Biomechanics of Repair in Invertebrates

Maeve O'Neill

Department of Mechanical & Manufacturing Engineering

Trinity College Dublin

Ireland

2019

A thesis submitted to the University of Dublin in partial fulfillment of the requirements for the degree of Doctor in Philosophy

Declaration

I declare that this thesis has not been submitted as an exercise for a degree at this or any other university and it is entirely my own work.

I agree to deposit this thesis in the University's open access institutional repository or allow the library to do so on my behalf, subject to Irish Copyright Legislation and Trinity College Library conditions of use and acknowledgement.

____

Maeve O'Neill

Signed on this the ____________ day of ___________________ 2019

Abstract

Repair is a ubiquitous process in nature, and it is one of the many features of biological materials that humans are constantly attempting to recreate. Though the process of repair has been studied in mammals, very little work has been done on other organisms, despite mammals representing just a minuscule percentage of global biodiversity. This thesis bridges some of these gaps in the knowledge, focusing of the repair process in two different organisms, the desert locust (*Schistocerca gregaria*) and the common limpet (*Patella vulgata*).

For the locusts a link was drawn between age and repair capabilities, similar to that observed in mammals, finding that older insects are less capable of repair. Both young and old insects repair damage by the deposition of fresh material. Older cuticle was also found to have a decreased fracture toughness. This has implications for energy storage for jumping manoeuvres which was found to involve the deformation of the stiff tibial cuticle. This deformation causes microdamage to the cuticle, in addition to the viscoelastic changes in behaviour, and poses the potential risk of fatigue failure in cuticle. This damage is repaired in a week, similar to the repair of microcracks in bone. The fracture toughness of the limpet shells was similarly evaluated and found to be much higher than that of its main component, calcium carbonate. Several toughening mechanisms that help to achieve this were identified. The limpets were also found to be similarly susceptible to fatigue failure, though some remodelling process may be occurring. The limpets are also capable to repairing damage to their shells, and like the locusts they achieve this by depositing fresh material, though another unidentified mechanism is at work.

Throughout this thesis comparisons were made to repair in mammalian bone. Bone has been very thoroughly studied and the mechanisms of repair are well understood. Several of the effects discussed in this thesis mirror effects observed in bone. Consequently,

comparisons to bone are drawn to give greater context and enable discussion about the studies.

Acknowledgements

I would like to thank my supervisor Professor David Taylor for giving me the opportunity to complete my PhD. He has been an endless well of guidance and support, even when I was convinced all was lost. He has taught me an immeasurable amount, whilst ensuring I was still enjoying my PhD.

To Peter O'Reilly for his endless patience and generosity with his time in helping me understand mechanical testing, as well as always being a friendly face. Muchas gracias, lo aprecio. To Mick and everyone in the workshop for their help in developing rigs. To everyone in the main office for being so friendly and making me feel welcome.

I owe a huge debt of gratitude to Collie Ennis for all of his help and guidance with the locusts, as well as enabling me to take Christmas off from feeding the plague. Additionally my thanks to Alison Boyce, Martyn Linnie and the zoology building for allowing me to house the locusts there over the years. Thank you to Clodagh, Eoin and Jan-Henning for their guidance with various techniques, and willingness to help.

A big thank you to Diego, Diana, and Riccardo who all contributed enormously to the work presented here here.

A big thank you to my Parsons friends (and Jenny!) for their constant support, company and commiserations; you got me through this. Thank you to my non-parsons friends both here and abroad, who listened patiently to the ups and downs, in particular to Rebecca and Hannah for always being at the other end of a phone to make me smile.

Thank you to my family who despite not understanding what I do always listened patiently and pretended to be interested. And to my goddaughter Laragh for always encouraging me to be better (and for allowing me to help in wrecking my aunts kitchen with our experiments).

And to Jason for the bleps and always encouraging me to believe in myself. 🐳 ❤️

List of Publications

This is a list of all publications and conference presentations associated with this work.

- M. O'Neill and D. Taylor ”Microdamage in insect cuticle” *J. Exp. Zool. A.*, In Review.
- M. O'Neill, D. DeLandro, D. Taylor ”Age related responses to injury and repair in insect cuticle”, *J. Exp. Biol.* In Press
- M. O'Neill, R. Mala et al. (2018) ”Repair and remodlling in the shells of the limpet Patella Vulgata”, *J. R. Soc. Inter.*, **15:145**
- M. O'Neill, D. Cafiso et al. (2018) ”Fracture toughness and damage development in limpet shells”, *Theor. App. Frac. Mech.* **96**, 168-173
- M. ONeill, R. Mala et al. ”Science with Impact; Fracture toughness and repair in limpets”, World Congress of Biomechanics 2018 (Dublin, Ireland)
- M. ONeill, R. Mala et al. ”Impact Repair in Limpet Shells”, Society for Experimental Biology 2018 (Florence, Italy)
- M. ONeill, R. Mala et al. ”Fracture toughness and repair in limpets”, Bioengineering in Ireland 2018 (Enfield, Meath, Ireland)
- M. ONeill, D. DeLandro, D. Taylor ”Age-related changes in the mechanical properties of insect cuticle.”, International Conference of Mechanics of Biomaterials and Tissues 2017 (Waikoloa Hawaii, U.S.)
- M. ONeill, D. DeLandro, D. Taylor ”Biomechanics of Insect Injury Repair”, Society for Experimental Biology 2017 (Gothenburg, Sweden)

- M. ONeill, D. DeLandro, D. Taylor "Biomechanics of Insect Injury Repair", Sir Bernard Crossland Symposium 2017 (Dublin, Ireland)
- E. Parle, C. Dooley, M. ONeill, D. Taylor , "Age related changes in the stiffness of insect cuticle" Society for Experimental Biology 2016 (Brighton, United Kingdom)
- C. Dooley, E. Parle, M. ONeill, D. Taylor "Age related changes in the stiffness of insect cuticle", Bionegineering in Ireland, 2016 (Salthill, Galway, Ireland)

To Butt. The goodest dog.

Contents

List of Figures **xv**

List of Tables **xxiii**

1 Introduction **1**

1.1 Thesis Outline 3

2 Theory & Background **7**

2.1 Bone 9

2.1.1 Bone structure 12

2.1.2 Bone repair 14

2.2 Chitin 15

2.3 Repair in Invertebrates 16

2.4 Locusts 17

2.4.1 Cuticle 18

2.4.2 Wound Repair in Insects 21

2.5 Limpets 24

2.5.1 Shell Structure 27

2.5.2 Repair in Molluscs 30

2.6 Mechanics 33

2.6.1 Insects 33

2.6.2 Limpets 40

2.7 Summary & Conclusions 44

2.8 Objectives 44

3 Materials & Methods 47

3.1 Insect Cuticle 48
  3.1.1 Mechanical testing 49
3.2 Limpet Shells 51
  3.2.1 Impact Testing 52
3.3 Statistical Analysis 55

4 Age Related Responses to Injury and Repair 57

4.1 Introduction 58
  4.1.1 Ageing Effects 58
  4.1.2 Injury Type 59
4.2 Materials & methods 60
  4.2.1 Ageing Effects 60
  4.2.2 Injury Type 61
  4.2.3 Cuticle Deposition 63
4.3 Results: Scalpel cuts 64
  4.3.1 Ageing Effects 64
  4.3.2 Cuticle Deposition 64
  4.3.3 Mechanical Results 65
4.4 Results: Puncture Injury 66
  4.4.1 Injury Type 66
  4.4.2 Mechanical Results 69
  4.4.3 Microscopy 70
4.5 Results: Fracture Toughness 72
4.6 Discussion 73
  4.6.1 Ageing Effects 73
  4.6.2 Injury Type 74
4.7 Conclusions 76
4.8 Future Work 77

5 Repair of Microdamage Caused by Cyclic Loading in Insect Cuticle 79

5.1 Introduction 80

5.1.1 Development of dyes 82

5.2 Materials & Methods 82

5.2.1 Staining and imaging cuticle 84

5.3 Results 85

5.3.1 Early investigations 85

5.3.2 Repair results 86

5.3.3 Staining of insect cuticle 91

5.4 Discussion 93

5.5 Conclusions 97

5.6 Future Work 98

6 Additional Studies on Insect Cuticle **99**

6.1 Introduction 100

6.2 Sex and mating differences 102

6.2.1 Materials & Methods 102

6.2.2 Results 103

6.2.3 Discussion 104

6.3 Water content 105

6.3.1 Materials & Methods 107

6.3.2 Results 108

6.3.3 Discussion 111

6.4 Conclusions 112

6.5 Future Work 113

7 Fracture Toughness of Limpet Shells **115**

7.1 Introduction 116

7.2 Methods 117

7.3 Results 121

7.4 Discussion 123

7.5 Conclusions 126

7.6 Future Work 126

8 Repair & Remodelling in Limpet Shells 129

8.1 Introduction 130

8.2 Materials & Methods 132

8.2.1 Compression testing 132

8.2.2 Damage Repair 133

8.2.3 Fatigue & Remodelling 134

8.3 Results 135

8.3.1 Quastistatic testing 135

8.3.2 Mechanical repair 137

8.3.3 Thickness and Deposition 138

8.3.4 Crumple Zones 141

8.3.5 Fatigue Behaviour 141

8.4 Discussion 146

8.4.1 Quasi-static testing 146

8.4.2 Repair 146

8.4.3 Crumple Zones & Fatigue Behaviour 149

8.5 Conclusions 151

8.6 Future Work 152

9 Conclusions 153

10 Future Work 161

References 165

List of Figures

1.1 A sketch of da Vincis flying machine. The resemblance to a bat wings is evident. ‘Design for a flying machine‘ circa 1488. 2

2.1 3D-printed biomimetic shark skin foil membrane. Taken from Wen et al 2014 [6] 8

2.2 Schematic of a BMU, bones repair mechanism. The osteoclasts break down and absorb old bone as the osteoblasts generate new bone. Taken from Taylor et al. (2007) [18] 10

2.3 Hierarchical structure of bone across multiple length scales. Taken from Sabet et al (2015) [30] 12

2.4 (A) Sketch by Wolff [31] of the predicted lines of stress in a human femur under normal loading. (B) Cross section of adult femur [32] showing trabeculae oriented in the same direction as predicted stress lines. 13

2.5 Stages of bone repair. The appearance of the hematoma and its subsequent replacement with bone can be observed [39]. 15

2.6 Chemical structure and hydrogen bonding in α chitin. Taken from [49]. . . 16

2.7 Adult female desert locust *Schistocerca Gregaria* 18

2.8 Chitin microfibrils formed of single sugar chains arranged in an antiparallel fashion. These are then embedded in a proteinaceous matrix. Taken from [49]. 19

2.9 19

2.10 Hierarchy of the main structural levels and microstructure elements of the exoskeleton material (referring to the exocuticle and endocuticle layers) of *H. americanus* (American lobster). Taken from [62]. 19

2.11 Schematic of the histological layers through a cross section of cuticle. . . . 20

2.12 (A) Schematic of adult cuticle repairing an excision in 5^{th} instar cuticle with a milipore filter. The epidermis can be seen to be migrating. Taken Locke [66]. (B) Epidermis of adult insect 4 days after injury; *ct* indicates margin of excised area, *cz* zone of congested cells, *nz* normal unchanged cells, *sc* cells spreading over injury site, *sz* zone of sparse activated cells, undergoing division. Taken from [67]. 21

2.13 Schematic of coagulation in *Drosophila* larvae. Coagulation begins with the disintegration of hemocytes, resulting in a soft clot. Crystal cells within additional hemocytes activated rupture and release phenoloxidase, causing the clot to melanize. Taken from Dushay [70]. 24

2.14 *Nautilus* shell cut in half, exposing the inner iridescent nacre layer [83]. . . 25

2.15 Intact limpet shell. The scale bar represents 5 cm, with 1 cm markers. . . . 26

2.16 Layered structure of the limpet shell taken from Taylor (2016) [93] 27

2.17 Micrographs of **P. vulgata** shells stained with Feigls solution, staining aragonite crystals black, leaving calcite unstained. (A) Cross section of shell. Calcite can be seen to be main component of apex and rim of shell, with a stained intermediate layer. (B) Layer M, M-1, M+1 layers can be seen to be composed of aragonite, with a transition to the unstained M+2, M+3 layer. Both images taken from Oritz and et al. [94] 28

2.18 (A) Optical microscope image of the radula containing many rows of teeth. (B) SEM image of a close up view of a tooth depicting the nano goethite structures. Both images taken from Barber et al. [98] 29

2.19 Photograph of repaired bivalve shell with damage scars evident as protrusions from the smooth surface. Taken from Harper and et al. [99] 30

2.20 Steps in patch formation. After one day the arrows represent the limits of the organic layer. By 4 days a thin patch begins to cover the hole. After 7 days this layer covers one third of the hole and has begun to mineralize. After 15 days the layer covers most of the hole and is almost fully mineralised. All photos are of the same section, however T4 and T15 are at twice the magnification. Taken from Fleury and et al. [101] 31

2.21 Schematic of the external and internal anatomy of the joint of the metathoraic (jumping) leg. Taken from Bennet-Clark [118]. 34

2.22 Diagram depicting the failure modes of slender tubes; 1 depicts fracture, 2a Euler buckling, 2b local buckling, 2c ovalisation and 3 depicts splitting[126]. 37

2.23 Prediction and experimental results for the locust tibia loaded in bending and axial compression respectively. The vertical lines indicate the optimum r to t ratio for axial compression and bending. It can be seen that the tibia lies much closer to the bending prediction. Taken from [126]. 39

2.24 Spalling concrete: the loss of smaller amounts of materials from the surface is evident [137]. 43

3.1 Image of the zoology setup; it spans two shelves. The glass tank is typically covered with black plastic to keep put light; this has been removed in the lower shelf so the tanks can be seen. Red heat lamps maintain the temperature, and white LEDs (not visible) give light. 48

3.2 (a) depicts the set up for the mechanical testing: the leg is implanted at its proximal end and the positioning of the pointer can be observed. (b) depicts a typical (nominal) stress-strain curve; The red line is a linear fit to the early part of the curve, to obtain Young's modulus 51

3.3 Aerial map of the test site, taken from Google maps. The test area is marked with a black square. 52

3.4 (A) Apparatus used to impact the shells. The weight weighs 123g: the pin and the holes in the tube allow the weight to be dropped from a known height, thus delivering an impact of a known energy. (B) An intact limpet shell. (C) Shell of a limpet after an impact test (17). The failure manifested as the formation of a hole in the apex. For both (B) and (C) the scale bar indicated represents 5 cm, with 1 cm markers. 53

3.5 Plot of survival or failure of shells as a function of their size for a given energy. A step function can be determined, defining some critical length (indicated here by the line), that minimises the error, allowing a fit of the ideal size to be found. 54

4.1 (a) is a repaired scalpel injury taken from a sample injured at 12 weeks and allowed to repair for 3 further weeks. The red colouring indicates the fresh cuticle laid down underneath the scalpel injury, evident as a fracture surface, whereas the scalpel injury can be seen as a smoother surface. (b) is a schematic of an insects hind tibia. *T1*, *T2* and *T3* indicate the dorsal, ventral and the medial/lateral sides respectively where cuticle thickness was measured. 60

4.2 (a) is a schematic of a puncture injury, the cuticle is pierced on the dorsal side without coming into contact with the ventral side. (b) Is a repaired puncture injury, after 2 weeks of repair. The fresh cuticle has been coloured in red. 62

4.3 (a) depicts the relevant sides of the hind tibia to aid understanding (b) and (c) depict the cuticle thickness after 3 weeks of repair for young and older insects respectively, along with their control counterparts. *T1*, *T2* and *T3* carry the same meaning as before. 64

4.4 Image of puncture injury caused by a large needle captured using a light microscope. 67

4.5 SEM image of a large needle puncture wound on insect cuticle. 68

4.6 Section of tibia of the dead animal. The injury is obscured by the darker mass of oat flakes. 69

4.7 (a) SEM image of a repaired puncture injury, from an insect injured at 8 weeks and repaired for 3 weeks. Fresh cuticle deposited after the injury can be seen marked in red. (b) SEM image of a puncture injury, looking at the dorsal side of the hind tibia. The injury was made at 8 weeks and the image taken after testing, i.e. with no time for repair. The injury is marked with a circle and is evident as a dark hole with extensive cracking extending from it. (c) Close up of a cross section of a repaired puncture injury (2 weeks repair). Fresh cuticle has been highlighted in red for emphasis. (d) Close up of a needle injury on a horizontal sample, with the same view as in Figure 4.7b. This image was taken without any repair time. The injury is indicated with a circle. Cracks can be seen protruding from the injury. . 71

4.8 Fracture toughness of cuticle tested at different ages. Value for 14 days is taken from Dirks and Taylor, 2012 [65]. Values shown are the means ± one standard deviation. The line indicates the samples that are not statistically different from each other. 72

5.1 Image of a locust taking off and a schematic of the corresponding anatomy [124]. 81

5.2 (A) Rear view of cyclical loading setup. The animal is secured against the blu tak using play-doh, and one hind tibia is extended into the orange cube filled with cement. (B) Schematic of lateral view of the test; the leg is implanted into dental cement, inside a 3D-printed cube. The animal is secured in plastic tubing, and the pointer connected to the Zwick descends. 84

5.3 Graph of stress versus strain for 5 cycles to a displacement of 3 mm at a rate of 150 mm/min. 86

5.4 Graph of stress versus strain for 5 cycles to a displacement of 0.5 mm at a rate of 0.6 mm/min. 87

5.5 (A) Graph of stress versus strain for 5 cycles to a displacement of 3mm at a rate of 5 mm/min. (B) Graph of early parts of 3 tests for the first and second cycle of the initial test, and the first cycle of the test after 1 hour of repair. Stiffness is found by taking the slope of the first 0.5 mm of displacement (once the sample is in contact with tester) and corresponding force. 88

5.6 (A) Graph of changes in Young's modulus between samples after various repair periods **(L-R)** 1 hour repair, 24 hours repair, 1 week and 4 weeks. (B) Graph of changes in UTS between samples after various repair periods **(L-R)** 1 hour repair, 24 hours repair, 1 week and 4 weeks. For both the line indicates the median and the circled dash the mean. In the 4 week UTS set the star indicates an outlier. 90

5.7 Percentage change in Young's modulus when compared to the original test for both the repair samples (i.e. samples tested once-original test- before being tested again after a given repair period) and for the other limb, used as a control. 91

5.8 A series of SEM images of part of the surface of one of our specimens after cycling: no microdamage was observed. The blue boxes indicate the region magnified in the subsequent image: i.e. the section marked with a square box in a is the image in image b, shown at a higher magnification. The images were taken at the part of the tibia closest to the cement, where the force would have been the highest. 92

5.9 Samples of cuticle stained with basic fuschin. Some cracks are visible as they are darker in colour, particularly in (a). However in (b) it is less clear if what can be seen is a crack or an air bubble or liquid inside the tibia itself. 93

5.10 (a) Data from Schaffler et al. [179] showing reduction in Young's modulus during cycling at applied strains of 0-1200 μ ϵ) (b) Results from O'Brien et al. [171] showing the typical appearance of a microcrack in bone after treatment with a fluorescence dye to enhance its visibility. 96

6.1 Increase in Youngs Modulus (right axis) and UTS (left axis) against cuticle thickness [140]. 100

6.2 Changes in Exocuticle thickness in comparison to total thickness over the first 10 weeks of adult life [140]. 101

6.3 (A) UTS for insects allowed to mate and the controls. (B) Young's modulus for insects allowed to mate and the controls. (C) Bending moment for insects allowed to mate and the controls. 103

6.4 Relationship between Young's modulus and percentage water content for a variety of failure modes [194]. 106

6.5 (a) Spectra of % transmittance against wavenumber recorded over the course of 12 hours, the peak associated with O-H bonding can be seen to decrease in this time period. (b) Peak intensity versus wavenumber, for old and young fresh cuticle. The height of the O-H peak can be seen to be drastically different between the two images. 109

6.6 Average of peak intensity heights for (L-R) mid-age, young and old insects 110

6.7 Loss of mass (as a function of mass per unit length) for insects of various ages 111

7.1 Instron machine used during testing. 118

7.2 Slope of the load-displacement curve for a shell before and after impact. . . 119

7.3 Images of the polishing machines used. 120

7.4 Different regions and crack types indicated on the shell. Example images of the three different crack types can be observed. 121

7.5 SEM photos depicting the layered structure of the shell, along with the nano-structured pleats. (a) and (b) are images of shells polished to reveal the surface. (c) and (d) are of spalled material after a fracture and by Dr. Dooley. 123

8.1 Plot of E_n against N_f. The straight line represents a constant value of the total accumulated E_n, here 8.06 $MJm^{-4.6}$. Graph taken from Taylor [93]. . 131

8.2 Typical load-displacement curve produced by the Instron. The different colour lines represent different tests. 132

8.3 (A) Regression models fitted to data from both fresh and beach shells. The gradients indicate a strong relationship between size and force to failure. (B) Force for failure for size bins of beach (yellow) and fresh (blue) shells. Data for the fresh shells bigger than 40 mm is not included as only two values occurred here, one of which is a significant outlier, disrupting the graph. 136

8.4 (A) Increasing apex thickness for impacted shell, over time. This correlates with the increase in impact strength depicted in the lower plot. It can be seen that the mechanical strength approaches the control values even as the thickness remains reduced. (B) Increasing thickness for shells that were abraded and then left to repair. The same trend is observed as for the impacted shells. 139

8.5 (a) Depicts a shell polished down to expose the thickness through the apex. In this way thickness can be measured and the internal structure and damage can be seen under SEM. The apex of the shell has been indicated with a black rectangle. (b) Depicts a shell impacted with 0.3J and left to repair for 60 days. Evidence of damage is still clearly present. (c) Depicts a shell abraded and left to repair for 30 days. In contrast to (b) there is little evidence of damage. 140

8.6 (a) Depicts a variety of shells with holes either on or slightly off the apex that have failed. (b) Depicts the effect of hole location upon the impact strength for shells with holes on their apex, and those with the holes moved slightly off centre. 141

8.7 (a) A shell found broken with the animal still inside (b) Imprint on a rock where a shell once was; the animal has gone missing and its grazing scar is left behind. Photos taken by R. Mala. 142

8.8 Survival rates of the three groups with varying impact energies evaluated, corrected for the effects of hurricane Ophelia. The red line marks the point where the accumulated energy meets the critical energy. 143

8.9 (a) Shell impacted at 20% of its critical energy every 14 days (shown here after reaching 160 % of the critical energy) (b) Shell impacted at 20% of its critical energy every 7 days (shown here after reaching 240% of the critical energy) 145

List of Tables

4.1 Numbers refer to the number of insects, not the number of samples tested. Except for controls in each case one hind tibia was injured and the other left intact for comparison purposes. For controls both hind tibia were tested as uninjured samples. ‘w‘ indicates the number of weeks. 63

4.2 Results for insects who received scalpel cuts across the dorsal side of the hind tibia at either 1 week (Young) or 12 weeks (Old) and UTS then left to repair for 3 weeks. Values for measured strength, bending moment to failure, and Youngs modulus are compared with uninjured control samples. μ and s.d. refer to the mean and standard deviation respectively, and σ, E and M refer to the UTS (MPa), Young's modulus (GPa) and bending moment (Nmm) of the samples respectively. 66

4.3 Results for insects who received puncture injuries on the dorsal side of the hind tibia at either 2 weeks (Young) or 8 weeks (Old). Uninjured refers to animals who received no injuries. Some insects were tested immediately with no time to repair and the remainder were then left to repair for 2 or 3 weeks. Values for measured UTS, bending moment to failure and Youngs modulus are compared with the uninjured control samples. μ indicates that all values are average values and *FS*, E and M refer to the UTS (MPa), Young's modulus (GPa), and bending moment (Nmm) of the samples respectively. 70

7.1 The number of samples in each group, the number of cracks, their length (mm) and a percentage breakdown of where in the shell cracks were found. 122

8.1 Number of shells tested for each type of damage and time period. For the apex hole shells the time period was actually 63 days as above. In cases where no data is given either an insufficient number of shells displayed repair at that stage to collect them, or the number of shells chosen were all of the same size. 134

8.2 Number of shells tested for each energy level and the repair periods. The final group are control shells; they were monitored to ensure no outside factor we were not aware of was influencing our results. 135

8.3 Number of shells lost across groups during Ophelia meteorological event. Results presented as percentages 142

8.4 Cyclical loading outcomes. The accumulated energy is written as the percentage of the shells critical energy, taken to be 8.3 $MJm^{-4.6}$. All results are percentages 143

9.1 N/A means this effect does not occur in this material. Scaling relationship displays the property that the UTS of the sample scales with. For cuticle all values are reported for insects 4 weeks after moulting. The scaling relationship is valid for the first 3 weeks. 154

Chapter 1

Introduction

The history of humankind is littered with thousands of attempts to imitate nature, and capture her ingenuity. One of the most obvious examples of this is our attempts to take to the skies, with nature informing every step of our aviation history. A key proponent of this was Leonardo da Vinci whose famous flying machine was inspired primarily by bats, which can be seen in Figure 1.1. And this trend has continued into modern history, with the evolution of Velcro, inspired by the clinging burrs of the burdock plant, and more recently the appearance of Speedos shark skin swimsuit - so good they have been banned from the Olympic Games for conferring too great an advantage to the wearer.

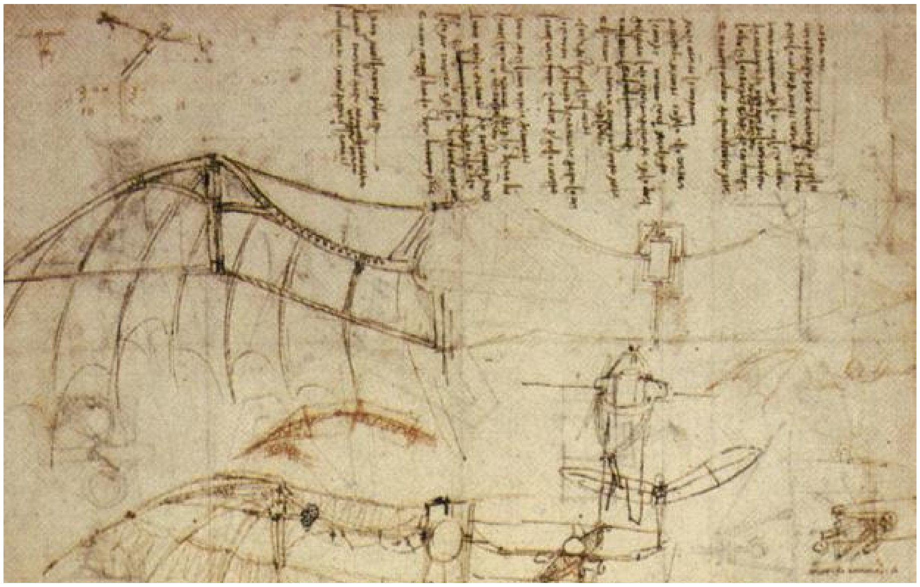

Figure 1.1: A sketch of da Vincis flying machine. The resemblance to a bat wings is evident. ‘Design for a flying machine‘ circa 1488.

This awareness of the potential of the natural world in solving many of humankinds problems, a field known as ‘biomimetics‘, has only increased in recent years. As of 2011, more than 2500 papers per year were being published in the field [1], a figure that one can imagine has continued to increase substantially since. Biomimetics have been used both in the design of structures, such as Velcro, as well as in material design - examining the microstructures present in materials such as bone that confer additional strength.

But despite the many advances made using biomimetics, one problem that humankind struggles with is the concept of repair. Repair is a ubiquitous feature found in nature, with organisms from most phyla demonstrating some capability for it [2–4]. In contrast many human-made materials come with a very fixed life, limited by the development of damage throughout them, requiring costly maintenance and outside help to repair the material.

As a result, nature may well hold the greatest insight into solving this problem, having mastered it in a variety of different environments, and typically under ambient conditions. This is also of grave importance when speaking about mimicking materials found in nature, such as nacre, more commonly known as mother of pearl. Many natural materials display incredible mechanical properties when compared to their individual components. For example a major component of nacre is calcium carbonate (chalk), yet nacre is much less brittle. This and similar effects are achieved through the advent of hierarchical layers or 'levels' at different length scales, often containing microstructures, with fine detailing on every length scale, from the nano right up to the macro-scale. However this system has a vulnerability in place. The failure of one of these levels can very rapidly lead to the failure of the others, meaning that repair is often a key factor in the maintenance of such structures. This also allows the structures to be light, containing less material than they would if they were not capable of repair. Consequently if one removes the ability to repair, they may no longer be as impressive, and certainly can be rendered less advantageous for applications.

However despite the ever increasing interest in biomaterials such as nacre, little work has been done to try and establish how these materials both withstand damage and how they are able to repair it; both important factors when considering their usage in our everyday lives.

The work contained here in this thesis seeks to address some of the gaps in knowledge of repair in non-mammals, along with the mechanical strength of some structures, focusing on members of the *Arthropoda* and *Gastropoda* phyla: The desert locust *Schistocerca gregaria* and the common limpet *Patella vulgata* respectively.

1.1 Thesis Outline

Chapter 2	Due to a lack of directly relevant literature this chapter instead aims to give the reader a broad overview of these organisms, to serve as a stepping stone when discussing the work done in the later chapters. It also gives an insight into bone and the repair mechanisms observed. Though no part of this thesis concerns bone, it is an ideal choice for drawing comparisons and parallels with when discussing the work here.
Chapter 3	An introduction to the methods and materials used in this thesis, describing those that are used repeatedly, as well as discussing animal care and housing. The statistical analysis and software used in this thesis are also discussed within this chapter. Any more specifics of tests are discussed within the relevant chapters.
Chapter 4	An investigation into *Schistocerca gregaria*, examining how age influences the animals ability to withstand damage, as well as the impact of age-related changes upon the animals repair ability.
Chapter 5	An investigation into the viscoelastic nature of cuticle and its ability to respond to microcracks, alongside the potential for energy storage in distortions of the hard cuticle.
Chapter 6	A combination of several smaller studies that serve to answer questions raised by the previous, larger studies
Chapter 7	An investigation seeking to establish the fracture toughness and work of fracture for delamination within the *Patella vulgata* shell, in order to draw a comparison to its more famous calcium carbonate counterpart, nacre.

Chapter 8	An investigation into the repair capabilities of the limpet shell. Examining the ability of these shells to respond to both large scale damage, and more minor damage, as well as their ability to detect and repair smaller stresses applied repeatedly over longer periods of time.
Chapter 9	Contains the conclusions of the work, summarising the thesis and its findings and their impact upon the field.
Chapter 10	Details the scope for further studies, continuing on from this thesis, as well as addressing further any questions left unanswered in previous chapters, and providing suggestions for how these questions could be addressed.

In this way we can begin to get greater insight into the steps necessary for developing self-healing materials, as well as understanding how nature has developed a variety of different solutions, to the same problem under various environmental and evolutionary constraints.

Chapter 2

Theory & Background

Since the turn of the 20th century the field of materials science, a field traditionally concerning itself with physics and chemistry, has expanded its reach into biology too, turning to nature for inspiration [1]. Though humankind has developed some amazing materials with excellent structural properties such as lightweight carbon fibres composites, and high strength alloys (titanium), there is still much that can be learnt from nature and biomaterials. This is due to the many desirable features that nature displays, distinguishing them from their synthetic counterparts. These interrelated features are: (i) Self-assembly, (ii) Multifunctionality (iii) Hierarchy (iv) Hydration (v) Ambient conditions (vi) Evolutionary and environmental constraints (vii) Self-healing [5].

And it is this final feature that this thesis focuses upon; the art of repair. Repair is ubiquitous on Earth - without the ability larger multicellular organisms may never have evolved, at least in their current form. Daily life is just too wearing.

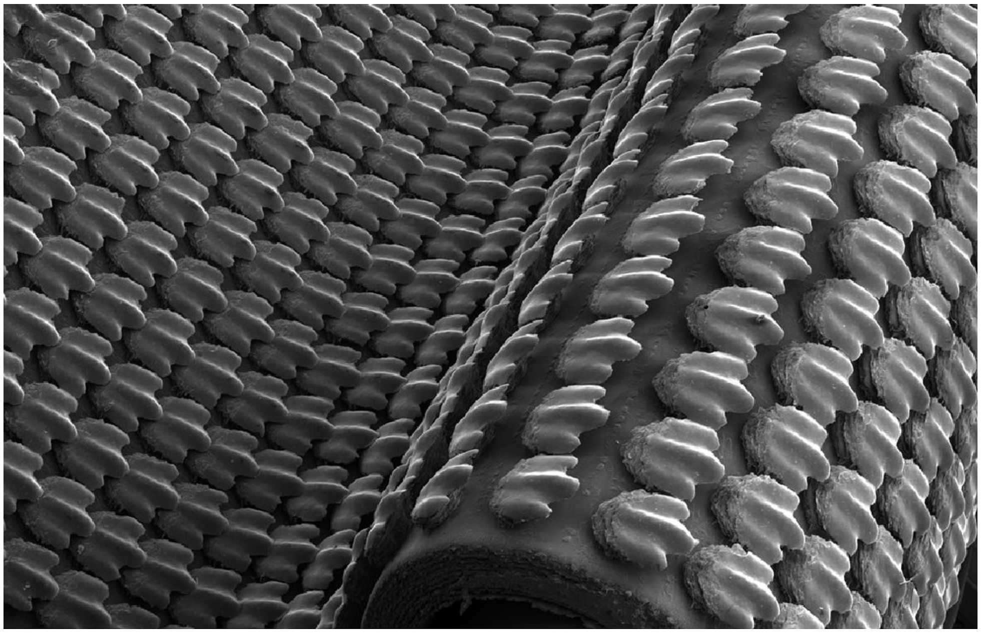

Figure 2.1: 3D-printed biomimetic shark skin foil membrane. Taken from Wen et al 2014 [6]

Biomimetics is an ever expanding field, and some of the most successful creations from this field, such as anti slip shoes with patterns similar to the waves on dogs feet, or the swimsuits with shark skin structure in Figure 2.1, have come from copying nature very closely. But when trying to recreate entire structures and materials things get more complicated.

And the reason for this is natures ability to repair damage. Natural materials are hierarchical structures [7], relying on the layer below them, with defects at one level potentially being catastrophic for the entire structure [8]. This can only be avoided by the layers being self-healing, able to restore functional and structural properties, whereas for human-made materials integrity is limited by our ability to inspect and keep quality control rigid. However there are some tissues that cannot repair themselves; enamel in human teeth that has been damaged is not able to repair itself, leading to the need for fillings and other dental interventions. Cartilage, a shock absorbing, tough tissue that cushions our joints has a very limited ability to repair itself, leading to problems such as osteoarthritis. Pain management was the main treatment option, until recent developments in tissue engineering [9]. Additionally some of the cartilage menisci in the body are not vascularised, further limiting their ability to repair [9, 10]. Conversely some man-made materials have been created that can self-heal, typically polymers such as thermoplastics. But in these cases repair generally refers to restoration of one or two properties, and is typically only possible under certain conditions, as well as only being described for certain type of injury such as puncture by a projectile [11, 12]. Though this is promising there is still a large amount of work to be done before man-made materials are able to respond to damage and repair it in a manner similar to mammalian tissues, which are able to detect not just large scale damage but also microscale damage, and do not require a very specific type of injury production in order to initiate repair.

2.1 Bone

This ability of repair and self-healing has been incredibly well documented, and is understood to quite an extent in mammals [13]. A classic example, that has been and still is an ongoing fascination for many scientists, is bone. It truly is a remarkable feat of engineering and how it changes as we age is understood to quite an extent [14–16].

Mammalian bones are able to constantly remodel - the bone we are born with is not the same bone we have as adults; our bones expand as we grow and get bigger and wider [17], and some fuse together - a new-born baby has approximately 270 bones in their body, which will eventually fuse to 206 by the time they are an adult. This ongoing growth is important; allowing a childs skeleton to be suitably sized for their physical proportions and activity, yet still strong enough to support the adult human. Though bone is not the subject of this thesis, it and its repair mechanisms are being included here to allow parallels to be drawn between different mechanisms of repair observed in nature, as well as between the work presented here and the wealth of existing work already performed on bone.

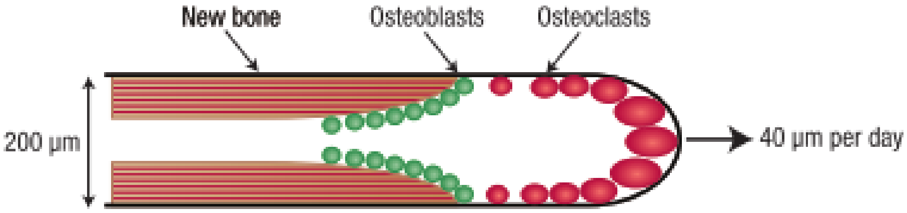

Figure 2.2: Schematic of a BMU, bones repair mechanism. The osteoclasts break down and absorb old bone as the osteoblasts generate new bone. Taken from Taylor et al. (2007) [18]

Bone must balance several evolutionary functions - it must be lightweight, providing maximum strength whilst minimising weight, as this allows a greater ease of movement, and it is less of a drain on an organisms energy supply. This trade-off is evident in larger animals such as pachyderms which are rarely renowned for their speed, instead fending off predators with their huge bulk. But this trade off for lighter weights leaves bones vulnerable to fatigue damage. Under normal circumstances bone is capable of functional adaptation - if subjected to high levels of stress or repeated cycling bones become stronger and thicker over time to compensate [18]. This relationship is governed by Wollf's law [14], with bones increasing in density and mass when placed under excessive loads or stresses.

This is achieved through a process known as remodelling. Bone is always constantly replacing itself, at a rate of a few percent a year [18]. There are two main phases to this; bone resorption and formation of new bone, involving two types of cells; ostetoclasts which use enzymes and acids to break down and resorb old bone [18, 19] and osteoblasts which produce the new bone tissue. Together the two are referred to as a Basic Multiceullar Unit (BMU) (see Figure 2.2), driving the growth of fresh tissue. Not only does this mechanism allow for growth, and for the bone to adapt to increased loads, but it also allows for the bone to respond to and repair any damage in the bone. Though initially the role of a

BMU in repair seems obvious; if bone is being replaced of course it is being repaired, but it has been verified to be a repair process, rather than a secondary effect, with a third type of cell, osteocytes, sensing cracks and alerting the body, actively targeting damaged bone [20, 21]. This has an evolutionary advantage allowing for more delicate bones than would be possible in a no repair situation.

However the down side of this state of active remodelling means that there is a small safety factor at work, and bones can easily be overloaded, leading to fracture. This is common in sports that require athletes to generate high forces such as running, rowing and weightlifting [22–24]. Baseball pitchers are another vulnerable group, though the safety factor when pitching is around two [25], they occasionally fracture their humerus [26]. Another group prone to damage is military cadets [27], with injuries typically occurring in the lower limbs in the first few weeks of training. These injuries occur when bones ability to withstand repeated loads is exceeded. Physical activity, especially weight bearing activity such as running or marching, loads bone via muscle forces and ground reaction forces. This typically leads to microcracks forming in the bone, which stimulates the body to produce additional, stronger bone. However when the rate of damage exceeds the rate of repair excessive strain on the bones begins to occur, which can often lead to a stress fracture. Another factor is that during remodelling, old bone is removed, before fresh bone is deposited, meaning there is a time lag, when bone may be more vulnerable to damage [23].

Several other factors may leave someone vulnerable to injury even just under everyday conditions due to reduced bone density or quality. One of the most prevalent causes of fracture is a reduced repair response or lowered quantities of bone in diseases such as osteoporosis [28]. These injuries are very common in an elderly population as the quality of bone becomes poorer with age. These sort of diseases are particularly prevalent in women due to the demands of childbirth. This is one of the many changes in the mechanical and material properties observed in various tissues in the body as the organism ages, such as the stretching of skin leading to wrinkles. Repair processes also become less effective with older adults requiring longer periods of time to repair any injuries. Alternatively if bones are underused due to periods of incapacity, bone responds to these mechanical loading conditions by becoming weaker, a condition known as disuse osteoporosis [18].

Once again this sort of bone loss is more commonly observed in an ageing population that may experience reduced mobility. Astronauts face a similar problem due to lack of force on the bodys musculoskeletal system [29].

2.1.1 Bone structure

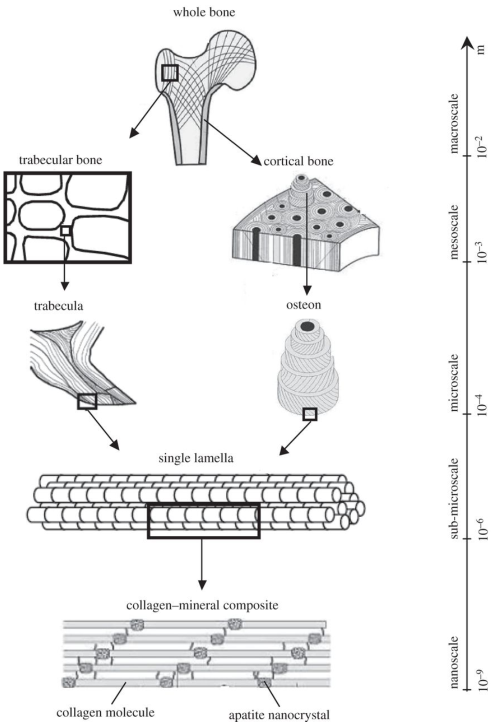
whole bone
trabecular bone
cortical bone
trabecula
osteon
single lamella
collagen–mineral composite
collagen molecule
apatite nanocrystal
m
macroscale
10⁻²
mesoscale
10⁻³
microscale
10⁻⁴
sub-microscale
10⁻⁶
nanoscale
10⁻⁹

Figure 2.3: Hierarchical structure of bone across multiple length scales. Taken from Sabet et al (2015) [30]

Bone is well adapted to resist loads and crack growth. Like most biological materials it has a hierarchical structure, with an order being clear on every length scale level from the nano to the micro to the macro scale. This can be seen in Figure 2.3. This structure contributes to bones impressive mechanical properties. There are two main types of bone; the first kind is compact cortical bone which is 20-30% dry weight of collagen, 1% other proteinaceous material and 70% calcium phosphate/hydroxyapatite [8]. Cortical bone forms the hard shell of our bones, conveying strength and stiffness. The second kind, is the more porous trabecular bone, which is spongy and makes up the interior of our long bones. Trabecular bone plays a role in energy dissipation.

The nanostructure of both materials are quite similar, both resembling sheets of plywood, composed of alternating lamellae [18]. These lamella are made up of collagen fibrils, containing small amounts of hydroxyapatite and non-collagenous proteins. Different arrangements of these lamellae give rise to the two main bone types: in cortical bone lamella orient themselves into concentric circles called osteons, aligned along the bones long axis [30]. In trabecular bone, such as that found in the femur, the lamella assemble into trabeculae, resembling rods [30]. These rods orient themselves in such a way as to resist the principal stresses. This can be seen in Figure **??** - **??** depicts the predicted lines of stress in a human femur when experiencing normal loading - 2.4b shows that the actual orientation of the trabeculae follows this predicted orientation.

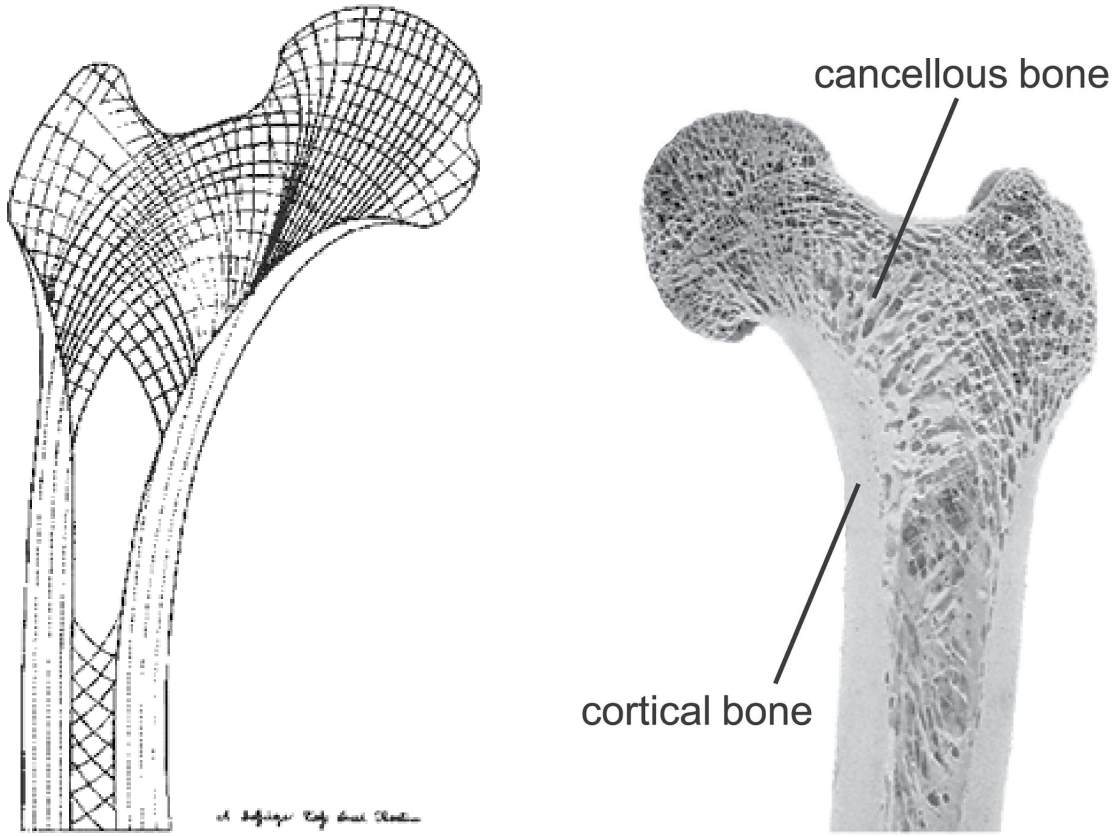

(a) **(b)**

Figure 2.4: (A) Sketch by Wolff [31] of the predicted lines of stress in a human femur under normal loading. (B) Cross section of adult femur [32] showing trabeculae oriented in the same direction as predicted stress lines.

This hierarchical microstructure that bone has also enables it to resist fracture. Bone is a quasi-brittle composite material, that prevents fracture through the formation of many microcracks which absorb and dissipate energy [33]. However these cracks are unable to grow any further due to a variety of ‘toughening mechanisms‘ (features that absorb energy that would otherwise be used to fuel crack growth). In bone these mechanisms tend to be structural interfaces such as mineral crystals, collagen fibrils, lamella and osteons where damage can form and energy can be absorbed [33]. NPCs at these interfaces can also absorb further energy. Such toughening mechanisms are common both in nature and in human-made materials such as metals where grain boundaries prevent crack propagation.

2.1.2 Bone repair

How bone actually detects microcracks and other damage relies upon a third type of bone cell; osteocytes. These cells are much longer than the two others with extensions of their cell processes - these meet at gap junctions (cell-cell contacts), forming a large network of cells, similar to the neural network within the brain [34]. These cells are highly mechanosensitive, and alter their production of signalling hormones when undergoing mechanical stimulus [35], orchestrating bone resorption [36]. When microcracks form in cortical bone this actually leads to the controlled death (apoptosis) of the osteocytes, but strictly only those at the original damage site. This disrupts the cell network leading to the activity of the osteoclast cells [37]. This has been confirmed experimentally - when osteocyte apoptosis is inhibited osteoclasts do not resorb bone [38]. However the exact mechanism by which the cells sense damage, and how they signal to other cells remains to be elucidated.

The repair process itself is quite interesting, as bone is one of the few mammalian tissues that can heal without the formation of a fibrous scar. Instead it is a form of tissue regeneration, involving both branches of the immune system, adaptive and innate immune functions. Immediately after injury a hematoma forms, causing an initial inflammatory stage where necrotic tissue is removed and angiogenesis is initiated. This causes the hematoma to coagulate around the fracture site, providing a template for a fibrin-rich callus to form on the bone [40]. This callus then mineralises, and is later resorbed - at the same time nascent bone tissue replaces the cartilage [41]. This bone is later resorbed as bone remodelling continues, with several cycles of bone remodelling and resorption taking place, as the bone is remodelled to it original structure [19]. At the same time marrow space is being re-established before extensive vascular remodlling occurs, restoring fluid

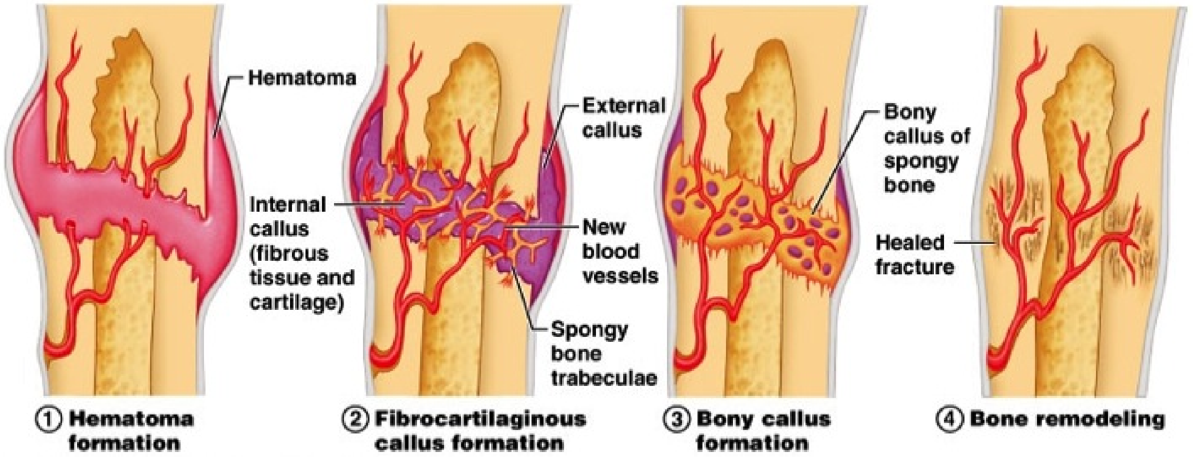
Hematoma
External callus
Internal callus (fibrous tissue and cartilage)
New blood vessels
Spongy bone trabeculae
Bony callus of spongy bone
Healed fracture
① Hematoma formation
② Fibrocartilaginous callus formation
③ Bony callus formation
④ Bone remodeling

Figure 2.5: Stages of bone repair. The appearance of the hematoma and its subsequent replacement with bone can be observed [39].

flow to the pre-injury rate [19].

Evidently the repair process in mammalian bone is quite well understood, both across large fractures and more minor cracks, along with the process of adaptive remodelling in response to large stresses. But outside of mammals, repair processes remain poorly understood, even though mammals represent a small amount of our global diversity. Taking a conservative estimate of the number of species to be 2 million, mammals make up $\approx$ 5,500 species (taken from [42]). As a result there is still a large gap in our knowledge. Furthermore, along with the ever increasing demand for cheap, low energy materials and a desire to further implement biomimetic design, there is huge scope for additional investigation and discovery in biomaterials. One such biomaterial is chitin, the second most abundant biopolymer on the earth after cellulose [43]. It is widely distributed throughout nature, being found in everything from fungal cell walls [44], the cuticle and integuments of arthropods [45] to the shells of mollusks [46].

2.2 Chitin

Chitin is a long, unbranched chain that is water insoluble, composed of 1,4-β-linked N-acetyl-d-glucosamine [47]. The structure and bonding can be seen in Figure 2.6. There are three types of chitin, α, β and γ chitin which possess different crystallographic structures. Chitin in the first two forms has been identified as an important structural component in both the exoskeletons of arthropods as well as the shells of molluscs, playing different roles in the two phylums. In arthropods chitin plays an important role in determining the mechanical properties and thus the function of the cuticle. For example chitin fibres that are loosely coiled will be soft and easily extensible. In contrast fibres that are tightly coiled or bonded together (a process known as sceloritzation, discussed in detail in Section 2.4.1) will result in a much harder, stiffer material. In molluscs chitin plays a vital role in the biomineralisation of the shells. Chitin orientation influences crystal orientation and aragonite inducing proteins [48].

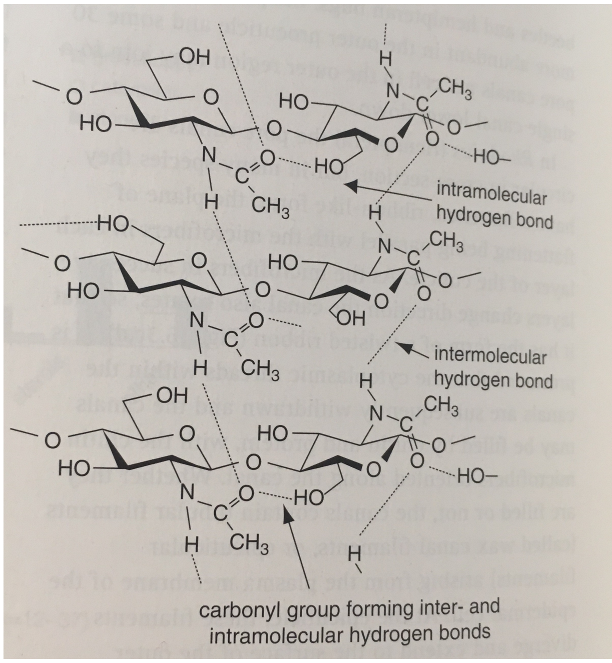
OH
O
HO
N
C
O
H
CH_3
intramolecular hydrogen bond
intermolecular hydrogen bond
carbonyl group forming inter- and intramolecular hydrogen bonds

Figure 2.6: Chemical structure and hydrogen bonding in α chitin.
Taken from [49].

2.3 Repair in Invertebrates

The trials and tribulations of everyday life demand that like mammals, invertebrates should be able to repair any damage they experience. This is especially true for longer lived species such as some gastropods that can live for decades. Famously the oldest living single organism was Ming the Mollusc, over half a millenia in age before being accidentally killed by researchers in 2006 [50]. Though Ming did not survive this encounter it is very unlikely that this was the only threat it ever encountered.

And the ability of invertebrates to carry out various forms of repair has been documented. Neural damage can be repaired [51] and the myth of an earthworms ability to regenerate the entire body from a small segment is not entirely untrue, though most of the animal must in fact be intact. However not all damage can be repaired. Muijres et al. (2017) [52] found that fruit flies are unable to repair any damage to their wings. But interestingly this has little effect upon their flight performance, with the animals capable of compensating for even extensive unilateral damage quite effectively. This raises the question of repair in insects and other arthropods, are they able to carry out repair, or is it even necessary for them to do so, have they simply evolved with body parts that are greatly over designed?

2.4 Locusts

The sub-phylum *Insecta* in particular makes up almost half of all arthropods [53], and have been incredibly successful. They are ubiquitous, having evolved to occupy virtually every ecological niche on our planet, save for the depths of our oceans.

They can be crucial to the ecosystem and to human life, such as the pollination of plants by bees, estimated to pollinate one third of all human crops. Yet insects can also be an extreme pest, such as the desert locust *(Schistocerca gregaria)*, see Figure 2.7 [54] infamous since biblical times (they are referred to in the Bible, the Quran, the Iliad and in Egyptian works of art) for their destructive swarming tendencies, which still pose an economic threat in many parts of the world today [55].

Insects have been used extensively in scientific research, *Drosophila* are utilised in numerous genetic studies and were amongst the first animals to have their DNA sequenced. On the far end of the arthropod spectrum, horseshoe crabs have had their blood harvested for years in order to produce the life saving vaccinations we all take as a given. In more recent years attention has turned towards the exterior of the insects. There is a growing interest from the biomedical fields in the cuticle that comprises the exoskeletons of insects, and its derivatives such as chitosan [56–58], primarily for both its biocompatability and biodegradability.

But despite recent interest a large gap in the knowledge still exists with regards to

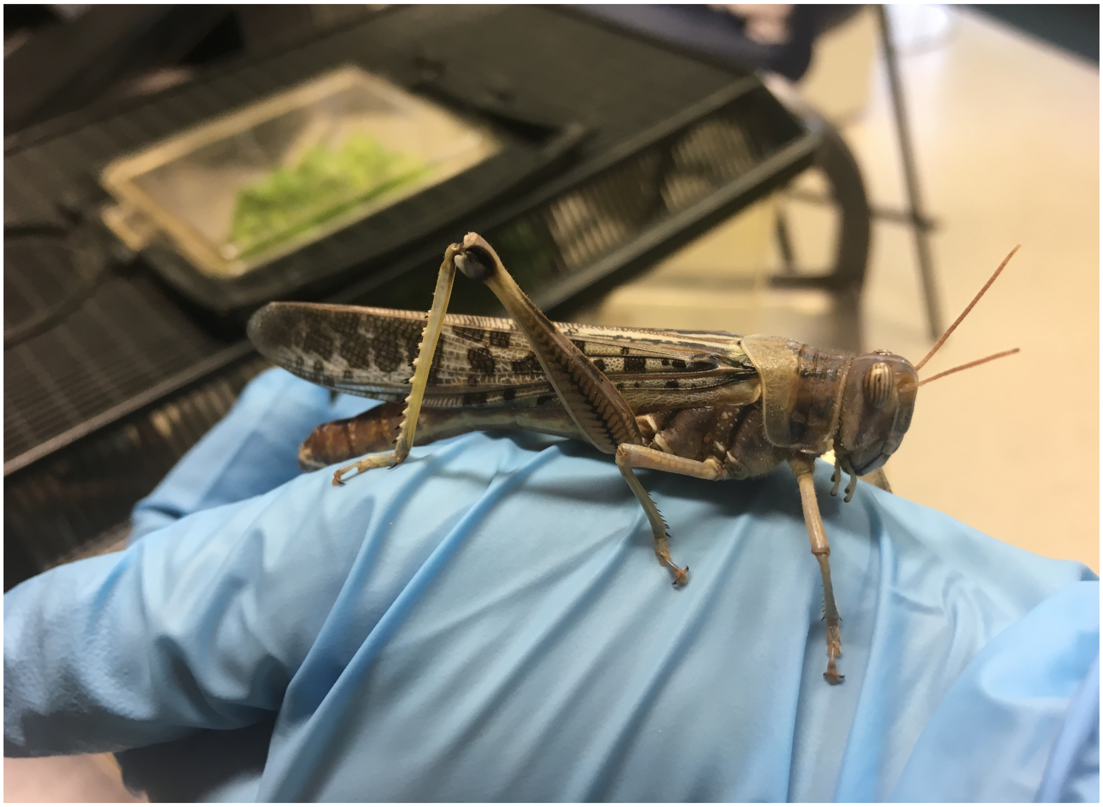

Figure 2.7: Adult female desert locust *Schistocerca Gregaria*

insects abilities to respond to injury or damage, that is the self-healing nature of their cuticle.

The insects in this study are the infamous desert locusts, though they rarely swarm in the wild, requiring certain environmental conditions to do so. This species exhibits phase polymorphism - the same species can display two different phenotypes, the solitarious and gregarious forms. Animals in the solitarious form are inactive during the day, bright green in colour and typically avoid other individuals. However when population densities become high enough, the presence of other animals drives a change into the gregarious form, which actively seeks out other locusts. This leads to increased population densities, with an exponential increase, creating the infamous swarms. All the animals used in these studies were of the gregarious form, which can be seen in Figure 2.7.

2.4.1 Cuticle

Cuticle makes up the skeleton of all arthropods and boasts a wide range of properties and functions even within a single insect. Cuticle is composed of individual chitin fibres embedded in a protein matrix [45, 49, 59], as can be seen in Figure 2.8. As cuticle is a hierarchical material, there are several levels at work. On microscopic level it is composed of individual monosaccharides joined by 1,4-β links. On the next level these chains ($\approx$ 3 nm long) orient themselves in an anti-parallel fashion creating α chitin. 18-25 of these form together to create nanofibrils of chitin crystallites [45]. These then cluster together and are coated with proteins, creating chitin-protein fibrils [60]. These further assemble into large fibres, eventually forming a planar network and orienting themselves in a ‘Bouligand structure‘ [61], resembling plywood. This arrangement can be seen in Figure 2.9.

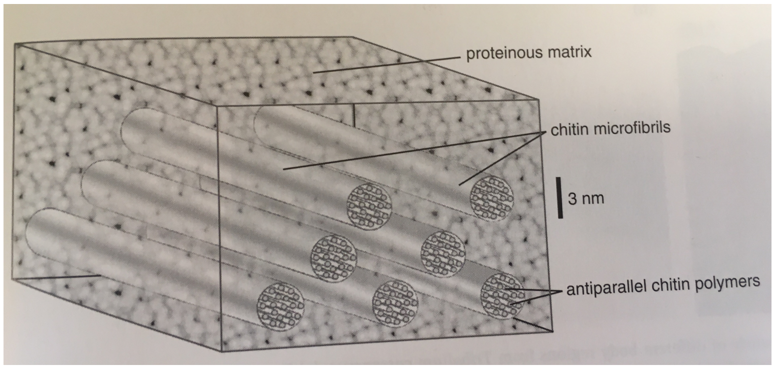
proteinous matrix
chitin microfibrils
3 nm
antiparallel chitin polymers

Figure 2.8: Chitin microfibrils formed of single sugar chains arranged in an antiparallel fashion. These are then embedded in a proteinaceous matrix. Taken from [49].

Raabe et al. / Acta Materialia 53 (2005) 4281

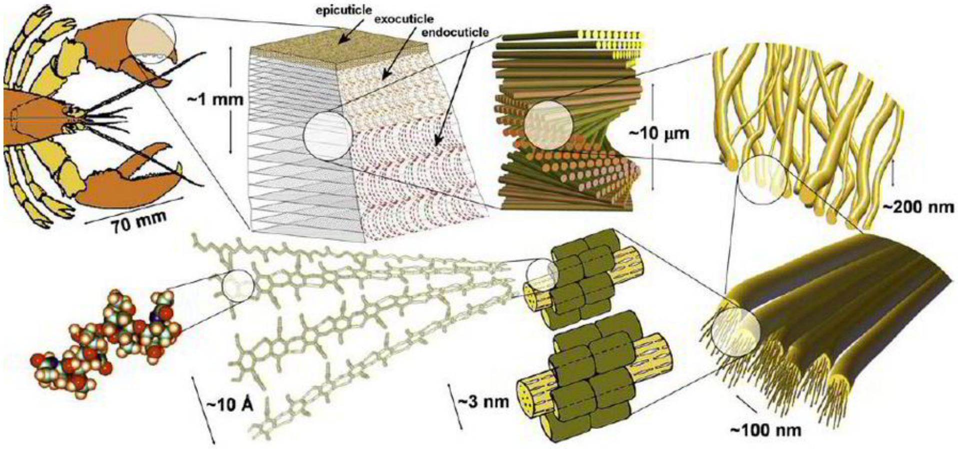
epicuticle
exocuticle
endocuticle
~1 mm
70 mm
~10 µm
~200 nm
~10 Å
~3 nm
~100 nm

Figure 2.9

Figure 2.10: Hierarchy of the main structural levels and microstructure elements of the exoskeleton material (referring to the exocuticle and endocuticle layers) of *H. americanus* (American lobster). Taken from [62].

The cuticle itself is composed of several histological layers, as can be seen in Figure 2.11 The outermost is a waxy epicuticle layer [59] similar in function to the stratum corneum found in mammals, both of which serve as a protective layer from desiccation. The layer below it; the procuticle, is acellular, it is the main determinant of material properties of the cuticle. It is composed of two further layers: the exo and the endocuticle. The exocuticle is hard and stiff giving the cuticle much of it's strength whereas the endocuticle is tougher and more flexible. Beneath these layers lies the epidermis, the first layer containing living cells. Insects and other arthropods - unlike mammals - have an open circulatory system. As a result haemolymph (comparable to mammalian blood) flows freely through their bodies - this is in contact with the epidermis providing the cells with nutrients.

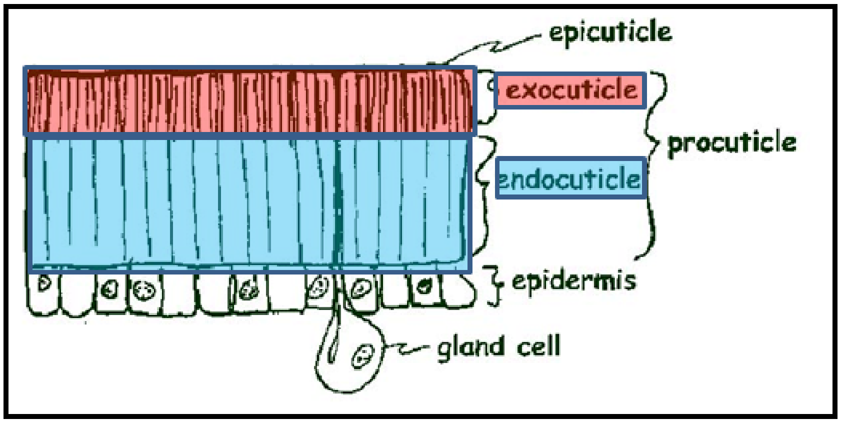

Figure 2.11: Schematic of the histological layers through a cross section of cuticle.

Scelortization

The mechanical properties of cuticle depend upon several factors such as cuticle thickness, the presence of dissolved minerals and the respective ratios of protein and chitin. However one of the most significant factors is the extent of sclerotization [63]. This is a process that occurs after each moult, a process known as ecdysis. As insects have exoskeletons, they cannot grow in the same way as mammals. Rather they shed their exoskeleton periodically through several cycles called instars. After each moult the cuticle must be soft so that the insect can swell and grow in size [49]. However this is not viable long term as the cuticle needs to be stiffer to allow normal locomotion. Consequently a couple of days after moulting the proteins distributed throughout the cuticle matrix cross-link, stiffening the cuticle considerably [49]. This causes the chitin layers to bind to each other, driving out water and tanning the cuticle, making it increasingly stiffer and harder. The extent of this process will depend on the final function of the cuticle; e.g. in the abdominal cuticle of *Rhodnuis*, which needs to expand quite dramatically, the cuticle will remain relatively soft with little cross-linking (60 MPa) [64]. In contrast, to the tibial flexor apodeme of the locust where the stiffness has been measured to be 20 GPa (parallel to chitin orientation) [45]. The tibia of the locust lies somewhere between these two [65].

2.4.2 Wound Repair in Insects

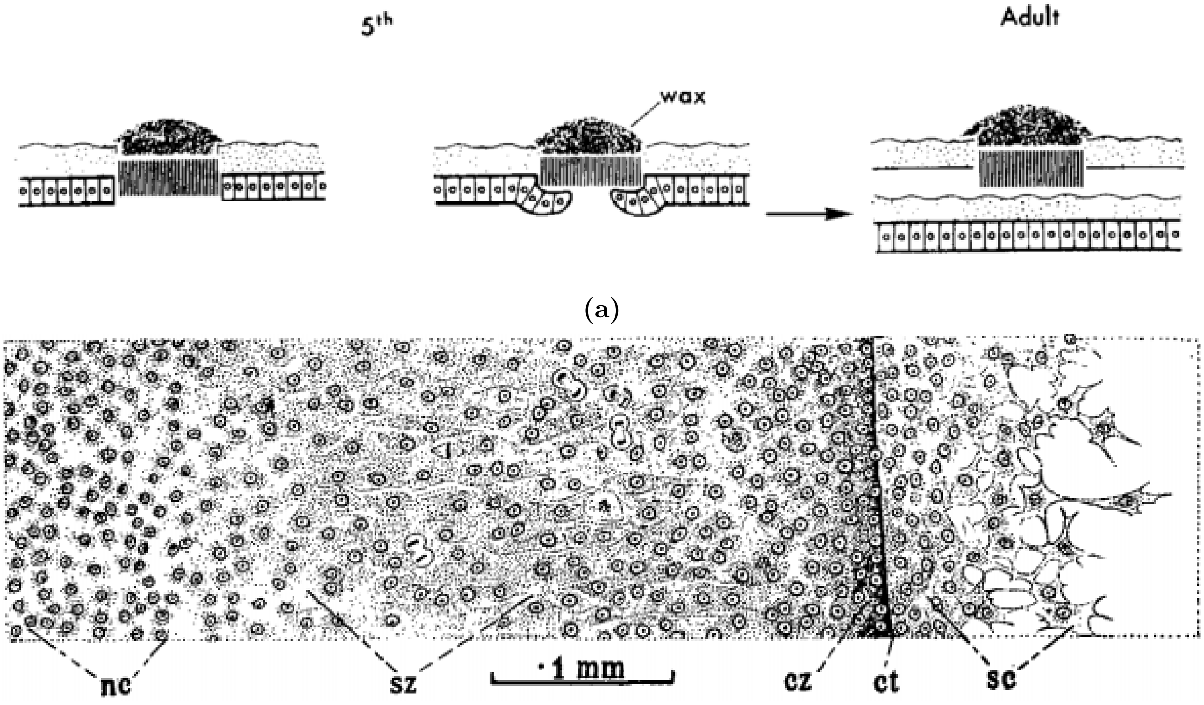

(a)

(b)

Figure 2.12: (A) Schematic of adult cuticle repairing an excision in 5^{th} instar cuticle with a milipore filter. The epidermis can be seen to be migrating. Taken Locke [66]. (B) Epidermis of adult insect 4 days after injury; *ct* indicates margin of excised area, *cz* zone of congested cells, *nz* normal unchanged cells, *sc* cells spreading over injury site, *sz* zone of sparse activated cells, undergoing division. Taken from [67].

Locusts, like all arthropods lack an adaptive immune response, relying solely on an innate system [68]. But it is one that is well developed and structured to prevent bacteria from entering the haemocoel and spreading from the wound; first there exists physical barriers such as the epicuticle, similar in function to mammalian epidermis. Then if the cuticle is breached, there exists a clotting response and cytotoxic molecules which are produced at the wound site.

Clots are essential to an insects survival for should a pathogen escape the humoral and cellular defence mechanisms at the wound site the insect has little defence against infection [69]. As a result, all of their immune responses centre upon preventing entry, and isolating pathogens at the injury cite. They do so via the appearance of a ‘scab‘ - similar to scab formation in vertebrates-to prevent the ingress and egress of fluids. This scab is a large chunk of melanin, the hard protein that strengthens the insects cuticle. This is process is known as coagulation, the formation of an insoluble matrix in the blood. In mammals the main function is haemostasis, but due to our more complex closed circuitry systems, we have also developed extensive anti-clotting measures, as excessive clotting could lead to thrombosis and other complications. In insects and other arthropods the clotting process proceeds much more exuberantly, because clots pose much less of a danger to their open circuitry system. For them, the more pressing urge is to prevent infection as well as to restore hydrostatic pressure and functionality to any soft tissue. Clotting is also of importance for preventing infection and disease, and this has been evidenced in fruit flies where loss of clotting factors leads to immune defects [70].

After clotting occurs, the next step is regeneration of the epidermal layer-the clot aids in this function acting as a scaffold for the cells to grow across. This movement of cells across the gap can be seen in Figures 2.12a and 2.12b. Once the epidermal layer has been successfully restored, the epidermal cells will begin to excrete new cuticle, gradually forcing the clot outwards from the insects body, though unless the insect has not yet reached its final moult, the clot will not be fully expelled and will remain as a dark melanised patch, visually similar to the concept of scars in mammals. The ability of the epidermal layers to realign is also crucial for repair, though the mechanism driving this migration is currently unknown. If it is prevented repair will not occur [66] and the animal could easily lose the damaged body part, with missing or shortened limbs being regularly observed.

Clotting & melanization

Clotting has four main steps [49, 69, 71];

- The hemocytes begin to disintegrate, forming extracellular aggregates, which along with extracellular matrix act for form a soft clot, sealing the wound.
- There is the activation of the PPO cascade, resulting in cross-linking which hardens the clot, helping to restore strength.
- Plasmatocytes are attracted to the wound, and begin to build under the clot, sealing it from the haemocoel.
- The epidermis begins to regrow underneath the clot, eventually growing it out.

Clotting occurs via the action of enzymes; the main ones responsible for the clotting process are include transglutaminase, which is phylogenetically conserved, and phenoloxidase, which is not found in vertebrates [69]. Though the cellular mechanisms responsible for clotting appear to be similar, requiring a mixture of haemolymph and plasma factors [70], the molecules involved are very different to those found in vertebrates; the proteins themselves typically do not have orthologues in vertebrates [69] but rather have novel architectures. These first two steps in *Drosophila* larvae are illustrated in Figure 2.13.

Clotting may have further purposes than just controlling fluid loss. Bacteria become trapped inside and possibly killed in the clots, though this response varies amongst species; clots in horseshoe crabs kill bacteria [72], but toxicity is not evident in *Drosophilia* clots [73]. It remains to be seen whether clots formed by *Schistocerca Gregaria* express toxicity. When the clotting proteins begin to cross-link and melanin is formed, highly toxic and reactive quinone intermediates form, due to the presence of phenoloxidase [74]. This results in visible melanin deposition [75], which gradually hardens to restore strength. The recovery continues at the site of the clot; repair of the epithelium and cuticle continue after clot formation, under the clot, which acts as a scaffold for repair. The clot attracts haemocytes [70] which are responsible for the repair and regrowth of new tissue.

Though the actual mechanism of wound repair has been well characterised and is understood to quite an extent, the actual mechanical properties of the insect cuticle under and after repair have been poorly investigated, with only one previous study by Parle

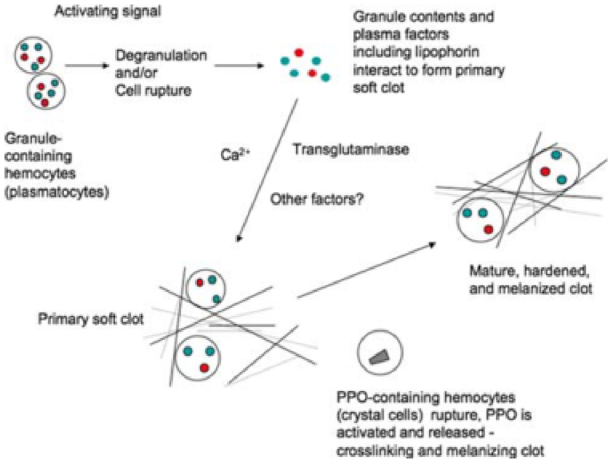
Activating signal
Degranulation and/or Cell rupture
Granule contents and plasma factors including lipophorin interact to form primary soft clot
Granule-containing hemocytes (plasmatocytes)
Ca^{2+}
Transglutaminase
Other factors?
Mature, hardened, and melanized clot
Primary soft clot
PPO-containing hemocytes (crystal cells) rupture, PPO is activated and released - crosslinking and melanizing clot

Figure 2.13: Schematic of coagulation in *Drosophila* larvae. Coagulation begins with the disintegration of hemocytes, resulting in a soft clot. Crystal cells within additional hemocytes activated rupture and release phenoloxidase, causing the clot to melanize. Taken from Dushay [70].

et al. [4] investigating the mechanical strength of repair. This is of grave importance; obviously if the animal is merely able to plug a wound without restoring any strength to the injured body part, using a leg as an example, it can be expected that the limb would break almost immediately upon the next attempt to jump, or even jut under normal locomotion. However this study only examined insects of one age, 5 week after moulting. Additionally only about half of the animals were actually able to repair their injuries; this is believed to be due to misalignment of the cuticular layers, preventing cell migration [4], but this could not be confirmed. More recently Parle and Taylor [76] published a similar study, investigating how the mechanical properties of the insect cuticle get stiffer and stronger over time, as the animal ages. How this may influence repair and other mechanical properties of the cuticle remains to be seen.

2.5 Limpets

Composites formed by nature are a source of inspiration for engineers and material scientists alike. Nature can produce composites and structures that often have remarkable properties [7, 8, 77]. Of particular interest are the hard biocomposites observed in bone and nacre, which frequently convey high strength stiffness and toughness [78, 79], typically mutually exclusive properties, giving inspiration for novel biomaterials [77, 79].

A classic example of this is nacre, the irridescent material on the inside of abalone shells (such as in Figure 2.14, and the outer coating of a mother of pearl. Nacre is composed primarily of calcium carbonate, a traditionally poor engineering material. Yet once included in a biomatrix, where $CaCO_3$ can make up to 99% of the structure, with the rest being an organic matrix [80], the fracture toughness is an order of magnitude greater than that of pure aragonite. This impressive feat is achieved via a ‘staggered structure‘ - a mix of high aspect ratio pieces (calcium carbonate plates in nacre) embedded in a ductile organic matrix [7, 81, 82]. In nacre this gives the appearance of a brick wall, with protein and polysaccharide layers at the interfaces [7, 81], with the calcium carbonate plates conveying high strength, and strain dissipated through viscoelastic energy dissipation throughout the organic layer [79]. Evidently nature has evolved a way to tightly control crystal growth to give exact properties. Even more impressively it has achieved this under ambient conditions, making it very exciting for those interested in single and poly crystalline materials.

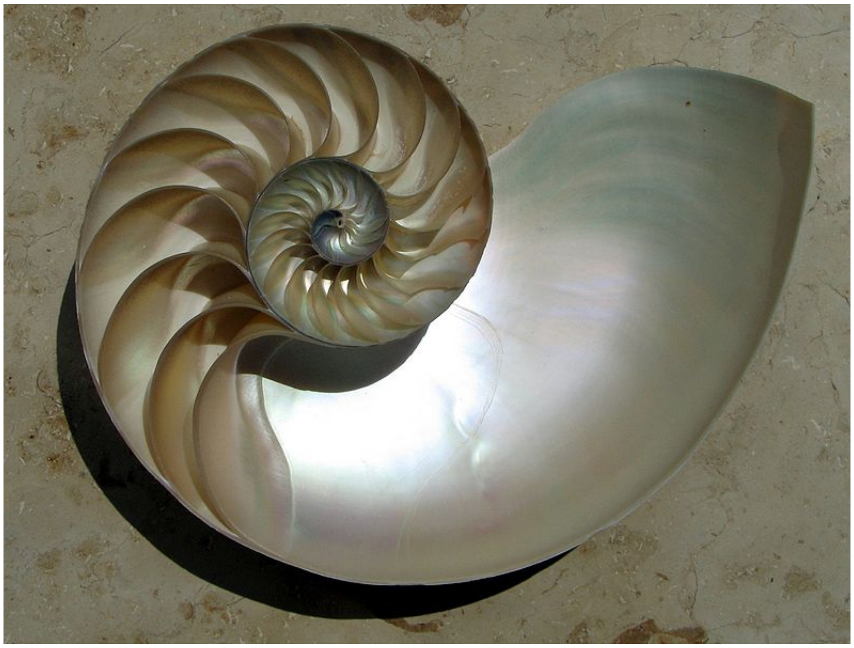

Figure 2.14: *Nautilus* shell cut in half, exposing the inner iridescent nacre layer [83].

As such the growth of these biomineralised shells is appealing as a solution to the demand for low-energy solid materials [84]. This is evident in the large number of papers published on the topic of nacre (nearly 4,000 in ten years on sciencedirect.com). This interest in shell structures is what led to the following work on limpets; due to climate constraints Abalone is not typically found in Northern European shores, favouring warmer climates in the Southern hemisphere.

‘Limpet‘ is a very broad term, comprising all aquatic snails with conically shaped shells. The limpets in this study, *Patella vulgata* (see Figure 2.15, are members of the *Patellidae* family, being true limpets. This means they are capable of some locomotion, but they return to a fixed spot, their home. *P. vulgata* like many other limpets [85] creates a grazing scar at its home; the limpet is capable of movement to locate other sources of food yet always returns to the same spot, which can be observed as a worn part on the rock. Finally, when threatened limpets will press themselves close against the rock substrate, increasing friction, resisting shear movement of the shell along the substrate. Limpets tendency to stay in the same spot has an advantage as their shells grow very precisely into the rocky substrate increasing friction and resistance to shear forces [86, 87]. They are common across Northern Europe in inter tidal zones, and can live for decades. They affix themselves to rock faces using suction forces generated by their strong muscled foot to hold their shell against the rocks [88, 89].

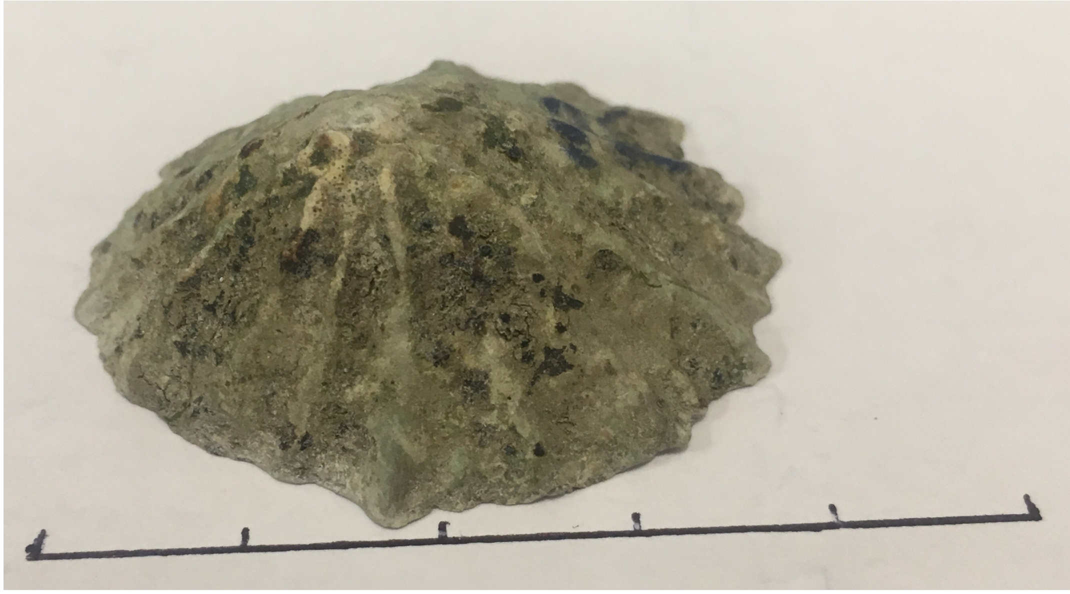

Figure 2.15: Intact limpet shell. The scale bar represents 5 cm, with 1 cm markers.

Their success and proliferation is largely attributed to their shells; a multifunctional structure. They serve multiple purposes, protecting the animals from dehydration and predators, as well as support for the internal anatomy of the soft bodied animal [90]. The animal continually produces its shell, resulting in older limpets being larger. Limpets also increase the thickness of their shells as they age [91]; this is an important adaptation, as if the shell thickness stayed the same as the animal got bigger, the shell would eventually cave in under natural forces. Consequently older animals can be identified compared to the younger ones by examining shell thickness and size.

2.5.1 Shell Structure

The primary function of the shells is to protect the molluscs soft body from both debris and predators. Consequently they are designed to be strong in particular directions, optimised to withstand impact and crushing forces. The shells do have some macrostructures to support their structural ability to resist damage such as curvature, spines and ribs [92], but it is the manner in which the calcium carbonate micro-structure is composed that plays the biggest role.

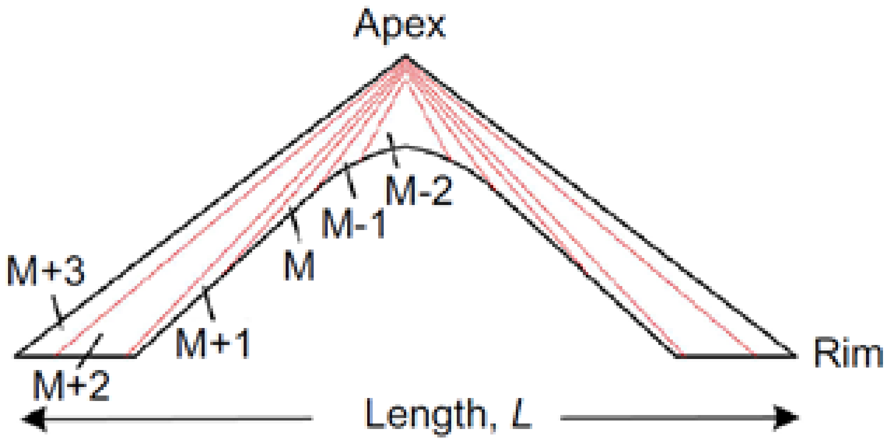

Figure 2.16: Layered structure of the limpet shell taken from Taylor (2016) [93]

The microscopic structure is very precise and ordered and there is a large amount of inter species variation [94]. Figure 2.16 depicts a simplified version of this layered structure for *P. Vulgata*. The M-layer is the myostracum, where muscle insertion into the shell occurs. The other layers above the myostracum are denoted with a M+n and

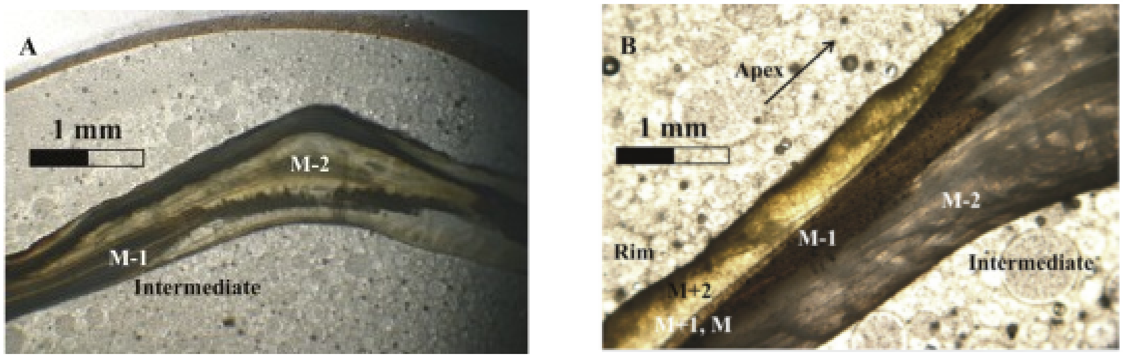

(a) (b)

Figure 2.17: Micrographs of **P. vulgata** shells stained with Feigls solution, staining aragonite crystals black, leaving calcite unstained. (A) Cross section of shell. Calcite can be seen to be main component of apex and rim of shell, with a stained intermediate layer. (B) Layer M, M-1, M+1 layers can be seen to be composed of aragonite, with a transition to the unstained M+2, M+3 layer. Both images taken from Oritz and et al. [94]

those below are denoted with M-n. The rim and apex are primarily composed of calcite, with the intermediate M±1 layers being composed mainly of aragonite [94]. This can be observed in Figures 2.17a and 2.17b, where the aragonite can be seen to be stained in black, with the calcite layers unstained.

The orientation of the layers, as well as the prismatic and lamellar arrangement also vary from layer to layer; The myoscratum is very thin, with a prismatic structure, where the crystals are large and oriented perpendicularly to the shell surface [94]. In the layers closest to the myoscratum where aragonite dominates (M-1, M+1), the structure is a complex crossed-lamellar structure, with a feather like pattern [94], with first, second and third order lamellar layers being identified [92]. Contrastingly the microstructure of the layers at the rim (M+3, M+2) have a concentric crossed lamellar pattern with crystals oriented parallel to the shell edge [95]. Layer M-2 makes up the apex and its microstructure shows an irregular to radial crossed-lamellar pattern [94]. The layers composed of calcite contain higher levels of organic matter than those composed of aragonite.

The outermost layer of the shell is the periostracum, a thin, organic coating made up of tanned proteins. It is excreted from the mantle, from the periostracal groove [96] and similar to scelortization process in insects is tanned via a quinone driven process. This layer serves to protect fresh growth of shell material from the external environment. The shell itself is formed and mineralized by the mantle - a thin sheet-like organ that lines the inner surface of the shell - depositing extracellularly both the crystalline and organic materials [97]. Fresh shell material is deposited in a small compartment called the extrapallial space, enclosed by both the mantle and the existing shell and the periostracum. This allows for calcium ions to build up in high enough concentrations for crystallisation to occur [96]. Additionally the periostracum also acts as a framework for calcium carbonate deposition with the outer layer being laid down here. The organic matrix shapes the forming crystals.

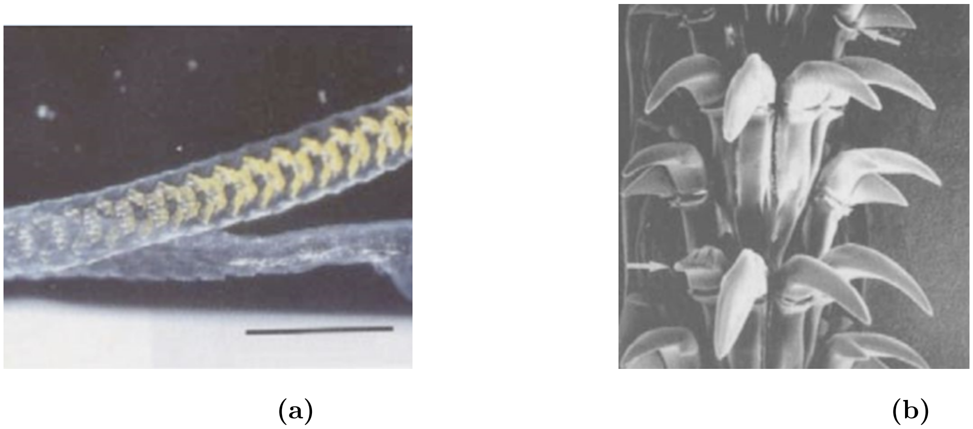
(a) (b)

Figure 2.18: (A) Optical microscope image of the radula containing many rows of teeth. (B) SEM image of a close up view of a tooth depicting the nano goethite structures. Both images taken from Barber et al. [98]

In order to achieve the necessary supersaturation conditions for calcium crystallisation to occur molluscs posses membrame-bound ionic pumps, recruiting calcium and bicarbonate ions from the teguments and the gills and the gut and transported by the haemolymph [90]. These ions are then stored before being pumped into the extrapallial space by specific channels in the calcifying epithelial cells [96].

Underneath the shell the underside of the animal consists of a single muscular foot, used for gripping surfaces. Like insects their circulatory system is open, with haemolymph flowing through. Limpets feed using an organ called the radula, rasping algae off of the rock (see Figure 2.18). These teeth are iron-mineralized and act in a conveyor belt like fashion with teeth in the front rows being replaced as they wear away. These teeth are amongst the strongest natural materials in the world, exceeding even spider silk [98].

2.5.2 Repair in Molluscs

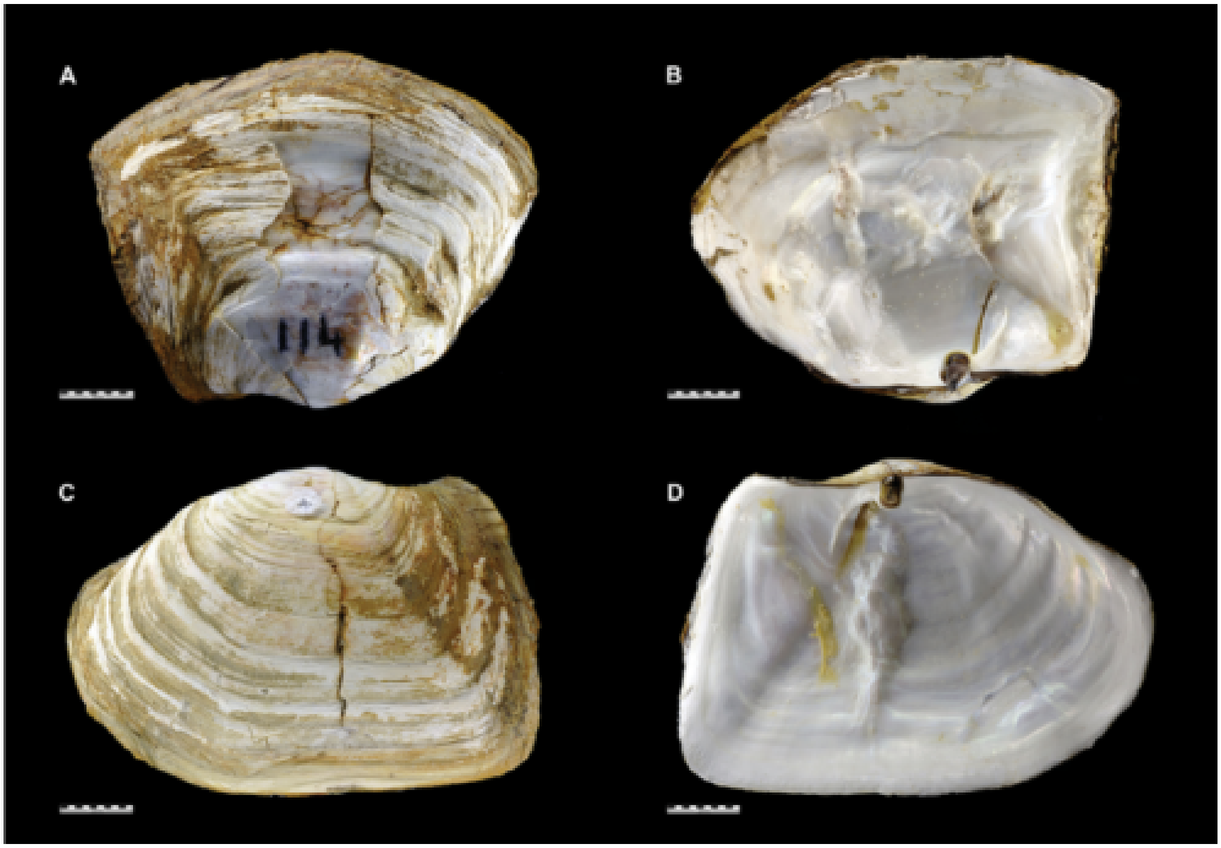

Figure 2.19: Photograph of repaired bivalve shell with damage scars evident as protrusions from the smooth surface. Taken from Harper and et al. [99]

Damage to the shell of a mollusc requires immediate repair to prevent anything from piercing the soft body of the animal inside. Shell repair requires the replacement of both the crystalline layers and the protein matrix, and is carried out in a similar fashion to the normal growth of the shell, with the mantle excreting both the organic component of chitin and proteins and the inorganic phase of calcium and other minerals. Typically the shell does not perfectly regenerate, especially if there is damage to the mantle, with protrusions often evident, as in Figure 2.19. Generally the type or morphology of the new crystal layers differ from the normal shell, as does the organic matrix in both structure and composition [90]. Additionally the rate of calcification is increased during repair compared to normal shell growth [97], though for molluscs in the water, repair still typically takes several months [80, 100].

The stimuli for shell regeneration have not been clearly defined, though it could quite possibly come from mechanical effects on damaged parts of the shell, or the exposed mantle detecting a different medium, especially in marine molluscs. But it proceeds in a series of steps;

Once the shell is pierced the mantle retracts from the injury site, remaining in place in the rest of the shell. This creates a gulf in the shell, creating a physiological seal against the external environment [101], which is important for the function of the extrapallial space. However this only occurs if the damage is near the edge of the shell. If damage occurs away from here, where the mantle cannot contract the shell will still repair but in these cases the new shell will differ in structure and morphology [90].

Within the first hour after damage a thin membrane or fluid can be observed at the injury site [102] produced by the mantle epithelium. Shortly after a non-mineralized (organic) brownish layer appears [103], which slowly covers the extent of the damage. This layer is either periostracum or non-periostracum type depending on the location of the injury. In some species of marine gastropods an additional membranous layer similar to the organic matrix or a nacreous layer may be laid down before the periostracum layer, though this step has not been investigated specifically for *P. vulgata.*

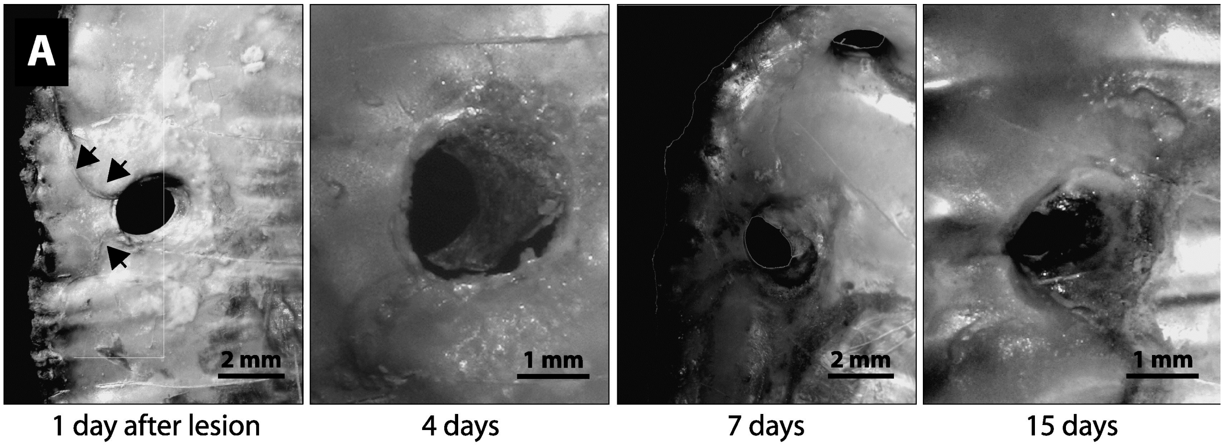

Figure 2.20: Steps in patch formation. After one day the arrows represent the limits of the organic layer. By 4 days a thin patch begins to cover the hole. After 7 days this layer covers one third of the hole and has begun to mineralize. After 15 days the layer covers most of the hole and is almost fully mineralised. All photos are of the same section, however T4 and T15 are at twice the magnification. Taken from Fleury and et al. [101]

In later stages these organic layers begin to mineralize from the inside (closest to the mantle) moving outwards, typically taking a month for the mineralization to begin [101][103]. This calcification process can occur in two ways: The first proceeds in the same fashion as typical shell formation only at an accelerated rate. The second and more common is the kind that leads to abnormal structures. This slow expansion of the organic layer and it's subsequent mineralization can be observed in Figure 2.20.

The exact mechanism of this calcification process is in dispute [101]: calcium granules have been observed in the connective tissue of the mantle but only in damaged shells, control shells do not display any granules. Which form of calcium carbonate they are is however unclear, as is the means by which they arrive at the repair site, as no such granules are observed in the epithelial cells and the epithelial barrier must be crossed. The two mechanisms proposed are re-dissolution of the calcium carbonate and subsequent ion transportation through the cells or the direct migration of the granules through trans epithelial channels. The role of hemocytes/ameobocytes is also still unclear. These immune cells have been reported to be involved in wound healing in some species for a long time. Kapur and Gupta [102] reported that hemocytes carry the histo-chemical substances necessary for calcification to the repair site, as well as acting as scaffold for the calcification process. More recently Mount et al. [104] reported that hemocytes bring single calcite crystal for the repair site, where they are remodelled and mineralized, though the mechanisms could vary between species [101, 105].

Crystal formation is either initiated in aragonite spherulites on the membrane or directly on the membrane itself [90, 106]. Thereafter the growth of a calcium carbonate polymorph layer will vary from species to species as some molluscs produce nacreous layers, and others such as *P. vulgata* do not. However Fleury and et al. [101] observed new microstructures in the green ormer (*H. tuberculate*) after repair. The reason for variation in microstructures in new patches of shell comes down to two factors: variation in the secretory regime during the repair process, as well as the orientation of the calcifying layer in the mantle to the repair site. This also explains why damage at the shell rim generally results in an identical microstructure to the rest of the shell, as the calcifying layer is in contact with the repair site in the same orientation as normal growth. The time it takes for mineralisation to complete will depend upon the species [101].

2.6 Mechanics

2.6.1 Insects

Locusts, like most insects have six legs and transport themselves across the ground via a six legged stride, slowly ‘walking‘ from location to location. However locusts are also incredibly effective jumpers, capable of comfortably jumping a metre, utilising their powerful hindlegs as a means of escape, to transport themselves up to higher locations, or to launch themselves into flight. Such movements require both high speed and power, overcoming the force-velocity trade off that constrains striated muscle [107–109].

Insects overcome this barrier using power-amplification mechanisms, though some animals, such as bush crickets also rely primarily upon the mechanical advantage of their very long hind tibia [110] and make use of a catapult mechanism [111, 112]. Energy is stored by slowly deforming elastic structures to maximise stored energy before producing a rapid recoil that delivers this energy, amplifying the power of the movement [113–115]. An excellent example of the effectiveness of this is the froghopper; accelerating in less than 1 ms at velocities of 4.7 m/s [116]. The power requirements for this (10^6 W/kg), far exceed the power that can generated through direct muscle contraction (250 W/kg) [111, 112, 117, 118]. The comparably slower desert locust (*Schistocerca Grgearia*) used in this thesis, accelerate in 20-30 ms and take off with a velocity of 3.2 m/s [118, 119].

There are three main steps in the jumping process for a locust. First there is the cocking phase, whereupon the flexor tibiae muscle contracts, flexing the femerotibial joint, so that the tibiae is pressed against the femur. Next is the co-contraction phase, which occurs over the span of 150-500 ms. In this stage the tibiae extensor and flexor muscles contract, the semi-lunar processes distort and the apodemes stretch, storing mechanical energy. Energy is also stored in the slight bending of the tibiae (approximately 3°) [120]. Though the flexor muscle is smaller and weaker than the extensor muscle, the tibiae do not move during this contraction phase, due to the mechanical advantage of the flexor muscle in the locked position, due in part to Heitlers lump, a chunk of cuticle on the inner surface of the distal end of the leg, which holds the apodeme in place [121]. Finally there is the jump itself where the flexor muscle relaxes, and the semi-lunar processes and apodemes extend the tibiae rapidly launching the insect into the air. The relevant anatomy can be observed in Figure 2.21.

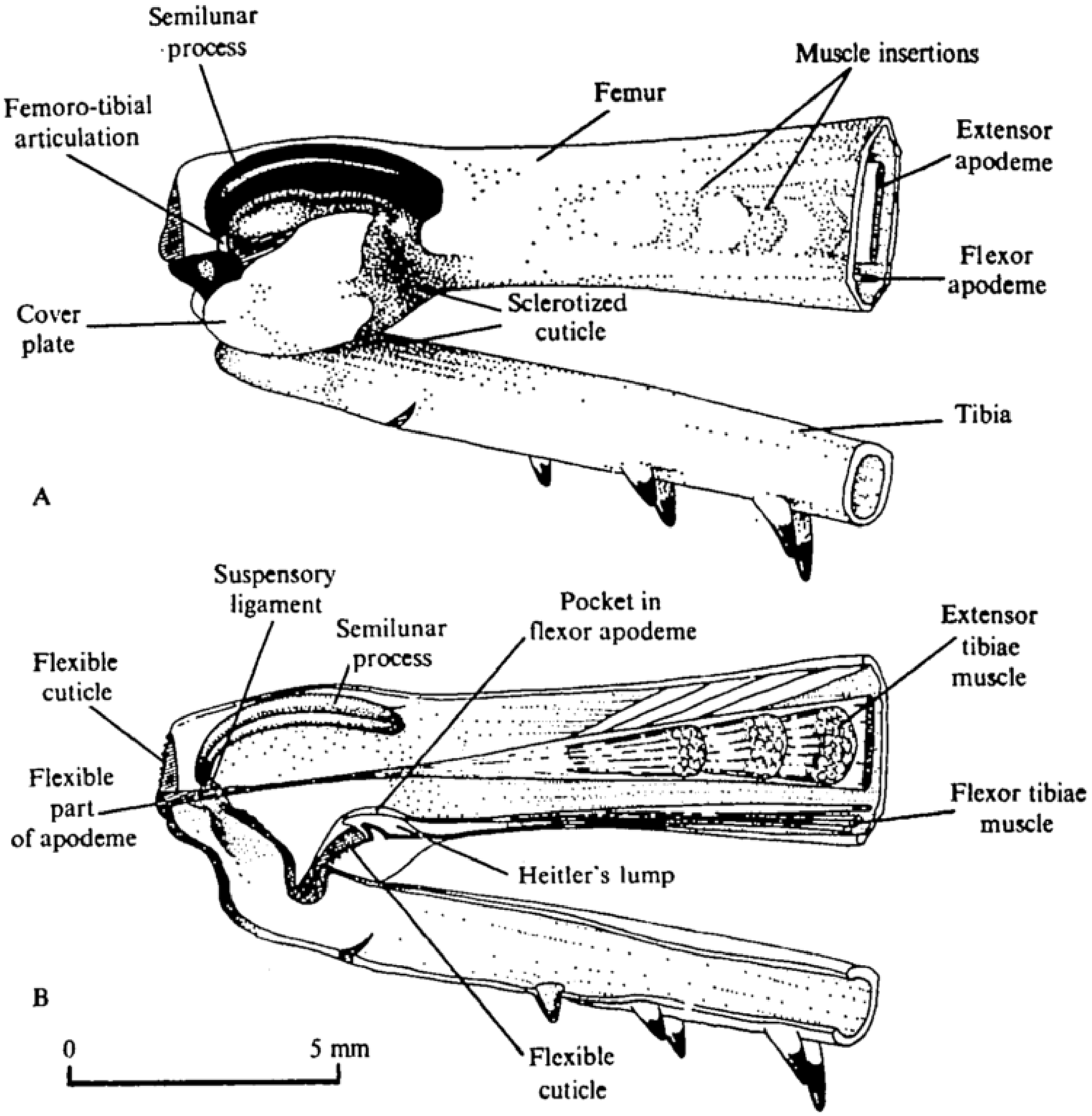
Semilunar process
Femoro-tibial articulation
Femur
Muscle insertions
Extensor apodeme
Flexor apodeme
Cover plate
Sclerotized cuticle
Tibia
A
Suspensory ligament
Pocket in flexor apodeme
Semilunar process
Extensor tibiae muscle
Flexible cuticle
Flexible part of apodeme
Flexor tibiae muscle
Heitler's lump
B
0
5 mm
Flexible cuticle

Figure 2.21: Schematic of the external and internal anatomy of the joint of the metathoraic (jumping) leg. Taken from Bennet-Clark [118].

The insects can also control their take-off velocity via careful control of three factors; speed, azimuth and elevation angle.

Azimuth is controlled by the position of the forelegs relative to the body before taking off, and rolling and yawing of the body, controlled by the forelegs and mesothoraic leg [122]. This indicates that proprioceptors and motor neurons play a key role. Similarly a locust controls its speed at take off by adjusting the tension in the extensor tibiae muscles [123].

The elevation is controlled independently from the azimuth and the speed, it is dictated by the orientation of the hind legs relative to the body and the angle set by rotation around the coxae before the tibia extend [124]. Thus with sufficient visual information, locusts are able to perform very precise jumps towards specific targets.

Synchronicity between the action of the two jumping legs is not essential for jumping but it does lead to a better conversion of stored potential energy. Locusts with only one leg are still capable of jumping, albeit half as far [118]. However this only considers locusts that have just lost a leg, perhaps over time they would adapt and be capable of performing jumps comparable to their intact peers. Additionally though normally the legs extend within milliseconds of each other, locusts are regularly observed to have one leg 'slip' or 'miss' the jump. This does not have catastrophic consequences as the angle of elevation is already determined and set before jumping by the position of the hind leg. Sutton and Burrows [124] observed that a locust with an angle of elevation originally set to 40°, that suffers a slip, will then take off with an angle of 36°.

This method of jumping means that the locust tibia is typically loaded under bending conditions and it has adapted to be effective at resisting both buckling and fracture [125].

Bending Moments

Bending moments occur when an object is placed under an external force, causing the object to begin to bend. The size of the moment is dependent upon the distance between the fixed point, or end of the element and the applied force.

$$M = l * F \tag{2.1}$$

where M is the moment (Nm), F is the external force (N) and l is the distance from the fixed point to the applied force (m). Consequently the bending moment increases with distance; this makes sense if one has ever attempted to open a door whilst pushing next to the hinges, instead of at the opposite end of the door.

Bending moments induce both compressive and tensile stress in the material, on opposite sides of the element. These increase proportionally with bending moment, however they also depend on the second moment of area of the cross section of the object in question. The second moment of area is a geometrical property of the object, and takes into account the resistance of different shapes to bending. Failure by bending will occur when the bending moment is sufficient to produce a tensile stress greater than the materials failure strength throughout the entire cross-section.

Other failure modes may still occur before the yield stress is reached, such as buckling, depending on the shape of the element being tested. Cracking and the presence of other defects can also dramatically reduce the failure strength.

Buckling failures

Insect tibia can be considered to be long slender tubes, when considering their slenderness ratio (that is the ratio of the radius of the tube to its length). This sort of beam or column is frequently used in structural engineering because they can provide a high strength to weight ratio, and reduce the amount of resources needed to produce the material. This is an important consideration both in manufacturing and in evolution. As a result slender beams can be seen in a variety of roles in both the natural world, such as insect legs, as studied here, the long tubes comprising bamboo, and the bones found in mammals and in man made industry e.g. aerospace engineering and automobile frames.

Unfortunately, these long thin beams, commonly referred to as columns, are susceptible to buckling failures. Also know as elastic instabilities, buckling failures are very hard to predict and are characteristic of such columns. They are characterised by the sudden sideways failure of a column experiencing compressive stress. As the load increases it will at some point, cause the element to become unstable and it will buckle and fail. What makes buckling failures hard to predict is that buckling failures occur long before the material has reached the ultimate compressive stress that it is capable of withstanding.

Leonard Euler in 1757 showed that there is a critical load that will cause buckling in a slender column. In Euler buckling a column experiencing compressive stress will become unstable with regards to transverse displacements. This critical stress is described as

$$\sigma_b = \frac{EI\pi^2}{AL^2} \tag{2.2}$$

Where σ_b is the stress at failure or Euler stress, E is the Young's modulus, I is the second moment of area, A is the area, and L is the effective length. This form of the equation applies where both ends are free to rotate. However for insect tibia the predominant

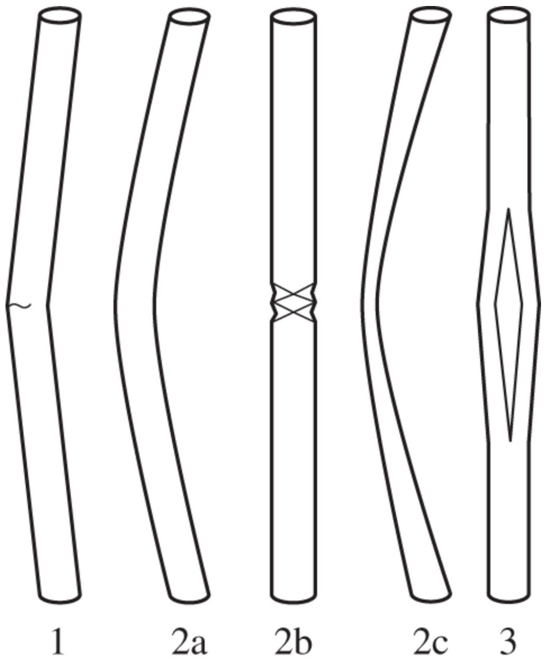

Figure 2.22: Diagram depicting the failure modes of slender tubes; 1 depicts fracture, 2a Euler buckling, 2b local buckling, 2c ovalisation and 3 depicts splitting[126].

methods of buckling are local and elastic buckling [4].

Local buckling is common in thin plates experiencing compressive stress, where local buckling can occur resulting in out of plane displacements called kinks. Whilst similar to Euler buckling, it does not depend on the length of the tube, rather upon the thickness to radius ratio. Timoshenko [127] described it as

$$\sigma_{lb} = \frac{E}{\sqrt{3(1-v^2)}}\frac{t}{r} \tag{2.3}$$

where σ_{lb} is the stress causing local buckling, E is the Young's modulus, v is Poissons ratio, t is the thickness, and r is the radius. However this formula tends to over predict the stress by 40-60% [126].

Alternatively the legs may fail due to ovalisation. Ovalisation was first discussed by L.G. [128], and it predicts how a perfectly circular tube under tensile and compressive stress will begin to flatten into an ellipse.

$$M = CEI \tag{2.4}$$

where M is the moment of the force, C is the curvature, E is the Young's Modulus and I is the second moment of area of the cross section. As E and I are properties of the material and shape one would expect them to be constant. However as the material deforms and curvature increases, I will no longer be constant, in fact it will begin to decrease as ovalisation increases. As such some critical moment will be reached whereupon the material will suddenly buckle and fail [129]. The critical value of this bending moment that will cause elastic instability is described as

$$M_{ob} = \frac{0.987rt^2E}{\sqrt{1-v^2}} \tag{2.5}$$

where M_{ob} is the critical value of the bending moment, E is the Young's modulus, v is Poissons ratio, t is the thickness, and r is the radius. However when a beam is loaded in bending one side is also experiencing compressive stress. As a result it is at risk for local buckling, which is predicted to occur at a slightly lower critical bending moment [126].

There is also always the possibility of different failure modes competing, especially if the failure loads are similar for two or more mechanisms, particularly when discussing Euler buckling and yielding. Taylor and Dirks [126] completed an analysis of this process for insect tibia, describing the total failure force (F_t) as

$$F_t = \frac{1}{\frac{1}{F_b} + \frac{1}{F_f}} \tag{2.6}$$

Where F_b is the failure force for buckling and F_f is the failure force for fracture [126]. This allows for the fact that at the yielding-buckling transition the load bearing capacity is reduced, being lower than either of the two forces separately. This is because as the stress approaches the fracture stress, nonlinear deformation processes begin to occur in the cuticle e.g. microdamage reducing the stiffness of the cuticle, and thus beginning to favour the buckling failure mechanism. However both of these mechanisms are dependent upon the ratio between the thickness of the tube and the radius of the tube, with different ratios precipitating different failure mechanisms. What Taylor and Dirks [126] found is that the locust tibia has a ratio of approximately 11, with the ideal ratio for bending being 7.2, and the optimum for axial loading being 29: locust tibia are thus optimised to resist bending forces. These results can be seen in Figure 2.23. They also found that the shape of the tibia is also optimised to resist ovalisation, as the tibia is not quite circular, more typically slightly elliptical, with the long axis in the direction of loading, so that when loaded ovalisation actually begins to make the tibia more circular. As the tibia are typically loaded in bending, and optimised to resist it, bending forces have been chosen throughout this work as the logical mechanism of loading.

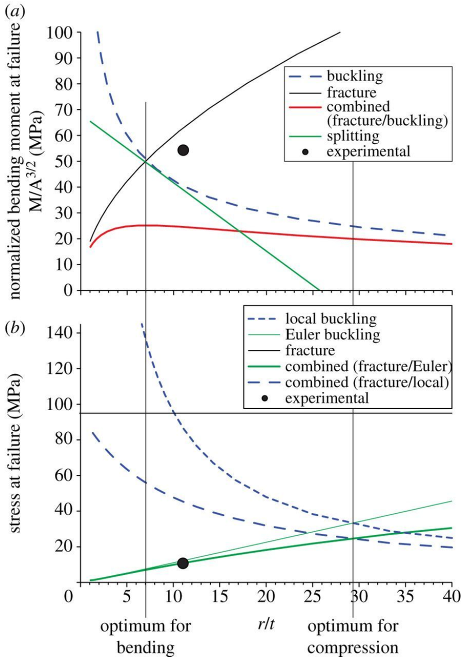

Figure 2.23: Prediction and experimental results for the locust tibia loaded in bending and axial compression respectively. The vertical lines indicate the optimum r to t ratio for axial compression and bending. It can be seen that the tibia lies much closer to the bending prediction. Taken from [126].

Brittle Fracture

The fracture toughness of the cuticle can be described as

$$K_c = F_b l_b Q \frac{r}{I} \sqrt{\pi a} \tag{2.7}$$

Here K_c is the fracture toughness, F_b is the maximum force before failure, l_b is the bending distance between the notch and the applied load. r, I are as before, and the crack length is $2a$. Q is a constant that depends on the type of loading and also upon the geometry of the sample and the notch. Approximating our sample as a hollow cylinder of constant radius and thickness [125], values of Q are attainable [130].

Studies carried out by Dirks and D.Taylor [65] reported a fracture toughness for the cuticle of the tibia of $4.12 \pm 0.4\ MPam^{\frac{1}{2}}$. This is comparable to other biological composites such as bone or wood or nacre, but is all the more impressive as cuticle lacks the mineral phase that reinforces the others. This also indicates that similar to bone, the cuticle in the locust tibia is ideally evolved to resist high impact loads without fracturing.

They also examined the effect of water content on insect cuticle and found that when the cuticle was allowed to dry out the stiffness and failure strength increased rapidly, but conversely the fracture toughness dropped substantially. For fresh cuticle the tibia could withstand a cut of 0.9 mm before the bending stress was affected, whereas desiccated cuticle could only withstand a cut of 0.06 mm, an order of magnitude smaller. This gives an insight into the trade-off occurring in the insect tibia, as increasing strength brings reduced fracture toughness, requiring the insects to optimise the combination of mechanical properties.

2.6.2 Limpets

In stark contrast to insects, the animals in the phylum *Mollusca* and of the *Gastropod* class are not what are typically thought of as fast moving creatures; snails, slugs, and limpets etc. are not renowned for their speedy getaways. Rather they have survived by developing a protective shell. They feed by walking around their local area, rasping algae off of rocks-this ability for movement is indicative of a true limpet. Consequently the loading experienced by a limpet shell, unsurprisingly, is very different to that examined in the previous sections. The literature contains many investigations and studies into the mechanical properties of the shells of limpets and other molluscs [91, 131], measuring properties such as tensile strength, toughness and Youngs Modulus. However most of these studies involved quasistatic tests upon the shells, or samples cut from them, gradually applying an increasing load or deformation. Currey and Taylor [132] for example machined dog bone samples out of shells and placed them in an Instron machine before applying a tensile load, with the test typically taking 5 seconds. Cabral and Jorge [91]) carried out similar tests, placing shells on a flat surface before applying a load at a rate of 2 mm/min.

The problem with these tests is that as they take place over a comparatively longer time scale they allow for the equal distribution of stresses and strains throughout the overall shell structure. In contrast impact tests are much more rapid involving a sudden localised force. As a result, the distribution of stresses throughout the shell could be very different to those experienced in a quasistatic test. Additionally an impact test would seem to be the more appropriate test for limpet shells as this is the sort of damage that would seem to be more likely due to debris in the waves. This has been verified by Shanks and Wright [133] who found that the mortality rate of shells in areas with lots of small pebbles and stones was close to half, whereas in more sheltered areas less than 10% of the animals perished during the study. This is in keeping with work carried out by Taylor [93]. They found that when loading shells both quasistatically and under impact loading, that the former produced a very large amount of scatter and the shells typically failed at much lower energies (often 20 times lower) than those observed by other researchers. In contrast, the shells impacted instead failed at energies comparable to those observed by other works such as Shanks and Wright [133]. The reason for this variation - as typically samples loading quasistatically tend to perform better than those experiencing impacts - can be explained due to the shape of the shell. Impacting an object produces a shock wave, that travels down through the sample, with the impact concentrating the stress at the impact site. However in this case it seems that the conical shape of the shell acts to prevent failure at any site except the apex [93], and as such may be acting in a similar fashion to the crumple zone in a car, though further study is required to confirm this.

Impact loading

The response of ceramics to shock loading conditions has been a subject of great interest for many years - compared to metals they have low densities, and much higher compressive strength. They are also much lighter with higher melting temperatures making them appealing for military and aeronautical applications. However they have an important limitation; they are generally very brittle and as such are prone to failing seemingly spontaneously when overloaded. There is little to no development of plastic deformation before failure of the component. As such their response to the sudden, rapid, high forces that occur during impacts- e.g. a bird striking more modern ceramic composite airplane blades- is of great concern to ensure that the blade is both strong and tough enough to withstand the blow.

This brittleness is linked to the fracture toughness of most ceramics; that is their ability to resist the growth of cracks. Ceramics are typically very brittle due to their inability to deform plastically, they have no means to absorb any energy from external forces and deflect crack growth which leads to failure. This is where nature is of interest, as many traditionally poor building materials such as calcium carbonate are utilised much more effectively in nature, where microstructures lend additional strength preventing catastrophic failure. This is seen in the microstructure of bone where the presence of osteons act as crack-stops, reducing the stress-instensity at the crack tip and thus deflecting its growth [134].

The fracture toughness of the shells is then an important factor to consider. Like most composites the main failure mode observed is the formation of delamination cracks, the running of smooth cracks along the edges where layers meet [135]. If this layer separation is extensive enough it will lead to the loss of material from the shell, a process known as spalling, though other failure modes such as crack propagation from the rim do occur occasionally. However measuring fracture toughness on biological materials can be quite difficult as there are two properties often conflated when reporting the toughness of the material. The first is the area under the stress-strain curve, quantifying the amount of energy required to increase the crack area by a given amount [134]. This is the crack propagation energy, G_C defined as

$$G_c = \frac{E}{\delta A} \tag{2.8}$$

Where E is the applied energy and δA is the increase in the area of the cracks. This energy can be influenced by a variety of toughening mechanisms such as viscoelastic behaviour and plastic deformation. The second toughness parameter is the fracture toughness K_C describing the ability of a material to resist the propagation of pre-existing cracks, defined as

$$K_c = \sqrt{G_c * E} \tag{2.9}$$

Where G_C is the crack propagation energy as defined in Equation 2.8, and E is the Young's Modulus of the limpet shells, obtained from Currey (1976) [136].

After an impact, energy is very rapidly transferred to the shell, which will undergo elastic deformations, before partially rebounding the weight. The remainder of the non-elastic energy will appear as damage inside the shell. As the shell is nearly pure ceramic, plastic damage and viscous flow can be assumed to be negligible. This leads to the formation of numerous delamination cracks, some of which can be extensive enough to cause part of the layer to become separated from the shell (a process known as spalling, see Section 2.6.2), or for failure to occur.

This is also of concern due to the poor impact fatigue behaviour of the shells. Taylor [93] found that the shells perform very poorly when subjected to repeated impacts, typically failing when the accumulated energy reached the critical energy [93]. This is very unusual even for ceramic composites. Even before failure occurred, loss of material due to spalling was observed, indicating that the energy threshold for delamination damage is much lower than that for total failure, which explains the poor impact fatigue behaviour, and indicates that the limpets rely on only having to withstand a single blow, rather than multiple blows.

Spalling

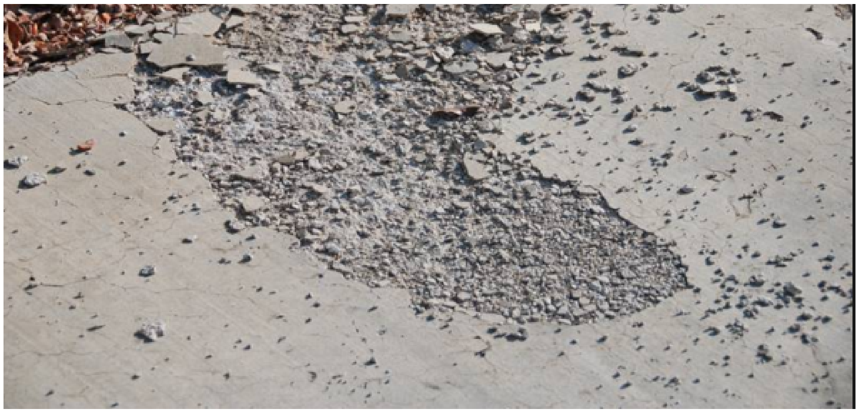

Figure 2.24: Spalling concrete: the loss of smaller amounts of materials from the surface is evident [137].

Spalling is a process that occurs whereupon a material fractures and appears to flake with smaller chips of material separating from the main body [138]. It typically occurs at high stress contact points, though mechanical weathering and high temperatures can also cause it. It is very common in building materials such as concrete [139]. It is the most common cause of failure observed in *P. vulgata* [93] due to extensive delamination cracking.

2.7 Summary & Conclusions

Despite the population of non-mammalians being greater than that of mammalian counterparts, non-mammalian mechanical behaviour of tissues is remarkably unexplored. This is despite the large leaps in biomimetics, often mimicking such animals, and despite the fact that as we struggle to develop man-made materials that can self heal we face battles due to a lack of cells. Yet many organisms from other phyla are able to repair acellular tissue, unlike mammals. This thesis attempts to explore this area of repair in non-mammalian organisms.

2.8 Objectives

Initially this thesis sought to build upon the work of previous researchers at the TCD biomechanics research group, particularly that by Parle [140]. Dr. Parle's research had investigated how mechanical properties change with age in arthropods, along with investigating their ability to restore mechanical strength to any injured limbs. This thesis combines these two, looking at insects of a much greater age to observe the previous tends in greater depth, but also examining the different response to injuries across insects of different ages, to establish if, similar to mammals, there are age related declines in repair abilities. This study also sought to answer another question raised by Dr. Parles work. Having observed that up to half of the insects were unable to repair injuries, it was speculated that the reason for this was due to displacement of the cuticular layers. This is examined in this thesis by examining another style of injury, one that guarantees displacement of the layers to examine the impact this has upon the repair rate.

This fed into the next study discussed in this thesis, aiming to establish if the insects were capable of detecting microscopic cracks in their cuticle, and if so are they capable of repairing them? This also has an additional consideration in insect cuticle as many insects that perform rapid movements do so by deforming their hard cuticle to store energy.

The final chapter on locusts in this thesis, Chapter 6, is a series of smaller studies that compliment the previous studies, and serve to answer some of the questions they raise, that were however, not large enough to comprise their own chapter. All of them relate to Chapter 4, seeking to provide an answer as to why there are changes in the mechanical properties of the cuticle as the insect ages, past simply labelling it an effect of old age. Consequently this chapter describes several different approaches to this problem, ultimately aiming to explain the ageing process observed in older insects, as well as attempting to elucidate the trigger for such a change.

Thereafter the work of this thesis, with the aid of several visiting students turned to the second model, the limpet, as described in Section 2.5. This study seeks to elucidate more information about the fracture toughness of limpet shells, and how they have evolved to withstand impacts. It is a natural follow on from the work done by Taylor [93], as having found that spalling is the most common mechanism for failure in the shells, and evidence of micro- and nano-scale roughness, knowing the work of fracture for these delamination phenomena would serve as valuable addition to the field.

This work outlined in Chapter 7 fed naturally into the work described in Chapter 8, which examines the ability of limpets to repair damage to their shell, building the bridge between the two halves of this thesis to make repair the focus. The ability of limpets to successfully repair significant damage is evaluated, along with their ability to detect and repair more subtle damage, that does not pierce the shell, similar to microcracks and other damage observed in human bone. This chapter also discusses investigations into the ability of the shells to actively remodel repeated loads, separated by various time periods. It had been previously observed by Taylor [93] that the shells display poor fatigue properties with damage accumulating in an approximately linear fashion. Consequently if shells are given small periods of time to repair, are they able to remodel their shell? Is there some maximum rate they can achieve, which if the rate of damage exceeds, they similar to the military cadets described by Kaufman et al. [27], will the shells fail? This chapter aims to understand whether or not limpets are able to detect and repair damage to their shells, and if so, how?

The final two chapters in this thesis, Chapter 9 and Chapter 10, outline the overall conclusions of the thesis, with the latter discussing future potential studies, and areas of this work with scope for further expansion.

Chapter 3

Materials & Methods

3.1 Insect Cuticle

Female desert locusts (*Schistocerca Gregaria*) were acquired as fifth instar nymphs (Blades Biological Kent England and later Monkfield Nutrition Ltd. Ely, England).

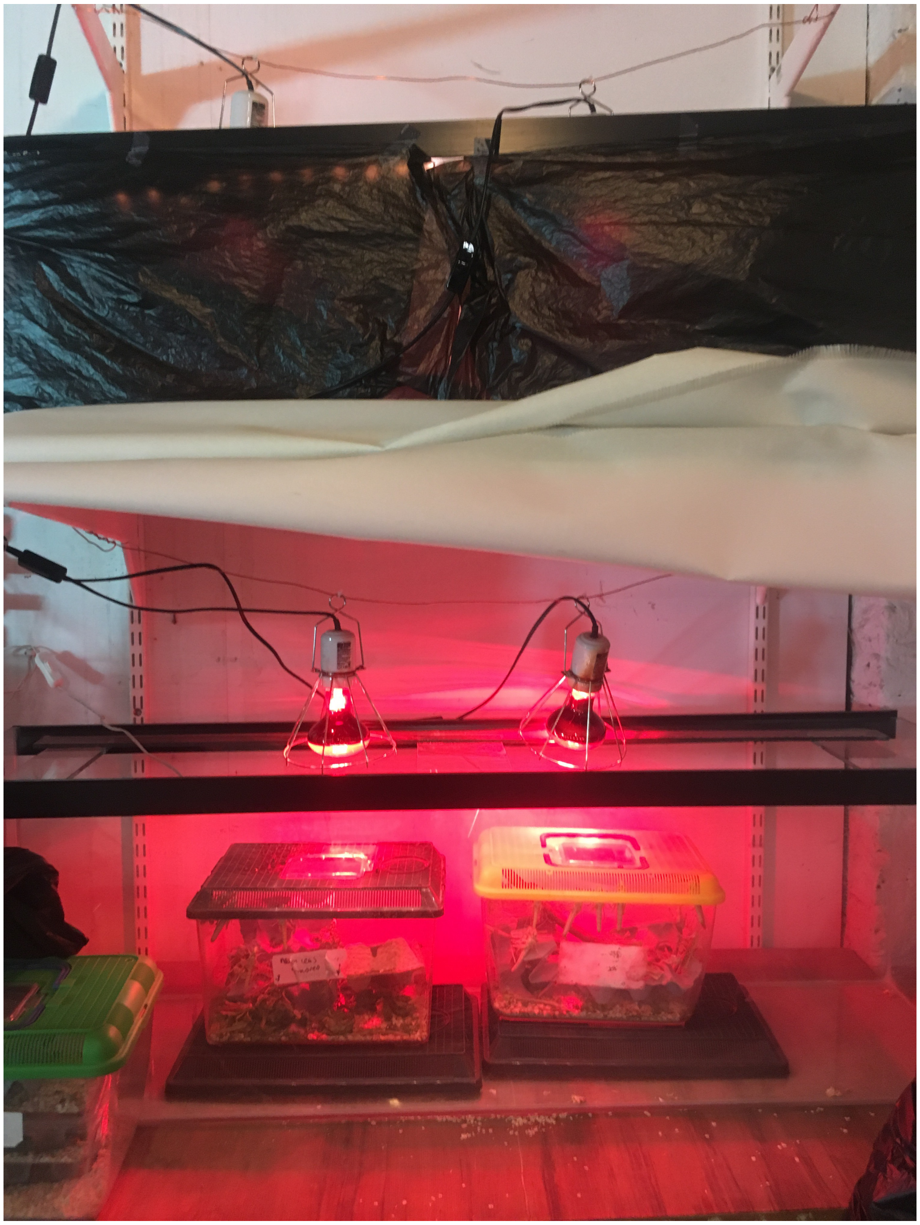

Figure 3.1: Image of the zoology setup; it spans two shelves. The glass tank is typically covered with black plastic to keep put light; this has been removed in the lower shelf so the tanks can be seen. Red heat lamps maintain the temperature, and white LEDs (not visible) give light.

All animals were housed in the Zoology Department at Trinity College Dublin, in large, ventilated tanks, under infrared heat lamps, with dried oats as bedding, as visible in Figure 3.1. They were raised with a 12:12 hour day:night cycle, created using white LED lights. The daytime temperature was 32-35°C, and the night time temperature 20-22°C. Temperatures were constantly monitored with digital thermometers. The animals were checked daily, and as they moulted, the adults were separated from the remaining nymphs into different tanks based on the date of moult.

Insects were fed ad libitum with fresh curly kale everyday or york cabbage during periods where weather conditions made kale difficult to obtain. Any faeces and/or corpses were removed daily. Tanks were cleaned twice a week.

3.1.1 Mechanical testing

Previous testing on insect cuticle have used nanoidentation techniques [141, 142], however there are several limitations to this technique. Firstly sample preparation for nanoindentation is quite time dependent and the mechanical properties of insect cuticle have been found to be very strongly affected by water content, with cuticle dehydrating very rapidly after excision [65]. Secondly, as outlined in Section 2.6.1, bending is the primary loading mode observed in jumping insects, and as such bending tests are a more appropriate test, as well as mitigating the dehydration effect once they are performed in a timely manner.

Animals were sedated by chilling them. Legs were then removed from the adult animals just below the tibia-femoral joint. Immediately after removal, legs were set into a well of 1:1 quick drying polymer cement (Howmedica Surgical Simplex P Bone Cement). The cement was placed inside custom made wells for the purposes of these tests, one can be seen in Figure 3.2a. The use of well of cement also allowed the effects of the buckling region [24], near the knee to be eliminated. This region is designed to absorb energy when an animal slips or 'misses' a kick or a jump. This is important, as the leg goes from accelerating the entire body to the comparably lighter leg and tarsus [24], causing the angular velocity to rapidly increase. The buckling region, as proposed by Heitler [143], dissipates this excess energy, preventing damage to the tibia. By eliminating this region in testing we prevent any effect this energy disspiation may have upon the results.

Cantilever bending tests were performed by applying a position controlled load to failure. This was done using a specially designed rig (see Figure 3.2a), made on site in the department of Mechanical Engineering's workshop. The positioning of the pointer was marked with a black marker in order to identify the point. Displacement was increased at a given rate using a ZWICK machine (Zwick/Roell Z005, Ulm, Germany) with a 5N load cell.

Failure was characterised by a sudden drop in the load. The distance between the applied force and the cement fixident was recorded with an electronic callipers for accuracy. Samples were then stored in 3.7% formaldehyde fixative for 24 hours before being transferred to 70% Ethanol for further storage.

Samples were prepared for SEM by mounting them in conducting carbon cement, before sputter coating them using an Au:Pd target and a Cressington 1080 sputter coater. The SEM images (taken using a Zeiss Ultra Plus SEM 5kV; Oberkochen, Germany) allowed us to record the dimensions of the tibia, which can be used to calculate nominal stresses and strains. Following previous models [4, 65] the tibia were assumed to be hollow cylindrical tubes, with a circular cross section. This allowed us to calculate the nominal stress (σ) and nominal strain (ϵ) using the following standard equations.

$$\sigma = \frac{FLR}{I} \tag{3.1}$$

$$\epsilon = \frac{3dR}{L^2} \tag{3.2}$$

$$I = \frac{(R^4 - (R-t)^4)}{4\pi} \tag{3.3}$$

Where F is the force, L is the distance from the applied load to the fixed end of the sample, R is the radius of the hind tibia, and I is the second moment of area of the sample. t is the thickness of the sample and d is the displacement of the sample. Using these nominal stress-strain curves can be plotted. The calculated stresses and strains are referred to as nominal values because there is some error involved in assuming that the tibia is a perfect circular tube. Previous work found this to be a useful approach to allow for differences in the size of the tibia from one individual to another and thus reduce overall scatter in the data.

Youngs Modulus of each sample was found by taking the slope of the initial part of the curve where the material still acts like a Hookean material with a linear slope. Failure strength is defined as the highest force experienced before failure. An example of such a plot can be seen in Figure 3.2b.

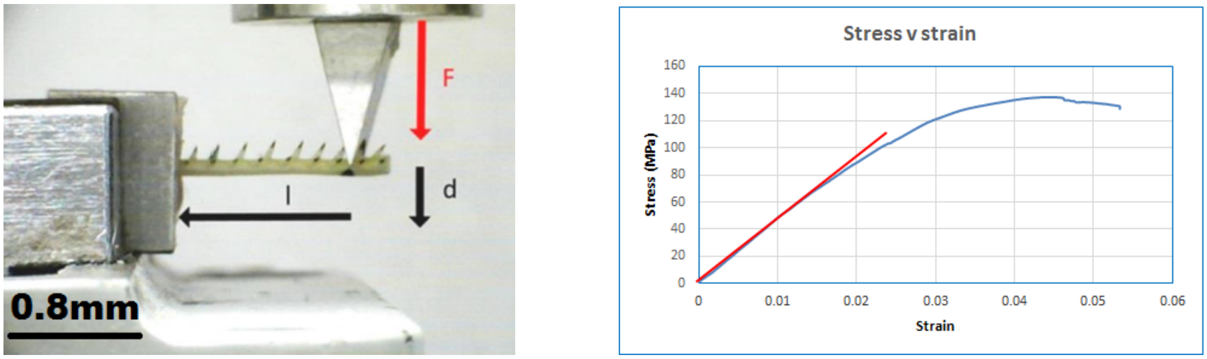

(a) (b)

Figure 3.2: (a) depicts the set up for the mechanical testing: the leg is implanted at its proximal end and the positioning of the pointer can be observed. (b) depicts a typical (nominal) stress-strain curve; The red line is a linear fit to the early part of the curve, to obtain Young's modulus

3.2 Limpet Shells

Shells were taken from a rocky outcrop in the intertidal zone. The location of the test site can be seen in Figure 3.3, located in the southern part of Dublin bay (co-ordinates 53°17'18"N; 6°6'42"W). There is a solid rock platform with numerous individual boulders, and relatively little sand or small pebbles. There is little human footfall as it is not attractive for recreational activities, and nearby there is a beach which is much more popular for tourists and water activities.

The animals in each particular study and any relevant controls were taken during the same period, specificed in the specific study. The chosen limpets (*P. Vulgata* [144]) were taken from the inter-tidal zone, where they had spent approximately half their time submerged. The animal was removed from the shell before cleaning the shell and storing it for subsequent testing. Any seaweed or barnacles on the exterior of the shell were removed.

Any shells taken as "beach" shells or as naturally abraded were taken from Sandycove beach. This is a sheltered sandy beach, and can also be observed in Figure 3.3. These shells were collected and cleaned before storage as above.

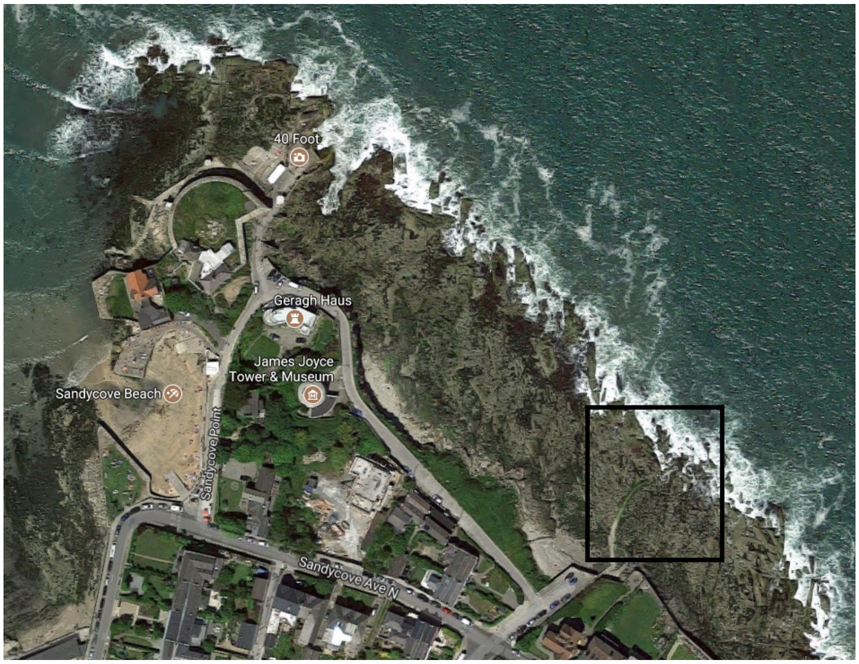

Figure 3.3: Aerial map of the test site, taken from Google maps. The test area is marked with a black square.

3.2.1 Impact Testing

In a previous study Taylor [93] devised a method of impact testing that was also used here. They found that the energy required to cause failure when the shell was impacted on its apex was related to the size of the shell raised to the power of 4.6 [93]. This allows the impact strength to be defined as a normalised energy value independent of shell size.

$$E_n = \frac{E}{L^{4.6}} \tag{3.4}$$

Here E_n is the normalised energy (MJ$m^{-4.6}$), E is the energy to cause failure and L is the length of the shell (defined as the largest diameter at the rim). The explanation for this scaling law with an exponent of 4.6 is unclear and merits further investigation. Shells were measured using a Vernier callipers. The failure energy of the shells was investigated by dropping a weight of 123 g a known height onto each shell using a simple apparatus (see Figure 3.4a) and noting whether failure occurred or not. The notches in the tube were at regular intervals allowing the height to be known. The tube and weight were crafted in the departments workshop.

Failure was defined as the formation of a hole or crack which penetrated through the

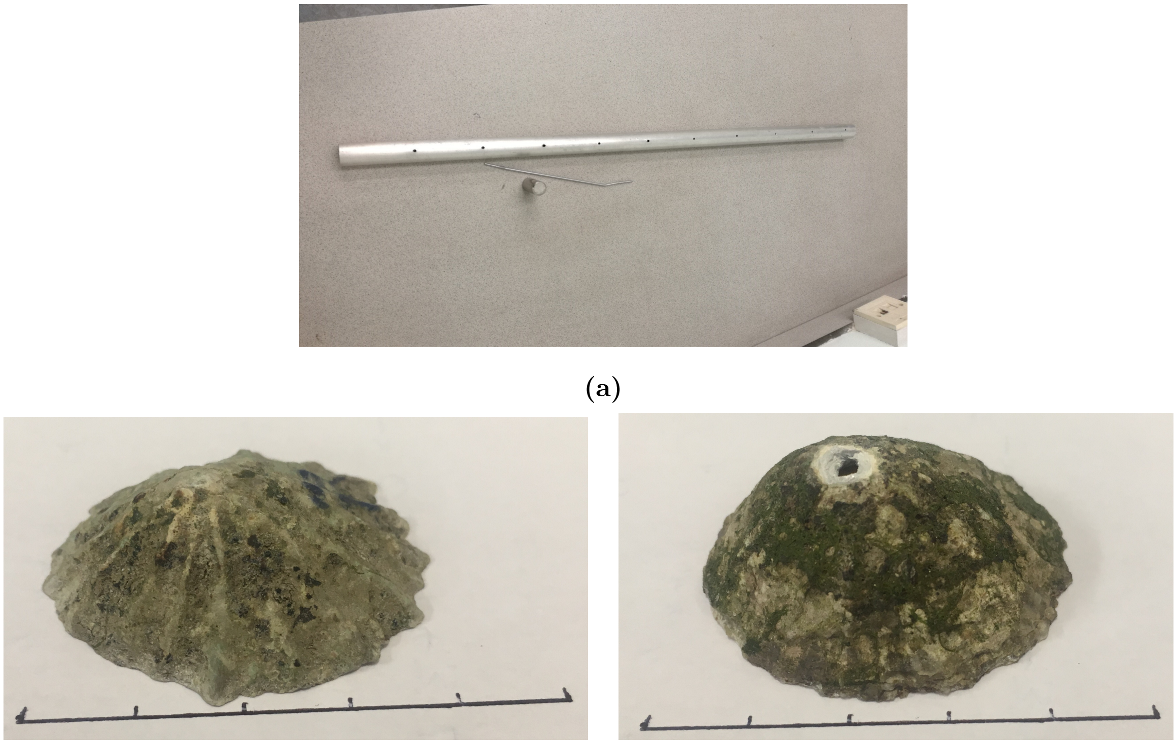

(a)

(b) **(c)**

Figure 3.4: (A) Apparatus used to impact the shells. The weight weighs 123g: the pin and the holes in the tube allow the weight to be dropped from a known height, thus delivering an impact of a known energy. (B) An intact limpet shell. (C) Shell of a limpet after an impact test (17). The failure manifested as the formation of a hole in the apex. For both (B) and (C) the scale bar indicated represents 5 cm, with 1 cm markers.

thickness of the shell. In almost all cases this took the form of a hole in the apex (as illustrated in Figure 3.4c), though occasionally cracks formed at the rim. Shell size varied from 23-48 mm. Typically the impact energy was 0.5 J. It is explicitly stated throughout the relevant chapters if the impact energy differs from this value. Shells were tested on a flat stone surface. A previous study [93] established that impact strength was not affected by removing the shell from its home location, or by removing the animal from the shell. Consequently shells were cleaned, stored and tested away from the site area.

Figure 3.5 shows a typical dataset from testing, some of the shells have failed and the larger ones survived, with a region of overlap. A step function can be defined for a given energy, as in Figure 3.5, indicating a transition from failure to non-failure at some critical

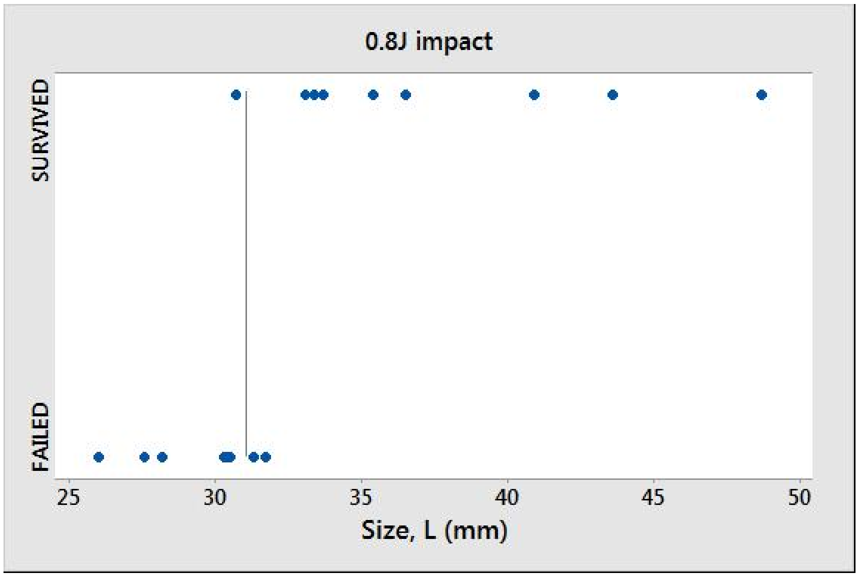

Figure 3.5: Plot of survival or failure of shells as a function of their size for a given energy. A step function can be determined, defining some critical length (indicated here by the line), that minimises the error, allowing a fit of the ideal size to be found.

length, L_{crit}. The error, ϵ_i can be defined as zero if a given point is on the line, and if not as

$$\epsilon_i = L - L_{crit} \tag{3.5}$$

In this way, by minimising the sum of the errors, L_{crit} for a particular dataset can be evaluated and from this the normalised energy for failure, E_n can be calculated, allowing comparison between groups.

A limitation of this method is that it requires a number of shells of similar sizes, all close to the expected critical length. If all of the shells were very large or very small, none or all of the shells would fail, meaning no such function could be plotted.

Shells were prepared for scanning electron microscopy (SEM) by extensive polishing of the samples, using silicon carbide paper (P360) to reduce the size of the sample, leaving only the point of interest (typically the apex intact). This was to reduce the time necessary for the vacuum to be reached in the sputtering and imaging equipment, as well as due to size constraints as to what can fit inside the equipment. Shells were coated using the same procedure as for the locust studies. The same sputtering and SEM equipment was used in both cases.

3.3 Statistical Analysis

All statistical analysis was carried out either in Excel (2013) or Minitab (2017). Data was first checked for normality using either Anderson-Darling normality test or Ryan-Joiner test where rounding could influence the result. All data is normal unless otherwise stated. In the event that data was not normal comparisons were made using either the Wilcoxon signed rank test or Mann-Whitney test depending upon the relationship between the data sets. Two data sets were compared to each other using either paired or unpaired t-tests depending on the nature of the data. The type chosen is stated in each case.

In the event of multiple comparisons either Bonferroni intervals or Scheffes test (when group sizes were unequal) were used to preserve the integrity of the test. ANOVA (analysis of variance) was used to find differences between groups. In the event of at least one group being different to the others, either Bonferroni intervals or Scehffes test were utilised to identify the relevant data points. All tests were performed at a 95% confidence interval unless otherwise stated. All values shown are means ± one standard deviation (s.d.) unless otherwise stated. Box and whisker plots show standard quartiles unless otherwise stated.

Chapter 4

Age Related Responses to Injury and Repair

4.1 Introduction

4.1.1 Ageing Effects

Recently there has been a growing interest in cuticle, to obtain better understanding of the biomechanics of insects and other arthropods. However, most previous studies only examined cuticle in the first few days of adult life [45, 145, 146]. The natural lifespan of insects is highly species-dependant and that of locusts is estimated to be 4-5 months from eclosion for females [147]. Considering the well-known changes in properties observed in mammalian tissue, such as bone, which suffers a decrease in impact strength and toughness with age [148], it is reasonable to consider whether cuticle experiences changes in its mechanical properties over the course of the insect's life. However there have been very few studies investigating this question.

Up until 2018 there has only been one study systematically examining the changes in mechanical properties in older insects, carried out by Parle and Taylor [76]. They found that the mechanical properties of the cuticle varies as the insect ages. They discovered that Young's modulus and ultimate tensile strength (UTS) for older insects is much greater than that for younger insects, though the mechanism governing these changes remains unidentified. This corresponds with Dr. Parles other work, having also published a paper showing that the desert locusts are not only able to close wounds to prevent infection, which was previously known [70, 149, 150], but that they are also able to restore mechanical properties [4]. This is an important factor in the insects life; The locusts' hind leg is crucial to their social interactions and survival in the wild. In captivity the insects can survive for extended periods of time without either of their hind legs, however they are essential for survival in the wild. The large leaps locusts produce are their escape mechanism from predators, along with their means to launch themselves into flight, so an insect suffering an injury that reduces the UTS of their limbs may not last very long. There are two ways an insect can approach this problem: They can be over designed and capable of sustaining damage whilst still being able to function successfully. Muijres and et al. [52] found that fruit flies *Drosophila* with damage to their wing can fly successfully, even when missing half their wing, but no repair process occurs. Alternatively insects can repair the injury, as observed in Parle et al. [4]. Scalpel cuts were found to have been repaired by targeted deposition, creating an internal patch - this mechanism is distinctly different from that used to repair mammalian bones [18]. But this study only examined insects at a single age and consequently any link between age and repair capabilities, such as that observed in mammals remains to be explored.

4.1.2 Injury Type

Most animals evolve to resist predation by a particular species, or similar species [151]. As a result it is probable that locusts have primarily evolved, to the extent to which it is possible, to resist predation by birds, their main predator, excluding efforts by humans to reduce their populations. This also fits into something observed by Parle et al. [4], that only some of the insects repaired their injuries, the others depositing no fresh cuticle. It was speculated that this was because the action of the injury displaced cuticular layers, preventing epidermal cells from migrating to cover the wound, meaning repair can not occur [67, 152]. Consequently it was decided to investigate different types of injury, attempting to more closely mimic the sort of injuries that would occur naturally.

Additionally there is also the role injury shape may play in the impact of the injury upon UTS. Insect cuticle is a reasonably tough material, with a value of 4.12 $MPam^{\frac{1}{2}}$ previously reported [65]. However many mammalian tissues become increasingly stiff and less compliant with age [148, 153]. And a similar age-related change has been reported in insect cuticle [76], with cuticle getting stiffer as the insects age. As stiffness and toughness tend to be mutually exclusive properties, it is quite possible that this is being accompanied by decreases in the toughness of the cuticle. Consequently if the cuticle is becoming stiffer and less compliant, any injury with a more jagged shape could create stress concentrations at the edge of the injuries, leading to failure at lower forces. The vulnerability of cuticle to crack growth from an injury, and how this may change with age, can be evaluated by investigating its fracture toughness.

Fracture toughness is a parameter which measures how easily a crack grows in a material and thus its susceptibility to brittle fracture, or more simply its defect tolerance. The fracture toughness of the insect cuticle was evaluated in the same manner as outlined in Section 2.6.1, using equation 2.7.

This approach would be expected to give an accurate estimate of K_c for the samples with scalpel cuts, and a reasonable indication for those containing punctures. After repair the value obtained for K_c will not be a true measure of the toughness of the material, but provides an indication of how effective the repair has been.

4.2 Materials & methods

4.2.1 Ageing Effects

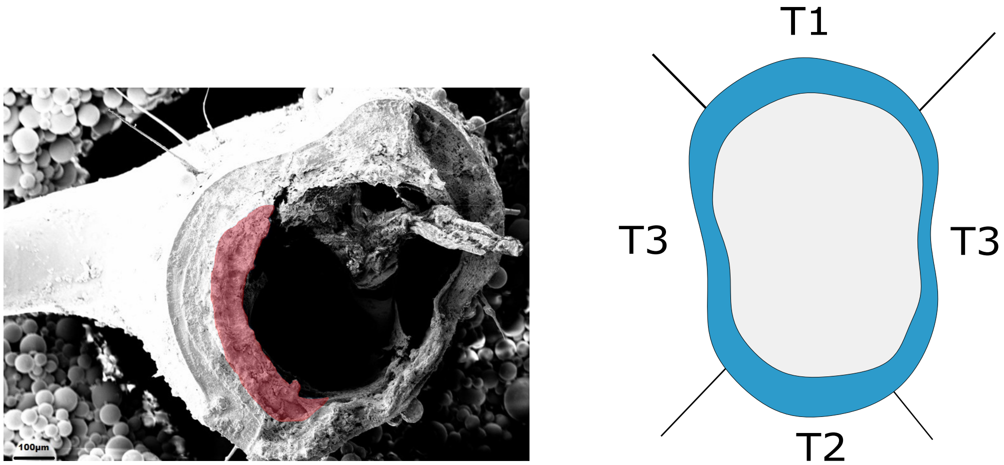

(a) (b)

Figure 4.1: (a) is a repaired scalpel injury taken from a sample injured at 12 weeks and allowed to repair for 3 further weeks. The red colouring indicates the fresh cuticle laid down underneath the scalpel injury, evident as a fracture surface, whereas the scalpel injury can be seen as a smoother surface. (b) is a schematic of an insects hind tibia. *T1*, *T2* and *T3* indicate the dorsal, ventral and the medial/lateral sides respectively where cuticle thickness was measured.

Subjects were tested at different ages (i.e. different times since the final moult): subjects will be referred to as either young or old depending on whether they were tested before or after 3 weeks of age, because previous work showed important changes in cuticle at this time point, due to the sclerotization that occurs post-moult in adult locusts [76].

Two different injuries were examined in this investigation, both on the dorsal side of the hind tibia. The first type of injury was a transverse cut made with a scalpel blade (see Figure 4.1a). Insects were injured at either 1 week or 12 weeks of age, and then left to recover for a subsequent 3 weeks. The injury was made by drawing a scalpel blade across the dorsal side of the hind tibia of a sedated animal. A specially designed cutting rig [4], was used to ensure the cut was always of the same size (average length L being 675 μm, $\approx 23\%$ of the total circumference) such injuries were regarded as severe but not serious enough for the animal to lose the limb immediately. This injury is the same as that made by Parle et al. [4], and will allow for comparison between insects of different ages here, as well as back to those in the original study.

4.2.2 Injury Type

The second type of injury investigated was a puncture style injury. We made these using acupuncture needles, chosen for their ease of availability and because they are provided pre-sterilised. Stainless steel acupuncture needles of three sizes were acquired, 0.3 mm and 0.22 mm diameter (TCM Supply Dublin, Ireland) and 0.12 mm diameter (The Acupuncture Supply Co). Injuries were made by pushing the needle into the dorsal side of the hind tibia, between spines, ensuring not to pierce the ventral side of the hind tibia. A depiction of the procedure and a repaired needle injury can be seen in Figure 4.2a and 4.2b below. These were performed in the same rig as used for the scalpel injuries ensuring that the location of the injuries were consistent, approximately 5mm from the tibio-femoral joint.

After injury some subjects were tested immediately to measure the effect of the cut or puncture on mechanical properties. Other subjects were kept alive to allow time for repair. These insects were kept in individual tubs of size 20x10x10 cm. This was the best compromise to prevent fighting amongst individuals that could lead to loss of the limb, yet still allowing full mobility and movement. They were raised in the same conditions as above for the desired length of time. Control animals were raised together in larger tanks.

All individual tubs were kept stacked and alongside other tubs to ensure the animals could see and smell each other to prevent them turning into the solitarious form. The tubs' locations were rotated frequently to ensure all animals spent most of their time surrounded by others. No animals showed any indications of becoming solitarious, interacting normally with other animals if reintroduced into communal tanks.

The number of insects used in each testing procedure and the time allowed for recovery is outlined in Table 4.1 below.

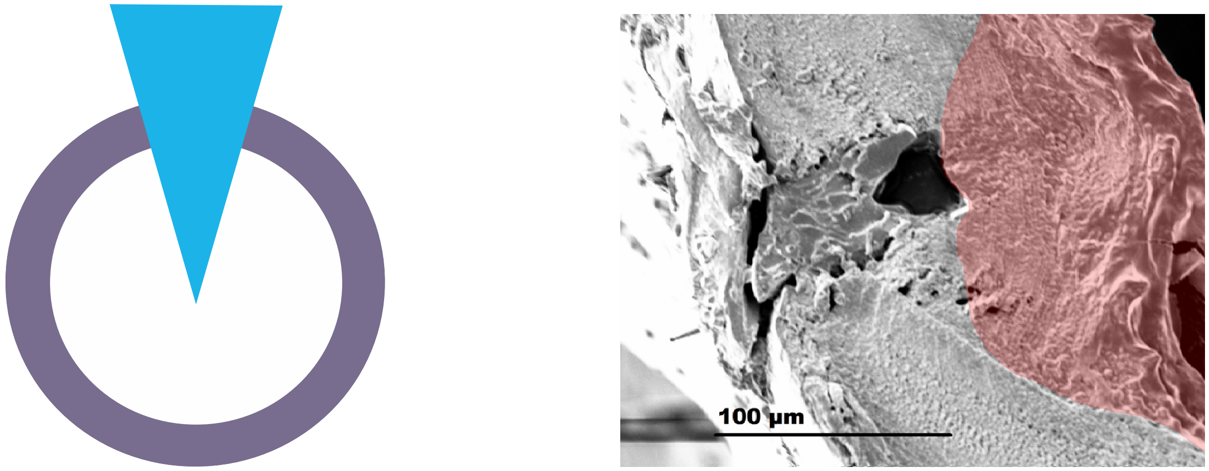

(a) (b)

Figure 4.2: (a) is a schematic of a puncture injury, the cuticle is pierced on the dorsal side without coming into contact with the ventral side. (b) Is a repaired puncture injury, after 2 weeks of repair. The fresh cuticle has been coloured in red.

The injured and intact hind tibia of each insect were tested in immediate succession to allow for paired comparison. To account for the possibility of the intact limb becoming stronger to compensate for the injured one, several age matched controls were tested as well. For insects of all ages no significant difference was found between the intact legs of injured insects and samples taken from the control insects, so they have been treated as a single group in the analysis.

Samples were mounted for scanning electron microscopy (SEM) and analysed in the same way as outlined in Chapter 3, in order to obtain the dimensions of the tibia, for both injured and intact samples. Nominal stress and strain can be calculated as before using Equation 3.1 and Equation 3.2. Young's modulus can be evaluated by taking the initial slope of the stress-strain curve, as outlined in Chapter 3.

For the uninjured control samples, the value of Young's Modulus gives an indication of the average value for the cuticle. When an injury is present this parameter will tend to be reduced due to the increased flexibility of the sample, and is no longer a true estimate of the materials modulus, however it is presented in the results here to give a sense of the changing stiffness of the leg as a whole, and how the ability to restore mechanical properties may vary with age.

Timeline		
Scalpel Injuries	Young (1w)	Old (12w)
3 weeks repair	35	23
Age matched controls	10	6
Puncture Injury initial test	Young (2w)	Old (8w)
Large (0.3mm diameter)	10	12
Medium (0.22mm diameter)	-	3
Small (0.12mm diameter)	-	4
Puncture Injury Repair	Young (2w)	Old (8w)
Large (0.3mm diameter) 2 weeks	-	4
Large (0.3mm diameter) 3 weeks	-	15
Medium (0.22mm diameter)	-	5
Age matched Controls	-	6

Table 4.1: Numbers refer to the number of insects, not the number of samples tested. Except for controls in each case one hind tibia was injured and the other left intact for comparison purposes. For controls both hind tibia were tested as uninjured samples. ‘w‘ indicates the number of weeks.

4.2.3 Cuticle Deposition

Using the SEM images, we measured the thickness of the cuticle, at three locations. These can be observed in Figure 4.1b, *T1* is the dorsal side, where the injury was made, *T2* is the ventral side and *T3* is an average of the medial and lateral sides. The lateral and medial sides were pooled as they displayed no difference. The aim of these measurements was to investigate whether additional cuticle was deposited during the repair period, and if so whether it was being deposited preferentially near the injury site. Parle et al. [4] found that repair was via targeted deposition of fresh cuticle; younger insects may achieve repair by a different process as they are already in a rapid growth phase after moutling, depositing cuticle much more rapidly than their older peers. Additionally this would inform us if the ability to repair is affected by age; if the mechanisms of repair are different amongst different age groups, as well as insight into whether or not the repair process is fine-tuned to the type of damage that has occurred.

4.3 Results: Scalpel cuts

4.3.1 Ageing Effects

In both groups samples were tested 20-22 days after injury. It was not possible to test all of the samples in one day due to time constraints. Controls were tested at the same time. Both the injured and uninjured leg of the animals were tested in immediate succession to allow for paired comparisons. No difference was found between the uninjured leg and the control samples (i.e. the animal had not been unduly favouring the uninjured leg making it stronger) so these data sets have been pooled when reporting for uninjured cuticle.

4.3.2 Cuticle Deposition

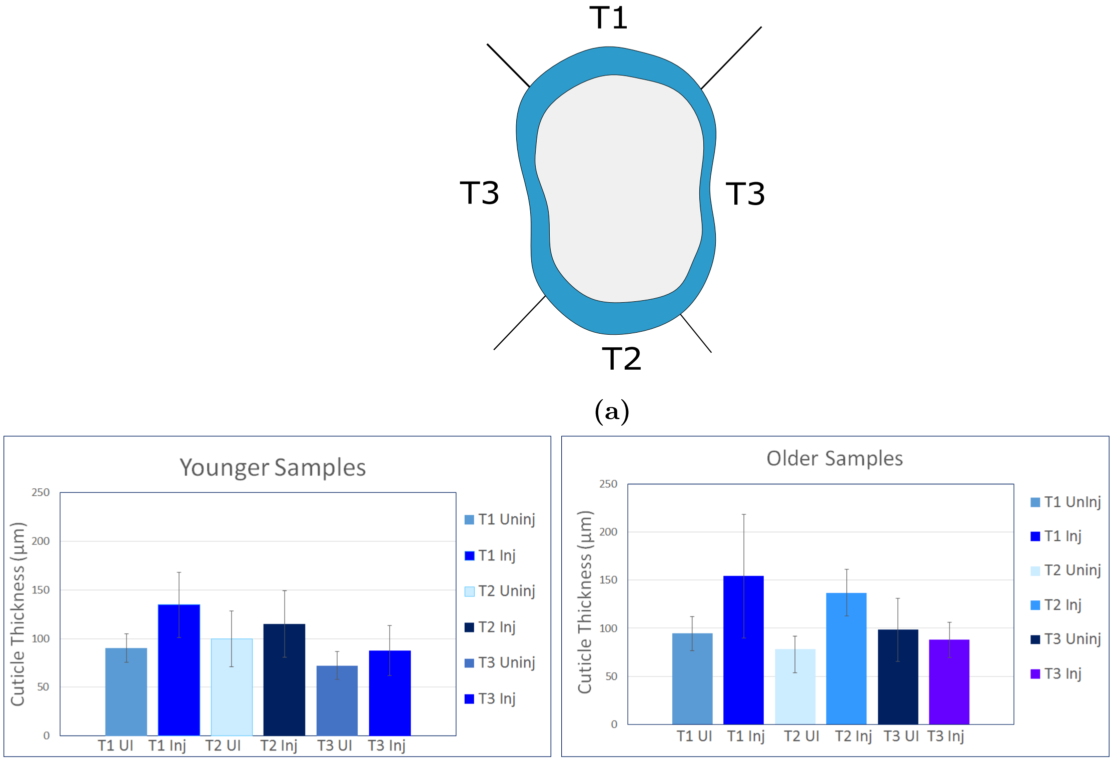

(a)

(b)

(c)

Figure 4.3: (a) depicts the relevant sides of the hind tibia to aid understanding (b) and (c) depict the cuticle thickness after 3 weeks of repair for young and older insects respectively, along with their control counterparts. *T1*, *T2* and *T3* carry the same meaning as before.

The deposition of fresh cuticle around an injury site has been previously identified as the main mechanism of repair in insects [4]. It was sought to see if there was a difference in the repair process between the younger and older insects, particularly as the younger insects are still in their post-ecdysis growth stage and are already rapidly depositing cuticle.

For the young insects ANOVA comparing the control and repaired cuticle groups indicated that the thickness was not the same across both groups ($p<0.05$). This was investigated this further using Bonferroni intervals and paired t-tests which revealed a significant difference in cuticle thickness on the *T1* side between the two groups ($p<0.05$). *T2* was also larger in the repaired group, however this difference was not significant ($p>0.05$). This data is presented in Figure 4.3b.

ANOVA was also carried out in the same way for the older samples, once again indicating a significant difference in the thickness between groups ($p< 0.05$). Paired t-tests revealed a significant increase in the thickness between the *T1* sides in the repaired and control groups ($p<0.05$. We also observed an increase in *T2* between the groups, and here it was significant ($p<0.05$). This data is presented Figure 4.3c. We found no differences in the *T3* side for either group ($p>0.05$)

4.3.3 Mechanical Results

There was a slight decrease in UTS after repair for the young insects, but this was not significant ($p=.11$). The bending moment to failure also indicated that full repair had occurred, with no statistically significant difference between the injured and uninjured groups ($p=.33$). The decrease in Young's modulus was statistically significant ($p=.04$), showing that the limbs were more flexible after repair.

In contrast, the repaired hind tibia of the old insects (those injured at 12 weeks) had significantly lower values of UTS, bending moment to failure and Young's modulus. The UTS for the older insects was on average $\approx 70\%$ of that of controls of the same age. Similar decreases were observed for Young's modulus and bending moment to failure. Paired t-tests showed that the decrease in UTS, Young's modulus and bending moment to failure were all statistically significant ($p<0.05$ for all 3).

Injuries seem to affect older insects more than their younger counterparts [4]. A similar trend was observed for young insects injured with a scalpel 7 days after their final moult;

their UTS of 59.6 MPa is comparable to values in literature for intact cuticle of insects of a similar age. [65].

Scalpel Injury	Young	σ	E	M	Old	σ	E	M
Controls	μ	158.86	5.38	8.85	μ	171.55	3.38	9.28
	s.d.	47.32	2.57	2.38	s.d.	27.08	1.06	1.50
Injured	μ	142.29	3.64	9.55	μ	137.26	2.739	7.82
	s.d.	30.49	2.02	1.99	s.d.	35.62	1.49	2.01

Table 4.2: Results for insects who received scalpel cuts across the dorsal side of the hind tibia at either 1 week (Young) or 12 weeks (Old) and UTS then left to repair for 3 weeks. Values for measured strength, bending moment to failure, and Youngs modulus are compared with uninjured control samples. μ and s.d. refer to the mean and standard deviation respectively, and σ, E and M refer to the UTS (MPa), Young's modulus (GPa) and bending moment (Nmm) of the samples respectively.

4.4 Results: Puncture Injury

4.4.1 Injury Type

This study began by testing the needles upon straws of similar diameter to the insects tibia to confirm that the needles were of a workable size. This also turned out to be very useful practice as at first the puncture holes were rather haphazard and irregular but after some practice it became quite possible to regularly make a perfectly circular puncture hole.

At this stage the next step was to begin trials with the needles on actual cuticle. For this purpose, several tibia samples were obtained. These samples were then repeatedly pierced with needles of varying sizes. The small needles were found to be too small to easily grip, and the lack of guide tube made them hard to aim, resulting in holes made at an angle, or even holes not made at all without any realisation. They had no impact upon the mechanical properties so they were abandoned at this stage.

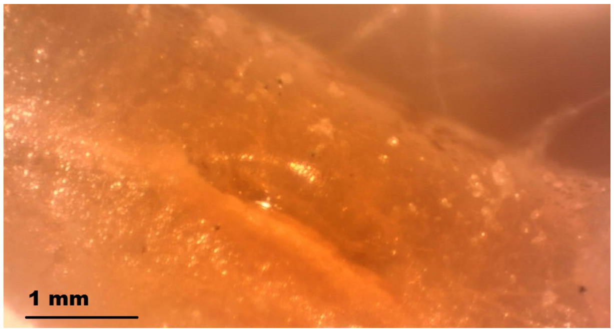

Figure 4.4: Image of puncture injury caused by a large needle captured using a light microscope.

The holes were initially examined under a light microscope. From viewing Figure 4.4 the presence of a hole is quite clear. It was measured to be 2 mm in length, and 0.4 mm in diameter at its widest point, indicating cracking and splitting of the cuticle from the needle pushing in. The hole is not circular but this is not too shocking. Insect cuticle is not isotropic, chitin fibres align and the act of pushing a needle in between the fibres may cause the cuticle to split, resulting in a hole that is longer than expected. Alternatively the stiffer nature of the cuticle may be resulting in crack propagation from the impact site.

However when the same holes were viewed under SEM (see Figure 4.5) it is evident that the hole is much smaller than thought based off the light microscope images, being more of the order of 150-180 μm in diameter, though if including the cracks in the length, up to 450 μm in diameter. What was thought to be the hole in the light microscope image is actually, for the most part a large portion of tissue that has been compressed in upon itself, and pushed inside the cuticle. Cracking is also evident, as suspected.

The presence of the cracks is of interest as they could compromise the UTS of the leg further than expected, growing rapidly when bent. The difficulty in interpreting images from the optical microscope led to its disuse, and the SEM was used thereafter.

Sudden Death

Early on in the needle wound repair trials a large death rate occurred amongst the locusts that had been injured with the large needle. In several cases the insects turned a bright red colour. In total 9 of the 27 adults injured with the large needle perished. None of the controls or other insects raised nearby passed away, discounting the possibility of an

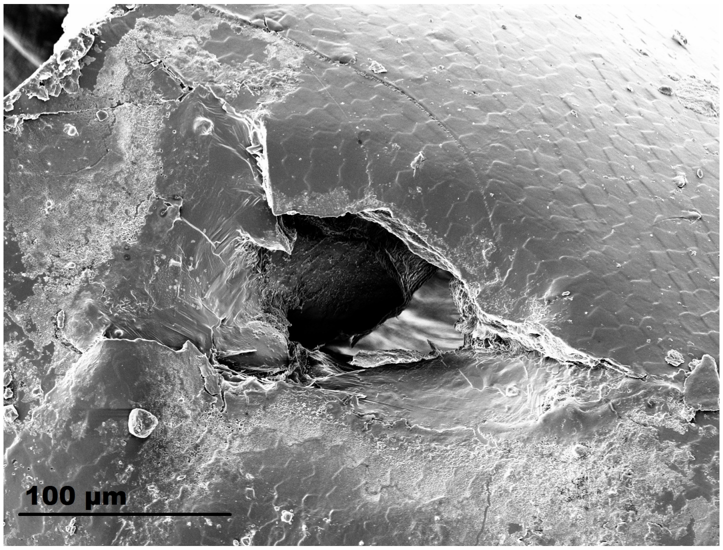

Figure 4.5: SEM image of a large needle puncture wound on insect cuticle.

airborne pathogen. As a fresh sterile needle was used for each insect there is no chance that a pathogen was spread from one insect to another. The good health of the medium needles and the fact that not all of the large needle injury locusts did not perish rules out the possibility that an insecticide was used to sterilise the needles. Additionally in that case the deaths all would have been rather immediate as opposed to over the span of a number of weeks.

One of the insects that turned red before death and its' enclosure were taken to the SEM to investigate the potential existence of any pathogens or contaminants. Samples of the tub side, bedding and egg carton in the tank were checked and no large colonies of any fungus or bacteria was found. A small number did exist, but this was to be expected as it is not a sterile environment, however nothing was discovered that could be the culprit for the deaths. Sections of the locusts leg around the injury site were also scanned and nothing in terms of microbes was observed.

It had previously been observed on the living insects that the injury sites tended to have large amounts of some unidentified matter clumped around them; Whilst observed all along the leg, it was always more concentrated at the wound site. After examining all parts of the insect tank it was realised to simply be flakes of oats, the material used for bedding. An image of the oats dust can be seen in Figure 4.6.

However the insects that perished had a much larger amount of oat flakes trapped at

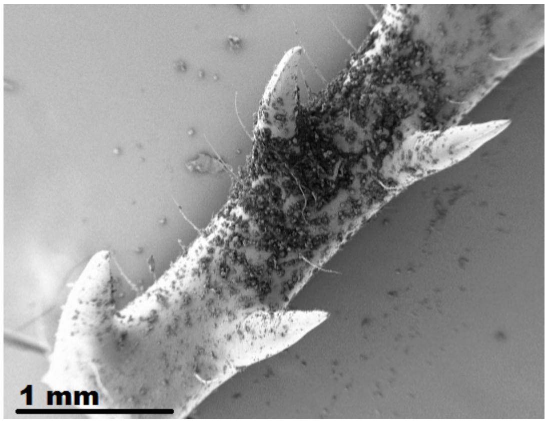

Figure 4.6: Section of tibia of the dead animal. The injury is obscured by the darker mass of oat flakes.

the wound site than others. The legs looked almost oily, as if large amounts of haemolymph had come up through the pore canals. This raises several possibilities. Perhaps in some insects oats get trapped inside the wound and enter the haemolymph where they illicit a foreign body immune response, and the oozing on the surface of the leg is the insects attempt to melanize the object, albeit too late.

Another hypothesis is that in some of the insects the wound did not heal properly initially, perhaps due to the misalignment of layers, and instead continued to produce melanin, but never closed the wound site, eventually resulting in dehydration and death. Or a combination of the two theories where the oat flake gets trapped in the wound site, preventing the immune system from healing the wound, causing dehydration. Ultimately the cause for these deaths could not be established. Evidently for future experiments where one wishes to see the outside of the entire hole as opposed to simply a cross section through it, that a different choice of bedding would have to be considered.

4.4.2 Mechanical Results

It is evident from Table 4.3 that the needle injuries had no significant effect on younger insects, those injured 2 weeks after their final moult, even without any time to repair. We found that uts, Young's modulus, and bending moment were almost the same for injured and uninjured hind tibiae. Paired t-tests showed no significant difference between the samples ($p>0.05$). As a result no repair studies were carried out upon this group.

However we found older insects suffered a significant reduction in their UTS after injury, down to ≈ 53% of their original UTS, when tested immediately after injury. When allowed to repair the cuticle, significant recovery was observed after two weeks. At this point the cuticle had been restored to ≈ 76% of its intact UTS. After three weeks the repair was relatively complete, with the UTS being ≈ 92% of the UTS of the controls. The bending moment at failure showed a similar restoration, as did the Young's modulus. Paired t-tests showed a slight decrease in the failure UTS between uninjured cuticle and cuticle that had repaired itself for 2 weeks ($p<0.05$). However after 3 weeks the two groups were not statistically different ($p>0.05$).

	Young	σ	E	M	Old	σ	E	M
Controls	μ	137.9±42	3.3±1.4	6.7±2.0	μ	160.8±34.4	4.4±2.08	7.4±1.4
0w repair	μ	130.8±26.2	3.2±1.5	6.4±1.3	μ	92.2±41	2±1.1	4.1±1.8
2w repair	μ				μ	133.1±44.2	2.9±1.78	7.1±1.1
3w repair	μ				μ	160.5±24.7	5.2±2.5	7.8±1.2

Table 4.3: Results for insects who received puncture injuries on the dorsal side of the hind tibia at either 2 weeks (Young) or 8 weeks (Old). Uninjured refers to animals who received no injuries. Some insects were tested immediately with no time to repair and the remainder were then left to repair for 2 or 3 weeks. Values for measured UTS, bending moment to failure and Youngs modulus are compared with the uninjured control samples. μ indicates that all values are average values and *FS, E* and *M* refer to the UTS (MPa), Young's modulus (GPa), and bending moment (Nmm) of the samples respectively.

4.4.3 Microscopy

In Figure 4.7b and 4.7d it can be observed that the damage done to the older cuticle is evidently more severe than just the hole made by the needle. We can see in Figure 4.7b that the injury is quite long, with a crack running away from the injury in both directions, along the length of the leg. This crack is close to 500 μm in length, corresponding to the cracking observed in the earlier samples. Figure 4.7d is a close up of a similar injury; the cracking of the cuticle away from the initial injury is evident, with the injury being almost triangular in shape.

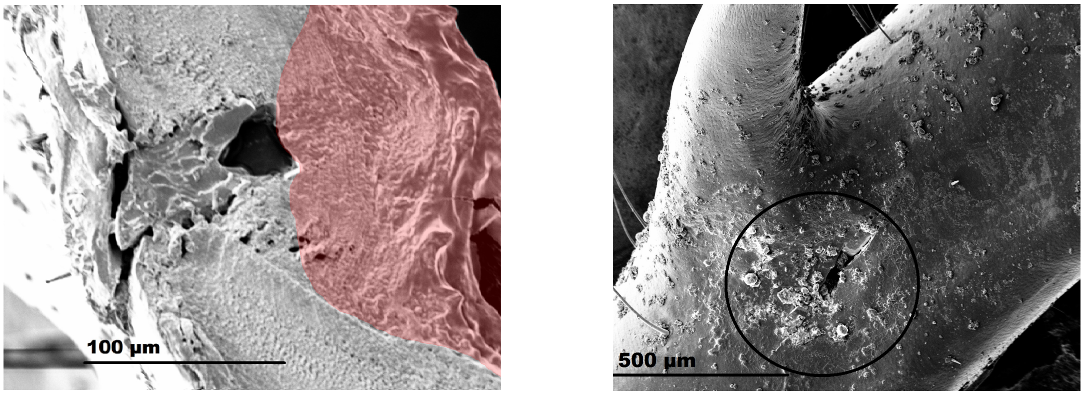

(a) Close up of needle injury **(b)** Horizontal view of puncture injury.

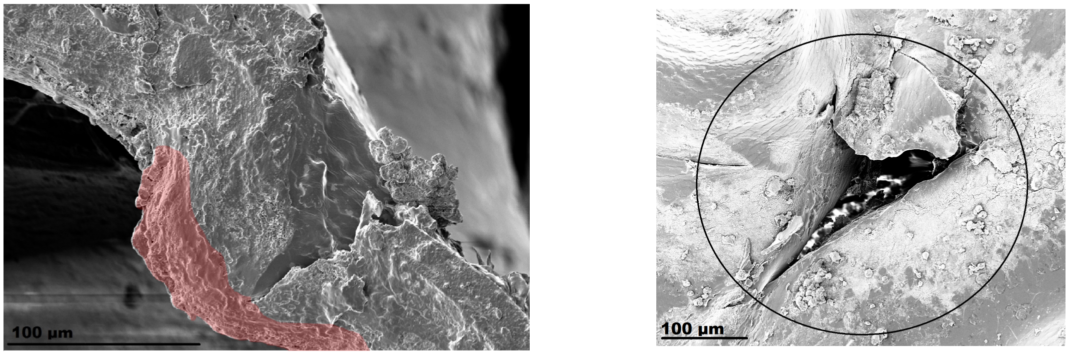

(c) Cross section of repaired puncture injury **(d)** Close up of cracks from needle injury

Figure 4.7: (a) SEM image of a repaired puncture injury, from an insect injured at 8 weeks and repaired for 3 weeks. Fresh cuticle deposited after the injury can be seen marked in red. (b) SEM image of a puncture injury, looking at the dorsal side of the hind tibia. The injury was made at 8 weeks and the image taken after testing, i.e. with no time for repair. The injury is marked with a circle and is evident as a dark hole with extensive cracking extending from it. (c) Close up of a cross section of a repaired puncture injury (2 weeks repair). Fresh cuticle has been highlighted in red for emphasis. (d) Close up of a needle injury on a horizontal sample, with the same view as in Figure 4.7b. This image was taken without any repair time. The injury is indicated with a circle. Cracks can be seen protruding from the injury.

However the older insects are able to repair such injuries by the deposition of new cuticle under the injury, in Figure 4.7a and 4.7c, where new cuticle has been marked in red. Once again this repair process appears to be targeted in nature, with all the fresh deposition being focused at the site of the injury. The wedge shape of the injury is also evident, indicating that some material was displaced at the time of injury, yet the epidermal layers were still able to realign.

4.5 Results: Fracture Toughness

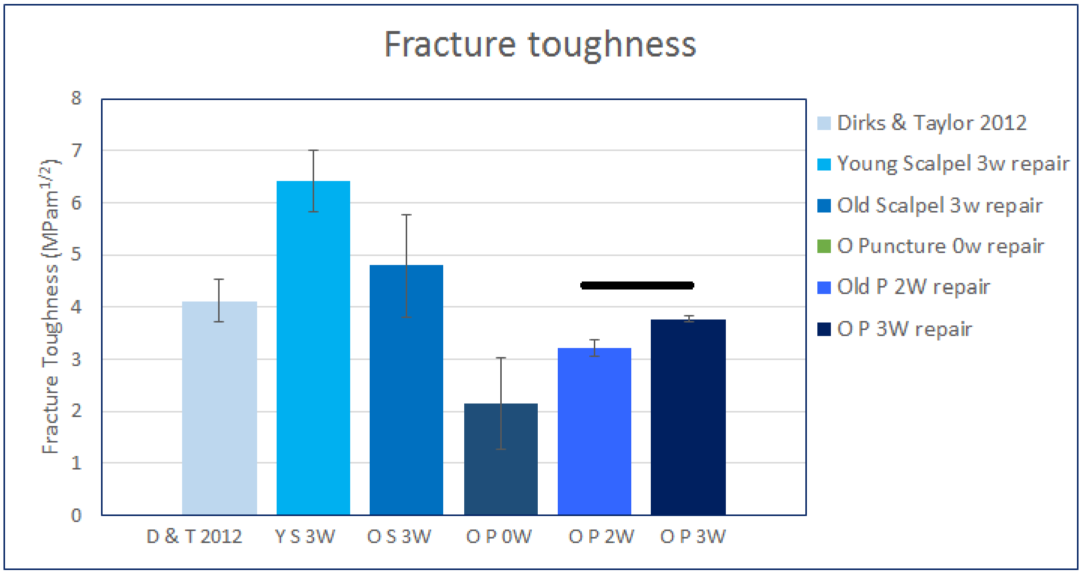

Figure 4.8: Fracture toughness of cuticle tested at different ages. Value for 14 days is taken from Dirks and Taylor, 2012 [65]. Values shown are the means ± one standard deviation. The line indicates the samples that are not statistically different from each other.

Fracture toughness for cuticle of insects 14 days post moult has been previously reported to be 4.12 $MPam^{\frac{1}{2}}$ [65]. It was found that insects injured at one week post moult and left to repair for 3 weeks reported an apparent fracture toughness of 8.48 $MPam^{\frac{1}{2}}$ a twofold increase. Older insects (injured at 12 weeks) that had 3 weeks to repair did comparably worse, only able to increase their apparent fracture toughness to 6.09 $MPam^{\frac{1}{2}}$.

For the insects receiving the puncture injuries, those injured at two weeks had a fracture toughness of 3.98 $MPam^{\frac{1}{2}}$, comparable to the value reported above [65]. When looking at the older insects, the same trend observed for the scalpel injuries occurred; older insects injured and immediately tested had a fracture toughness of 2.44 $MPam^{\frac{1}{2}}$, significantly lower than their younger counterparts, though it does suggest that the value seen in the older insects after recovery (6.09 $MPam^{\frac{1}{2}}$) is a large increase on the base value. The decreased fracture toughness reflects the trend of gradually increasing UTS and stiffness observed in the older insects.

4.6 Discussion

4.6.1 Ageing Effects

This work has shown for the first time that young and old insects have different responses to injury. It was found that young insects demonstrate a remarkable ability to withstand damage: the UTS of their hind tibiae was not significantly reduced even after a severe injury such as a cut over 23% of the legs diameter; almost complete restoration of UTS was observed in the younger insects, achieved via cuticle deposition. In contrast, a major decrease in UTS is experienced by the older insects, even after relatively mild injuries. The older insects were able to respond to these injuries by targeted deposition, but they were unable to fully restore UTS.

The UTS values reported here should be more than sufficient for normal activities, such as jumping for which the applied stress has been estimated to be 42 MPa [118, 126]. Complete repairs of the exoskeleton was not performed by either group ('scarring' is still evident at the wound site on the hind tibia) but the repairs appear to be sufficient for their continued survival.

It was found that the targeted deposition repair process reported by Parle et al. [4], occurred for both age groups. This is particularly interesting as the young insects are already in a rapid growth phase, depositing $1.8\mu m$ of cuticle per day [76], yet they are able to deposit even greater amounts. This high rate of deposition may be why the younger insects repair injuries to a greater extent than their older peers.

The toughness values calculated after repair showed significant increases. After 3 weeks of repair the older insects (12 weeks) were observed to have increased their fracture toughness to just 6.09 $MPam^{\frac{1}{2}}$. In contrast the fracture toughness of the younger insects (injured at 7 days) was increased to 8.48 $MPam^{\frac{1}{2}}$ after three weeks of repair. These changes do not reflect an increase in the toughness of the material itself, but rather the effect of the repair process which has made it more difficult for failure to occur by crack growth at the injury site [45, 154].

Consequently the targeted deposition of new material observed here serves two functions, it both plugs the wound and prevents infection, serving its innate immune function, as well as increasing the fracture toughness of the hind tibia, as reflected in the outlined results. However Taylor and Dirks [126] found that the tibia is optimised to resist both buckling and transverse fracture, so a trade off in the ability to resist both failure modes may be occurring as the thickness increases. Little difference in the absolute thickness was observed between both the young and old uninjured samples in all 3 directions of the cuticle. It was found that the increase across the *T1* (dorsal) side of the cuticle is comparable in both groups, though there is far more scatter in the older group. That the tibia are of similar thicknesses across by the end of the repair period is to be expected: cuticle is rapidly deposited by the younger insects immediately after moulting to reach the optimum thickness to radius ratio.

But the reason for the older insects being less capable of mechanical repair-despite having comparable amounts of cuticle deposited - must still be elucidated. These differences can most probably be attributed to the ageing process; though carrying out similar functions, a seemingly poorer performance is exhibited by the older insects. This could be due to the fact that the younger insects are still in their rapid growth phase at the time of injury, with cuticle being deposited immediately after growth so that an optimum radius to thickness ratio [65] can be reached and could be able to sclerotize some of the newly deposited cuticle, conferring additional strength. Alternatively there may be changes in the composition of the cuticle of the older insects; perhaps similar to bone, there may be changes in the mineral content of the cuticle. The fresh material laid down, though it looks the same as their younger counterparts under a microscope, may be of poorer quality, comparable to the reduced quality of older bone [28].

4.6.2 Injury Type

The puncture injuries had little effect upon the younger insects, which is perhaps not surprising because the holes created were relatively small and rounded, compared to the scalpel cuts. More surprising was the strong effect of the same puncture wounds on the older insects. The explanation for this appears to be that, owing to the lower toughness of the cuticle, cracks formed around the puncture wounds, turning them from relatively mild injuries to more severe ones, similar in their effects to cuts of the same size. These kinds of puncture wounds are important because they might be inflicted by bites from predators. Additionally as restoration of the continuity of the epidermal layer is necessary for repair [66, 152], their ability to repair the injury is surprising, as the needle displaces tissue upon entry, leaving a wedge shaped hole (Figure 4.7c), which could disrupt the healing process. But this is possibly dependent upon the size of the injury, and it may simply be the small size of the needle relative to the tibia that allows repair to occur.

Explanation for the varying effect of injury on the UTS lies in the relative values of fracture toughness and UTS of the cuticle as it ages. When receiving a puncture injury, younger insects were found to have a fracture toughness of ≈4 $MPam^{\frac{1}{2}}$ whereas older insects (8 weeks) had a lower fracture toughness of 2.44 $MPam^{\frac{1}{2}}$. Using Equation 2.7 the critical crack length (the length for which the failure stress is equal to the UTS of the cuticle) can be estimated. A reanalysis of the results of Dirks and Taylor [65] yields a critical crack length of 1.2 mm, which is approximately the same as the diameter of the leg. However the critical crack length for older insects (those at 8 weeks who received a puncture injury) is just 0.36 mm, which is significantly smaller than the diameter of the tibia (≈1 mm).

Combined with the lower fracture toughness, this means that small injuries could prove to be catastrophic at scales much lower than that of their younger counterparts. Thus the declining tolerance to injury can be seen to result from the tendency of the cuticle to become stronger but less tough over time. These findings are in agreement with those of some previous studies who noted that insect cuticle gets stiffer and less flexible as the insects age [21, 155]. This is also comparable to the changes observed in mammalian bone, which become increasingly less tough with age [148], leading to falls or damage being far more likely to cause failure. This is similarly observed in the insects where the lower toughness means damage can propagate and turn catastrophic far more easily.

It is not clear why these dramatic changes in both the UTS and the fracture toughness of the cuticle occur, nor why the repair capability is reduced in older insects. It could be linked to an animal becoming redundant to its species once it passes sexual maturity. Though 8-12 weeks may not seem like much, it is old for most insect species. Many insect species such as those in the Mayfly suborder only exist as adults for less than 24 hours, perishing immediately after mating. Locusts fare far better, experiencing sharp changes in the UTS of their tibia up until 3 weeks of age, when the post moulting sclerotisation and rapid deposition of cuticle cease. The insects typically begin to reach sexual maturity at around 4 weeks post moult and egg laying commences at around 2 months [147]. As the insects in this study were older than this, the role of sexual maturity in the changes is a possibility. The influence of gender in the insects is investigated in Chapter 6.

The endocuticle in older insects may also be getting less flexible as time passes; this would align with both the increased UTS and the reduced fracture toughness observed as the insects age. This would be comparable to the increased amounts of cross-linking of collagen fibrils observed in older mammalian muscle, leading to greater stiffness of the connective tissue [153]. In an anecdotal manner, insects that are older are far less inclined to jump in comparison to their younger counterparts. Whilst it may simply be an artefact of them getting more used to human presence, it may also be linked to their reduced stiffness, as they move far less. This could be due to the fact that jumping and other rapid movements require deformation of the hard tibial cuticle; if it is not as tough, the chance of a break increases. The role of microdamage in energy storage and movements is discussed later in Chapter 5.

The phenomenon of ageing, and in particular the changes in the mechanical properties of structural materials, is very widespread in nature, and the effects of ageing can have a large impact upon survival. Up to now the study of it has been lacking in insects: the present study has provided some new results in an area which merits further investigation. It also gives further insight into how ageing affects the repair process in insects, finding that similar to mammals, older insects are less capable of repairing injuries when compared to their younger counterparts.

4.7 Conclusions

It was discovered that younger insects are more capable of repairing injuries, displaying no significant decreases in UTS, stiffness or bending moment to failure after 3 weeks of repair. Older insects in contrast were only capable of repairing to $\approx 70\%$ of their original UTS comparable to the rate observed in insects injured at 5 weeks of age [4], indicating little difference in wound response between insects of 5 and 12 weeks old. Both older and younger insects carry out targeted deposition to repair injuries, with the younger insects capable of depositing cuticle at an even faster rate than normal post-moult growth.

Neither the small nor medium needles had any effect upon the UTS of the animals tibia, suggesting a reasonable resistance to minor damage. However the large needle had a significant effect upon UTS, but only in the older insects. It was discovered that this is because the cuticle of older insects is more susceptible to crack growth due to a large decrease in fracture toughness with age. As a result they are more sensitive to scalpel cuts and punctures. In contrast the puncture injury had no effect upon the UTS of the younger insects.

In the older insects repair did occur in the majority of samples, indicating that the needles were not large enough to cause displacement of cuticular layers to such an extent that repair was prevented. However a large number of the animals perished and the reason for this remains unclear. As there was no signs of pathogens and it only occurred with the large needle samples, this may be linked to displacement of cuticular layers.

4.8 Future Work

The reason for the increased stiffness remains unclear. Further histological studies into changes into the composition of the exo- and endocuticle with age would be an interesting path to pursue. One route is the use of confocal laser scanning microscopy or multi photon microscopy. As cuticle is autofluorescent, older cuticle may reveal itself to have higher amounts of sclerotised cuticle than that of its younger counterparts, which could be responsible for the increased stiffness observed. Another possibility is variation in the water content of the cuticle. Scleortisation, or ’tanning’ of the cuticle involves the loss of water from the cuticle [156] and increasing stiffness. Finally younger insects could be tested for shorter periods of time to investigate if they are capable of repair that is both more effective and faster.

Chapter 5

Repair of microdamage caused by cyclic loading in insect cuticle

5.1 Introduction

The phenomenon of fatigue, whereby a material becomes gradually degraded and eventually fails as a result of cyclic loading, is common to almost all materials. It is most frequently studied in metals [157] but is also well known in fibre reinforced composite materials [158]. A stress can be applied, less than that required to cause instantaneous failure, but if this stress is repeatedly removed and reapplied the sample may eventually fail. This happens as a result of irreversible processes in the material. In metals the main process is plasticity, whilst in fibre composites and other so-called quasi brittle materials the main process is microscopic damage in the form of small cracks and delaminations, which gradually increase in number and size after each cycle. Final failure occurs either by catastrophic build-up of microdamage or the appearance of a macroscopic crack capable of propagating rapidly.

Mammalian bone is essentially a fibre composite material and suffers in the same way as engineering composites from fatigue-induced microdamage [159]. However, it has been shown that living bone is capable of detecting and repairing this microdamage at an early stage. It has been estimated that in the absence of repair, human long bones such as the femur and tibia would all fail by fatigue within approximately one year [160].

This phenomenon has, until now, not been investigated for any other biological material. In previous work it was shown that desert locusts are capable of repairing macroscopic damage [4, 161]. We applied scalpel cuts and puncture wounds to the hind tibia, sufficiently large to induce significant loss of UTS, and found that repair occurred in the form of targeted cuticle deposition. Other researchers have shown that insects can repair areas which experience surface abrasion [162]. Other biological materials have also been investigated in this way: for example trees can repair scars by deposition [163], and plants can respond to surface abrasion of their leaves, restoring water resistance [2].

Insects and other arthropods place large stresses and strains on their skeletal members. They are capable of very rapid and powerful movement [111, 164, 165]. Such movements require both high speed and power, overcoming the force-velocity trade off that constrains striated muscle [107–109]. This is achieved by slowly deforming elastic structures in the cuticle, storing energy, before delivering a rapid recoil that amplifies the power [113–115]. In the locust 50% of the energy required for the jump is stored by bending the bow-shaped semi-lunar processes in the femoral-tibial joint of the hind leg [112, 118, 166], with the other half being stored in the muscles, tendons and distortions of the cuticle [112, 167]. A locust mid-jump and a schematic of the corresponding anatomy can be seen in Figure 5.1.

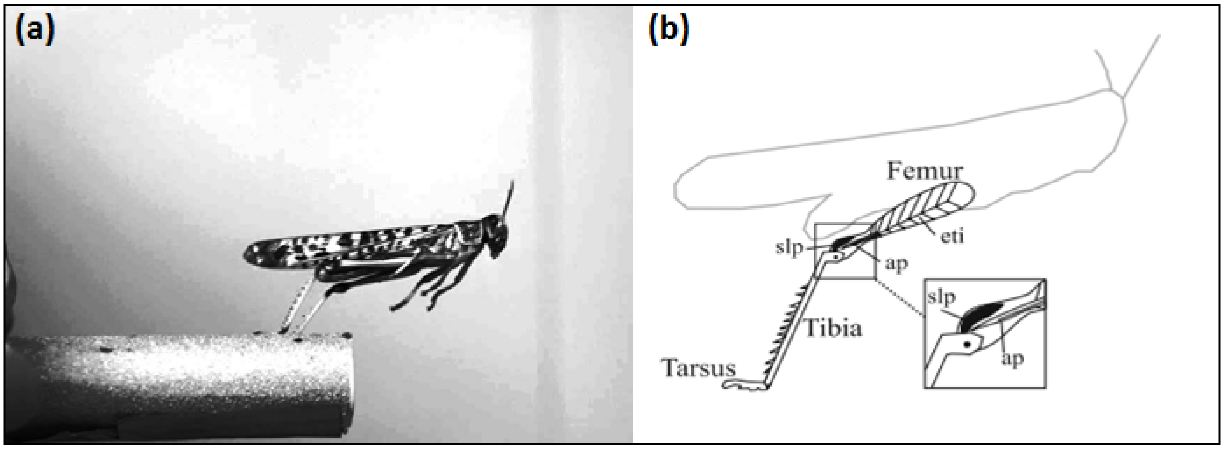

Figure 5.1: Image of a locust taking off and a schematic of the corresponding anatomy [124].

The idea that some of this energy storage is achieved by distorting the tibia was noticed by Katz and Gosline [120] who observed a substantial deflection of the tibia (13% of tibial length) under bending conditions. They found that this deflection is responsible for 10% of the total kinetic energy of the jump, showing that the tibia is capable of acting as a flexible spring. This is supported by Jensen and Weis-Fogh [146] who observed a plastic deformation of 8% under bending loads (bending is the primary way the tibia is loaded in vivo). This ability of cuticle to absorb energy is evident in the resilience observed in the cuticle for terrestrial insects including locusts, where it can be up to 90% [120, 168–170], allowing the cuticle to act as a damper and minimise perturbations. However if the stiff tibial cuticle is deforming and storing large amounts of energy it is possible that the cuticle is suffering microdamage at the same time.

There is some evidence for this: Bennet-Clark [118] found that insects would only jump approximately 10 times before needing a rest period: This is partly due to muscle fatigue but it may also be that the insect is damaging their cuticle with each jump. The forces during jumping are quite high, with the tibia of the locusts operating at a safety factor of just 1.2 [24, 118]. This means the insects are regularly coming within 20% of their UTS, raising the possibility of the development of micro-damage in the tibial cuticle during jumping.

Given the previous literature on bone and the evidence of strenuous use of insect cuticle, it was hypothesised that insect cuticle will sustain microdamage if loaded at, or beyond, the stress level at which it is normally used. We further hypothesised that cuticle is capable of detecting and repairing this microdamage so as to return the material to its original condition.

5.1.1 Development of dyes

Dyes have been instrumental in the study of cracks and fatigue in bone. These appear in the form of chelating fluorescent agents which bind to free metal ions. This works exceptionally well in bone due to the presence of free calcium ions during microcrack formation. Before the advent of such dyes, samples would have to be removed before failure occurred and histological staining performed, meaning samples could only be examined at one time point. The development of such dyes allowed for bone to be stained and cycled multiple times, giving an insight into how microcracks grow and accumulate over time [171].

One of these dyes is basic fuschin, used extensively to image microcracks in bone [172], appearing under both transmitted light and with fluorescent excitation. For this reason, (the ability to image stained cracks using a standard light microscope), basic fuschin was chosen for use as a dyeing agent for the insect cuticle, to investigate if it could pick up cracks, as insect cuticle also contains calcium, though whether or not it is released during damage is unclear.

5.2 Materials & Methods

Insects were acquired and raised as described previously in Chapter 3

Insects were sedated by chilling, before securing them in plastic tubing. During handling insects tend not to move when gripped around their pronotum (a saddle like patch on their neck). This grip was replicated using play-doh to ensure the animals remained stationary. The bottom of the tube was also lined with blu-tak. The tibia was inserted into a 3D-printed cube with a cutout (see Figure 5.2a) which was then filled with dental cement (Simplex), securing the tibia just below the tibia-femoral joint. This cube was then fixed inside the tube using another 3D-printed part. The tube was then affixed to a metal block for testing. The setup can be observed in Figure 5.2. Before testing began we evaluated the experimental setup to ensure there was no excessive motion of the tube and its parts. Videos of tests were recorded at the same speeds and loading as used in the actual experiments and no significant movement could be observed at the forces used, even when held at peak force (up to ≈ 1N).

Samples were tested using cantilever bending tests because bending is the primary loading mode experienced *in vivo* during jumping [173]. Early investigations involved carrying out a variety of tests up to different displacements (1.5-3 mm) and at different rates-the slowest being 0.6 mm/min and the fastest being 300 mm/min. Different hold times (the time the pointer of the machine stayed in contact with the sample for after maximum displacement was reached) were also experimented with, along with relaxation times between cycles.

Ultimately it was decided to cycle the left hind tibia 5 times, at a rate of 5 mm/min to a displacement of 3 mm by applying a position controlled displacement near the distal end of the sample (5 N load cell, Zwick/Roell Z005, Ulm, Germany). Based off of previous studies [76, 125] and the early investigations this was determined to be sufficiently close to buckling to feasibly be causing some damage to the cuticle, but not so much that the tibia would be expected to buckle during the test. A hold time of 10 s was also selected, with a 10 s relaxation time. The distance between the cement and the pointer was recorded, and marked on the insects tibia.

The insect was removed from the setup and left to repair any damage for a variety of repair periods: 1 hour, 24 hours, 1 week and 4 weeks. After each repair period the cuticle was tested in the exact same way as before. The markings on the hind tibia were used to try and ensure the same placement as in the previous tests, but in each case the distance between the cement and the applied force were recorded. At this point the right hind tibia was also tested, to act as control. This was done in the same manner as the other tests.

Concurrently, some of the tibia were removed after the initial testing (under sedation by chilling) before being fixed and stored as outlined previously in Chapter 3. At this point the tibia were either sectioned transversely or positioned longitudinally and prepared as before for scanning electron microscope (SEM) investigations. The samples were mounted

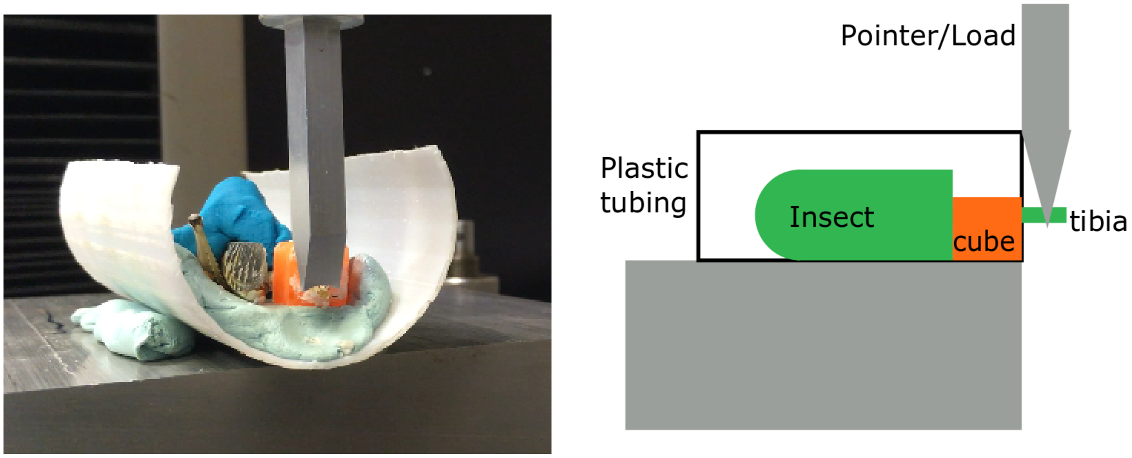

(a) (b)

Figure 5.2: (A) Rear view of cyclical loading setup. The animal is secured against the blu tak using play-doh, and one hind tibia is extended into the orange cube filled with cement. (B) Schematic of lateral view of the test; the leg is implanted into dental cement, inside a 3D-printed cube. The animal is secured in plastic tubing, and the pointer connected to the Zwick descends.

in carbon cement (Agar Scientific) before being sputter coated with an Au:Pd target. Longitudinal samples were investigated around the point where the force would have been at its maximum (i.e. close to the cement) for signs of micro damage. Transverse samples were used to record the dimensions of the tibia, using ImageJs Fiji software [174].As before, Young's Modulus of each sample was found by taking the slope of the initial part of the curve (up to a displacement of 0.05 mm) where the material still acts like a Hookean material with a linear slope.

5.2.1 Staining and imaging cuticle

Attempts were made to stain cuticle in order to help the visualisation of any microcracks forming. Basic fuschin, a common dye used for imaging microcracks in bone during fatigue testing was chosen [172].

Samples were placed in a 4% formalin mixture cooled to 4 degrees for two hours before being stored overnight in ethanol. Several samples were left intact (ie, stored and stained in the same manner as tested) whereas other had the ends removed to investigate if this aided the staining procedure. Various fuschin solutions were made up as required and the following progression was carried out:

- 1% fuschin 80% ethanol-twice
- 1% fuschin 90% ethanol-twice
- 1% fuschin 100% ethanol-twice

Samples were placed in a fresh fuschin solution approximately every 2 hours, and stored overnight in fresh ethanol solutions, taking care to avoid pipetting damage. Afterwards the samples were placed in fresh 100% ethanol for two hours, repeated twice. After this they were imaged using light microscopy.

A light microscope (Leica DMLM) was then used to observe the damage and record the damage (Dino lite digital microscope).

5.3 Results

5.3.1 Early investigations

Samples tested at higher speeds reached much higher loads for the same displacement than those tested at slower speeds. This is indicative of viscoelasticity; when tested at higher rates the material is much stiffer, and absorbs far less energy. Samples tested at 150 mm/min reached an average stress of 210 MPa compared to the values reported in the groups tested at 5 mm/min, typically of the order of 130-140 MPa. The stiffness of this group was also slightly increased, to 4.5 GPa, once again in comparison to an average of $\approx$ 3 GPa for groups tested at 5 mm/min. A typical example of one such sample can be seen in Figure 5.3.

Conversely samples tested at slower rates of 3 and 0.6 mm/min reach much lower average loads over the same displacement (see Figure 5.4), with the stiffness of the latter being just 1.02 GPa, indicating the rate dependent response of cuticle. Hysteresis loops are also evident in both graphs, further emphasising the the viscoelasticity of the cuticle, with the energy lost presumably going into the formation of microdamage.

The samples tested at the higher rate showed a plastic deformation via a change of 0.02 in the nominal strain after the first cycle, with the lower rate samples displaying

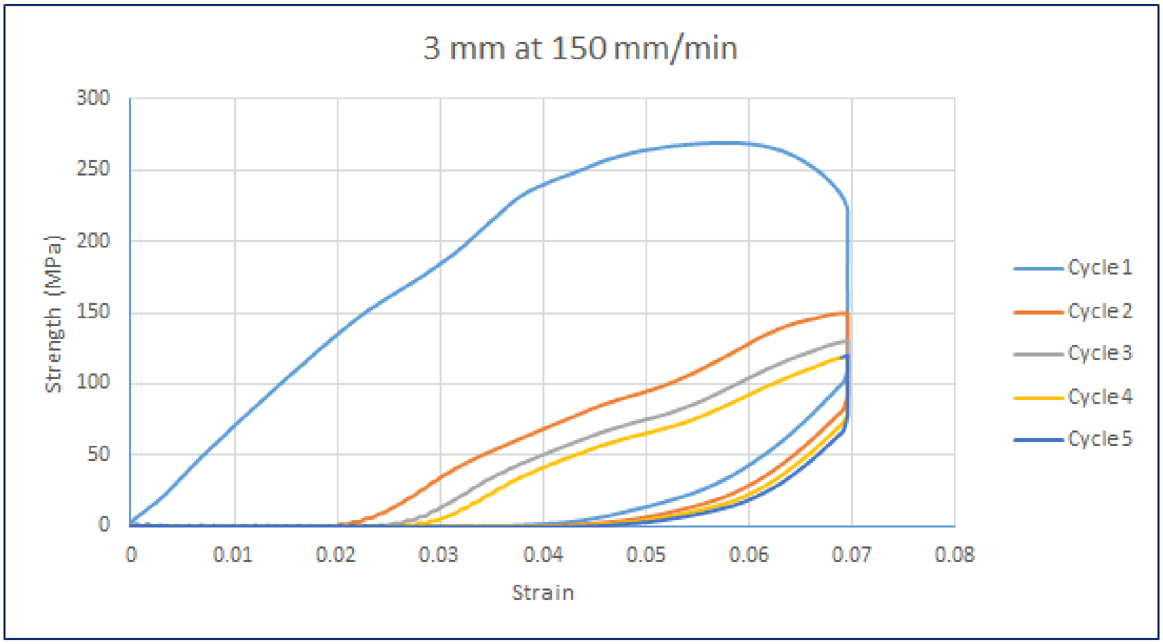

Figure 5.3: Graph of stress versus strain for 5 cycles to a displacement of 3 mm at a rate of 150 mm/min.

a deformation of just half that. However the higher rate samples go to a much larger displacement, and the occurrence of additional damage (despite the larger displacement occurring over a much shorter length of time) indicates some permanent damage is being done when the displacement begins to reach 3 mm. This is verified by the fact that samples tested up to 1.5 mm display a plastic deformation of via a change of 0.01 in the nominal strain, whilst once the deformation exceeds 2 mm the plastic deformation begins to double in samples, with the additional deformation present in all samples tested up to 3 mm.

As a result of these tests, a displacement of 3 mm was chosen as the ideal displacement to ensure all samples would come close to their maximum stress, but that few would fail. A rate of 5 mm/min was chosen to allow for comparison to previous studies [4, 76, 161], as well as the fact that using rates far exceeding this did not have a huge effect upon the observed properties, whilst still being substantially less than the rate that would occur in nature.

5.3.2 Repair results

Figure 5.5a depicts typical test results, showing stress versus strain during five sequential cycles for one sample. All samples showed essentially the same characteristics except that

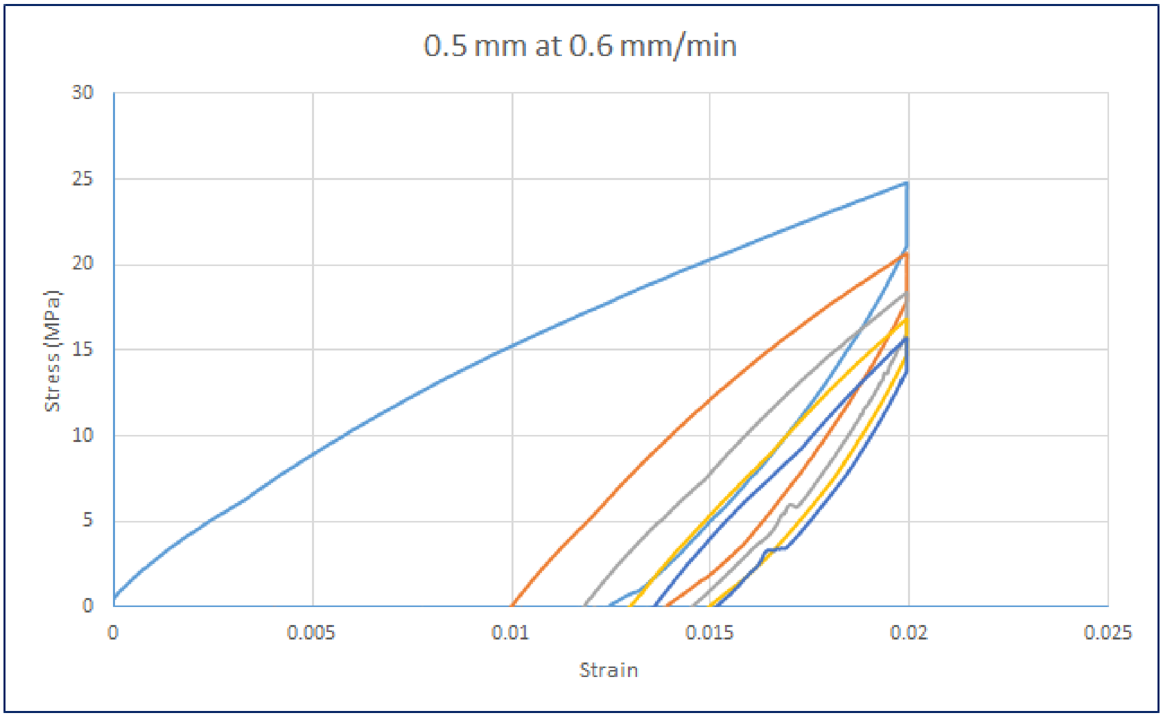

Figure 5.4: Graph of stress versus strain for 5 cycles to a displacement of 0.5 mm at a rate of 0.6 mm/min.

in some cases the peak stress value was reached during the 3 mm displacement, though in most cases it was not. The first loading line is seen to be initially straight but then curves downwards. During the first unloading line the stress decreases to zero at a positive strain value. This strain is referred to as the apparent plastic strain. At this point the loading pin loses contact with the specimen, re-establishing contact during the second cycle.

Cyclical softening, that is the reduction in the stress required to reach a given strain on subsequent cycles, is evident, especially between the first and second cycles and somewhat between the second and third cycles. The average decrease in stress between the first two cycles was 18%, followed by a further 7% decrease for the third cycle. Both of these decreases were statistically significant ($p<0.05$). The apparent plastic strain after unloading on the first cycle (which is 0.028 in the example shown in Figure 5.5a) was on average 27% of the maximum applied strain. This value gradually increased in the subsequent cycles, though by reduced amounts on each cycle.

Further interpretation of these curves will be presented in the discussion, Section 5.4. For the present purposes, the most important finding was that the initial slope during the loading phase, which indicates the Young's modulus, decreased significantly between

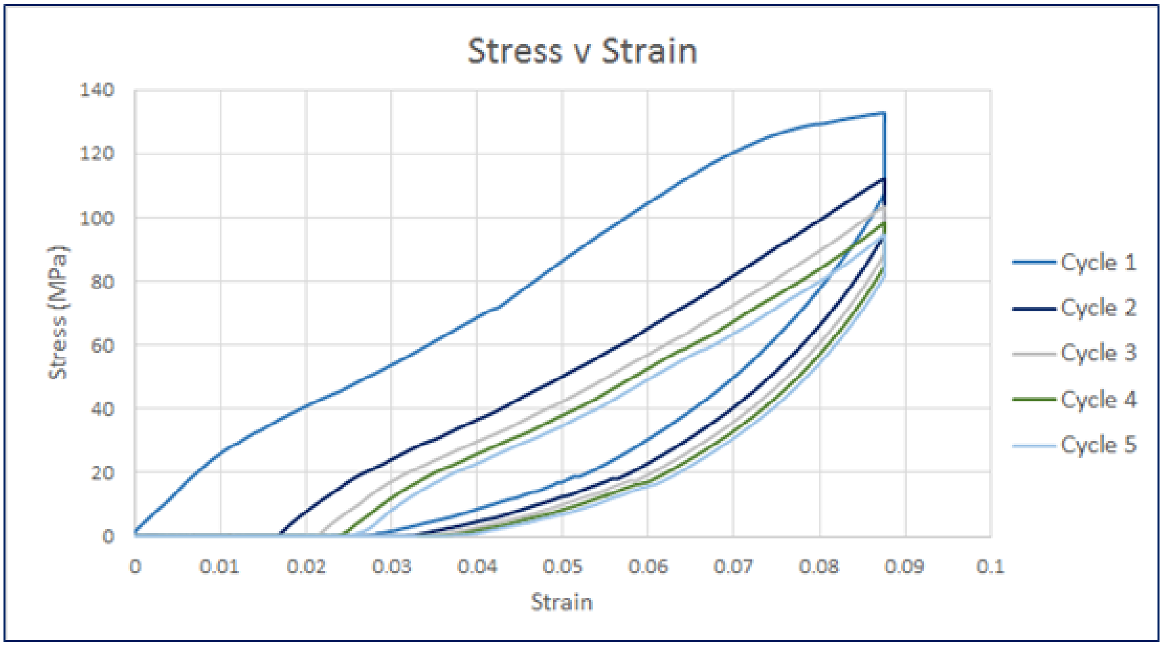

(a)

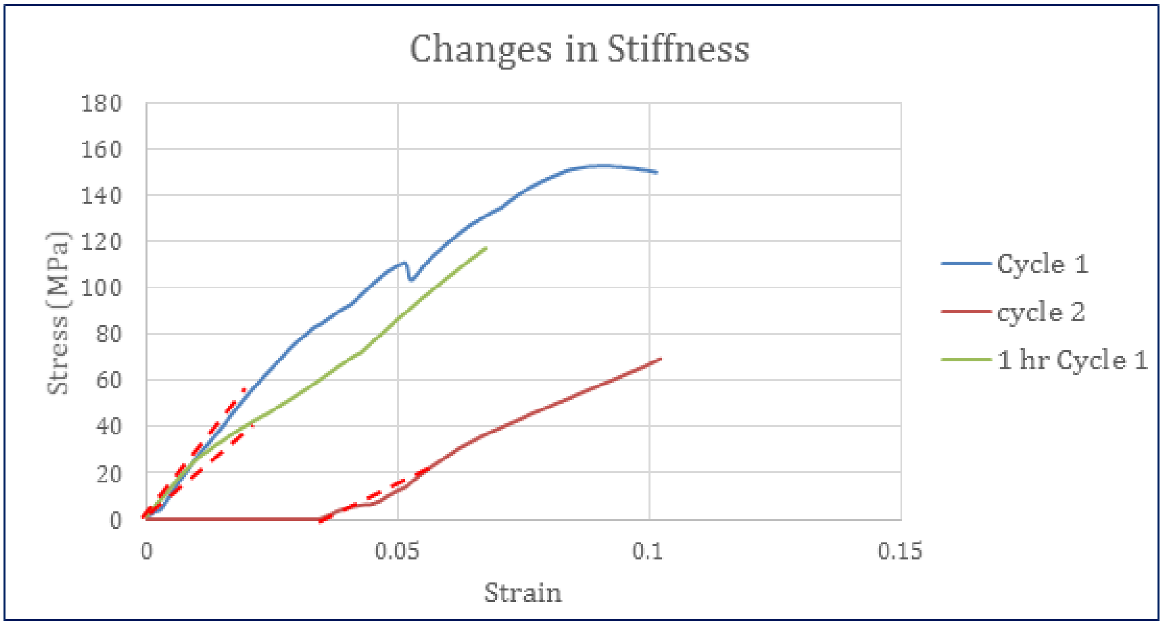

(b)

Figure 5.5: (A) Graph of stress versus strain for 5 cycles to a displacement of 3mm at a rate of 5 mm/min. (B) Graph of early parts of 3 tests for the first and second cycle of the initial test, and the first cycle of the test after 1 hour of repair. Stiffness is found by taking the slope of the first 0.5 mm of displacement (once the sample is in contact with tester) and corresponding force.

the first and second cycles. This indicates that damage (i.e. cracking) occurred in the specimen during the first loading cycle, increasing its elastic compliance. The average reduction in Young's modulus between cycle 1 and cycle 2 was 50% (standard deviation 28%) and this was not significantly different between the four testing groups. There were no significant changes in this parameter for the subsequent cycles 3-5.

Figure 5.5b shows an example of this reduction in Young's modulus, and also presents a loading curve for the same sample when it was retested after a period of one hour. The Young's modulus has now slightly increased compared to the cycle-2 value but is still less than that of the original cycle-1 value, being approximately 70% in this case. This indicates that damage still exists in the sample. Figure 5.6a shows the results of paired cycle-1 Young's modulus values for the various groups, both before and after the period of time allowed for repair. Figure 5.7 summarises this data, showing the percentage reduction in Young's modulus as a function of the time allowed for repair. For the 1 hour group the decrease in mean Young's modulus was 30%, just missing significance with a p value of 0.08. In the 24 hours group the decrease was also 30% and this was significant (p=0.01). For the longer repair times this decrease in stiffness had disappeared. There were small increases in the average stiffness, (11% at 1 week and 20% respectively at 4 weeks) but these were non-significant. This indicates that the induced damage had been repaired to bring the stiffness of the material back to its original value, or greater. Figure 5.7 depicts the repaired tibias Young's modulus as a percentage of the original test, along with the contralateral control limb as a percentage of the original test.

This confirms the reduction in stiffness for the 1 hour and 24 hour groups when compared to both the original test as well as the contralateral control, confirming that the noticed decrease is not just an artefact of the testing procedure. At 4 weeks the average stiffness for the control leg was somewhat higher than that of the tested leg (both initially and after repair) but this difference was non-significant (p=0.25 and 0.58 respectively).

The changes in UTS (shown in Figure 5.6b) broadly reflected the above changes in Young's modulus, showing a decrease in mean values for the shorter time periods but not for the longer ones. The p values just missed significance for the 1hr and 24hr groups (p=0.08 and 0.11 respectively). After 1 week a p value of 0.96 was returned, and after 4 weeks, surprisingly, an almost significant increase in UTS occurred, to 127% of the original

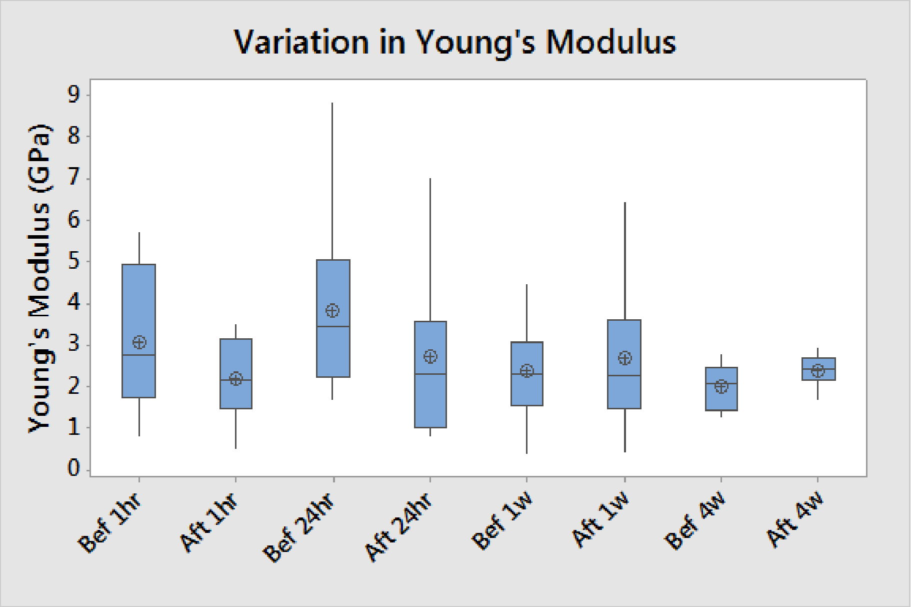

(a)

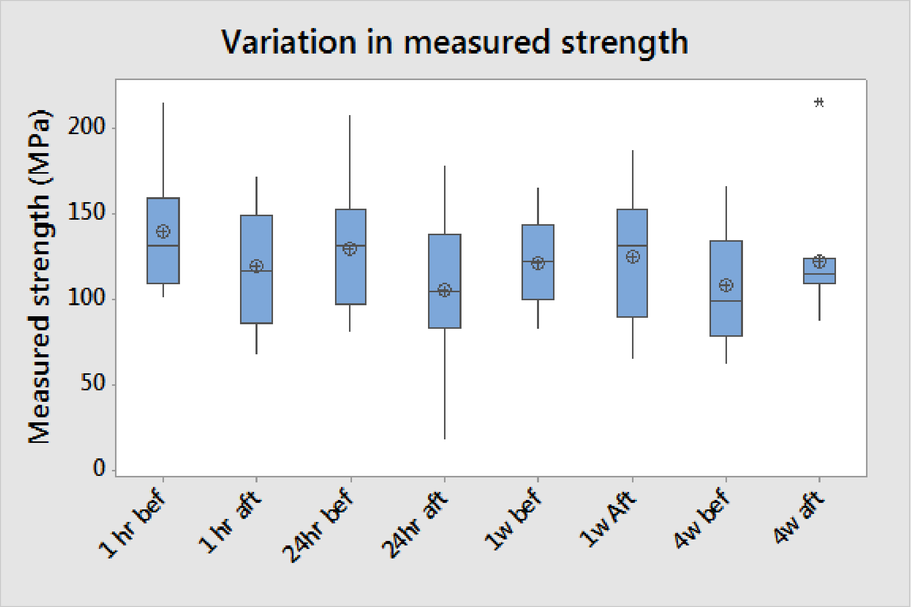

(b)

Figure 5.6: (A) Graph of changes in Young's modulus between samples after various repair periods **(L-R)** 1 hour repair, 24 hours repair, 1 week and 4 weeks. (B) Graph of changes in UTS between samples after various repair periods **(L-R)** 1 hour repair, 24 hours repair, 1 week and 4 weeks. For both the line indicates the median and the circled dash the mean. In the 4 week UTS set the star indicates an outlier.

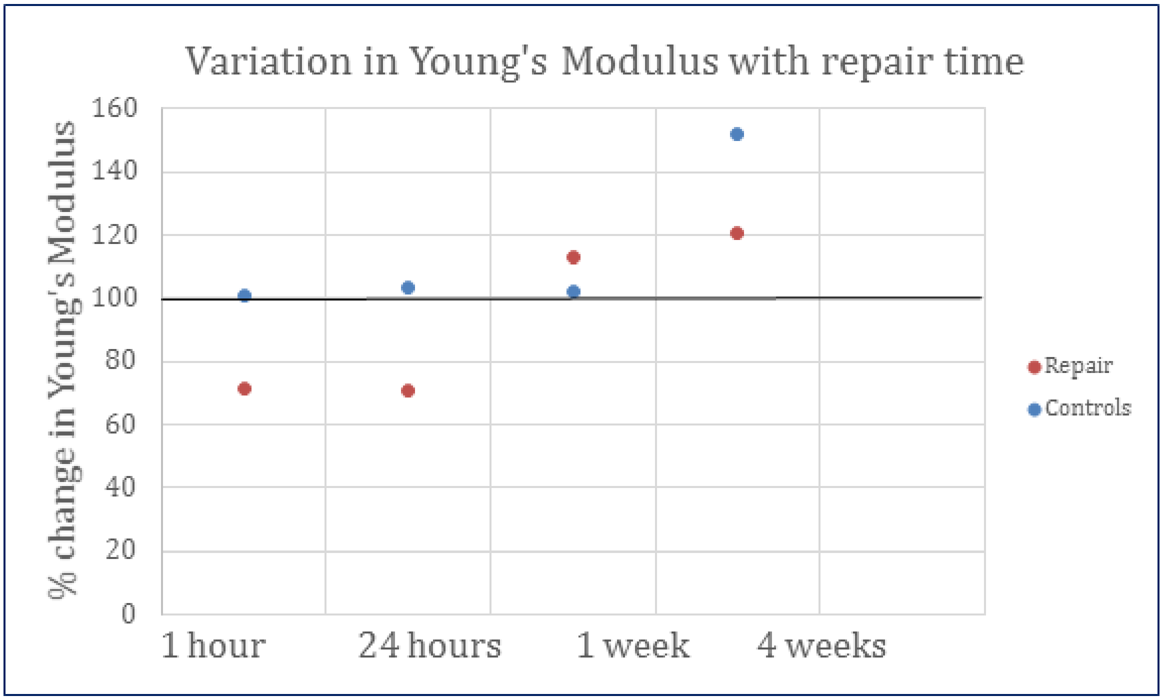

Figure 5.7: Percentage change in Young's modulus when compared to the original test for both the repair samples (i.e. samples tested once-original test- before being tested again after a given repair period) and for the other limb, used as a control.

value (p=0.11).

Examination of the surfaces of samples after the initial 5 cycles of testing did not reveal any signs of damage. Figure 5.8 shows the typical appearance of the tibia in the highly-stressed proximal region. No microdamage is immediately evident, at any of the magnification scales. In Figure 5.8d there is the appearance of a white line running up the image, however it could also be part of the textured surface of the cuticle, which can also be observed. No microdamage can be concretely observed.

5.3.3 Staining of insect cuticle

It took several days to stain the cuticle, and after 24 hours there was little evidence of it staining, though it did proceed more rapidly in the samples with the ends removed, as capillary action drew the solution up inside the hollow tibia.

Ultimately the dye was unsuccessful for the imaging of insect cuticle. Basic fuschin binds to free calcium, which is released when bones develop damage or cracking. Though

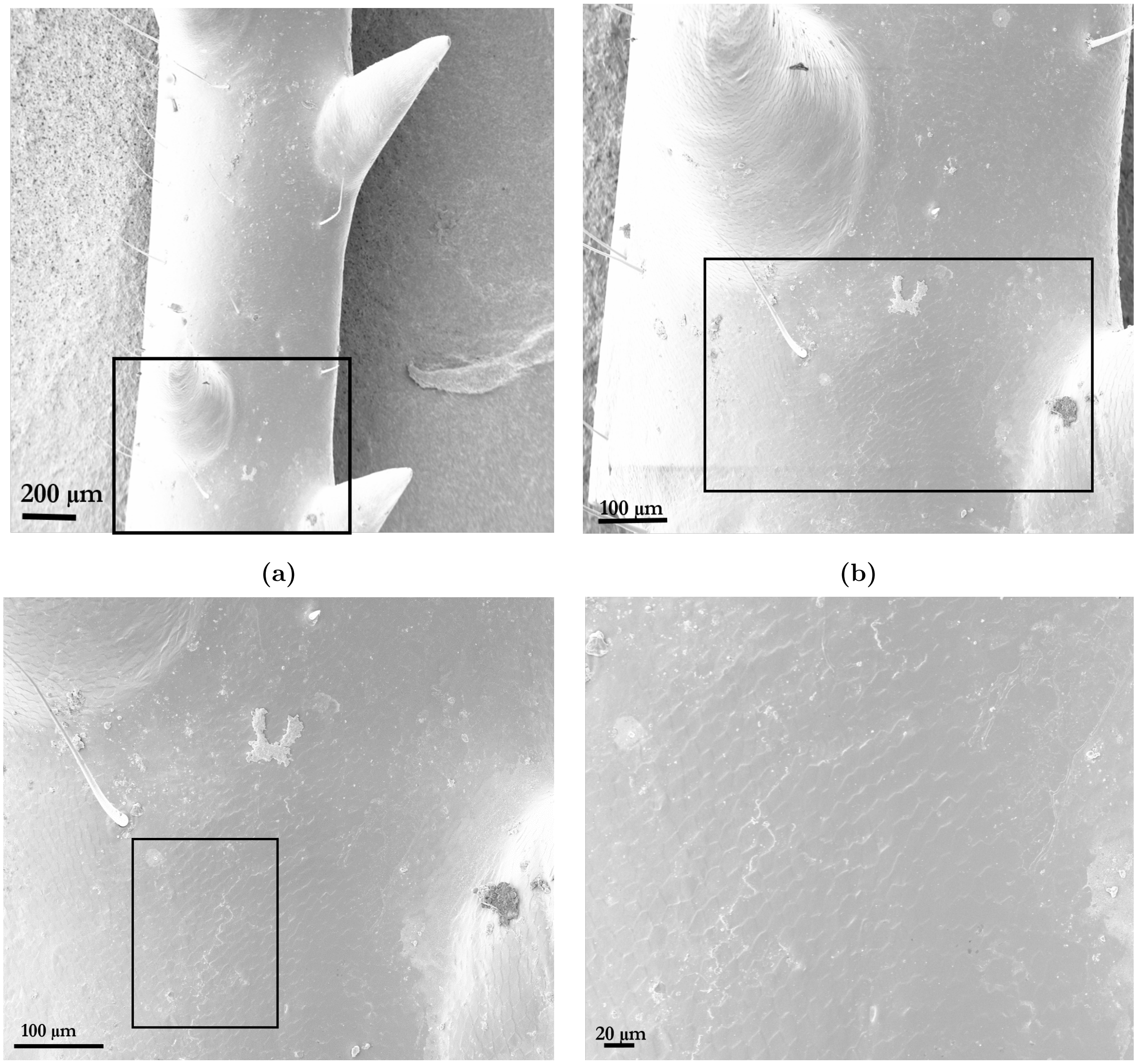

(a) (b)

(c) (d)

Figure 5.8: A series of SEM images of part of the surface of one of our specimens after cycling: no microdamage was observed. The blue boxes indicate the region magnified in the subsequent image: i.e. the section marked with a square box in a is the image in image b, shown at a higher magnification. The images were taken at the part of the tibia closest to the cement, where the force would have been the highest.

cuticle contains some calcium, evidently it is not being released when the cuticle is damaged. Though very large cracks can be seen, these are large enough to have been visible with a light microscope when unstained. There is also the problem with the fuschin-mixture inside the tibia, as this makes it hard to tell if a crack is being visualised or if it is

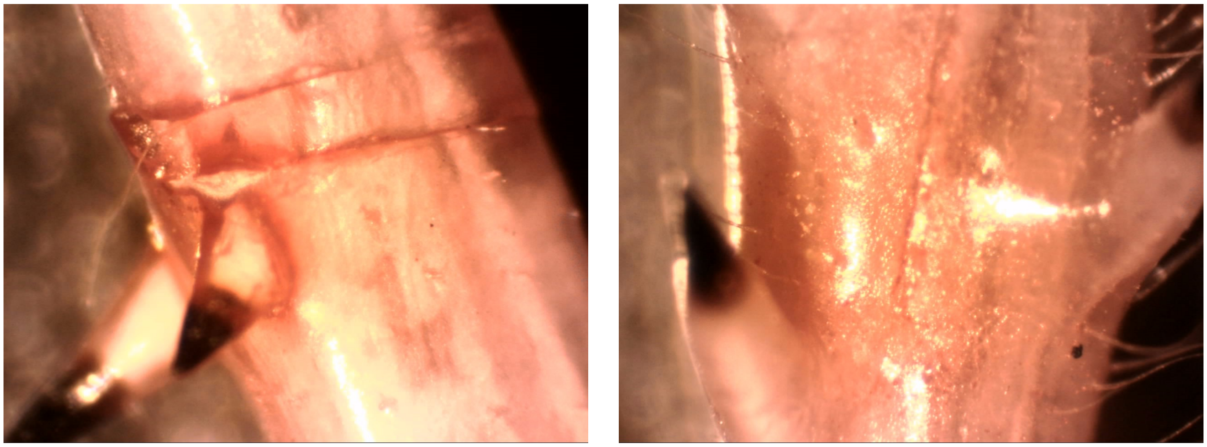

(a) **(b)**

Figure 5.9: Samples of cuticle stained with basic fuschin. Some cracks are visible as they are darker in colour, particularly in (a). However in (b) it is less clear if what can be seen is a crack or an air bubble or liquid inside the tibia itself.

a bubble inside the tibia. Additionally it took several days to achieve the staining and in this time several of the samples suffered damage, so it is difficult to confirm if any damage is due to this or as a result of the testing procedure.

5.4 Discussion

Cuticle is a viscoelastic material. Jensen and Weis-Fogh [146] observed plastic deformation visually during testing, and found that this recovered when the cuticle was left to rest. They explained this through cuticle being a viscoelastic material: the imposition of a stress causes an instantaneous elastic strain, followed by a viscous time dependent strain [175]. Once this viscous strain period does not break any primary bonds in the material, then there should not be any permanent effects. Bayley et al. [24] found a similar result; the energy absorbing properties returned within 24 hours, implying thixotropic behaviour [176, 177]. It was found that this is not the case; there is an active healing mechanism occurring when the insect experiences damage.

During the cyclic loading tests, viscoelasticity was evident in the decreasing slope of the loading line with increasing strain and the reduction in maximum stress from one cycle to the next, along with the increase in apparent plastic strain after each cycle. All these effects are due to an accumulation of viscous strain during the test. It was further highlighted by the increasing stiffness as the rate of strain increased in the early tests, with the cuticle behaving as a stiffer material when loaded more rapidly. The reduction in force, when the load is applied also fell farther when the maximum load was applied for longer periods of time. A large amount of hysteresis was observed, especially for the first cycle, even for the samples loaded at a lower rate, once again indicating viscoelasticity. This fits in with the cuticle absorbing a large amount of energy during deformation, and is comparable with what other researchers observed. Parle [140] reported that 50% of the energy during a loading cycle is absorbed by the cuticle, and Bayley et al. [24] found that the cuticle can absorb 78% of the energy during a kick.

It was hypothesised that cyclic loads of this magnitude would be sufficient to cause microdamage: this hypothesis has been proven by the observed reduction in Youngs modulus, which was not expected as a result of viscoelasticity alone. Since the deformation applied was within the range of values expected for insects in vivo, this finding is consistent with insects typical refusal to make multiple jumps consecutively - they may not continue to jump if there is a chance they will break their leg. Additionally the decreased stiffness of the damaged limb reduces its ability to store energy for subsequent jumps, which would presumably lead to jumps of shorter lengths or reduced heights.

It was further hypothesised that, given sufficient time, this microdamage would be repaired. This hypothesis has been proven by reference to changes in Youngs modulus over time, which show that repair occurs in a period between 1 and 7 days. This can be compared with previous findings which found that repair of macroscopic damage (cuts and puncture wounds) in the same limb occurs over a somewhat longer period of 3-4 weeks [4, 161].

Changes in UTS which were broadly similar to the above changes in Young's modulus were also observed, though with some differences. These changes were generally non-significant (though in some cases p values approached the limit for significance). This is not surprising: UTS as defined here would have included a large contribution from viscoelasticity and so will not be such a clear indicator of damage as Youngs modulus.

There are some limitations to this study; the tests were performed at quite a slow rate of 5 mm/min to allow comparison to existing literature on the mechanical properties of insect cuticle and repair. However physiological rates of strain would be much higher, and then the cuticle can be expected to behave as a stiffer material, absorbing less energy, and as such the extent of viscous deformation can be expected to be less. As the movement of insects are very rapid the use of slower movements as a proxy for the energy storage mechanisms of faster mechanisms is a well established when dealing with other arthropods [24, 178]. Additionally the lack of significant difference between samples at rates differing by an order of magnitude suggests the test are a reasonable estimate of the energy storage. Even if the energy being absorbed is higher than would occur naturally. The insects used were at least five weeks from their final moult, because previously it has been shown that cuticle stiffness and UTS increases significantly during the first three weeks [76, 161], an effect which would have complicated the measurements. Despite these precautions the overall values of Young's modulus measured here are rather lower than previously obtained for insects of this age; this might have been due to the use of a different animal supplier (there was no significant difference between the radius and thickness of the tibia).

The only other natural material for which similar studies have been carried out is mammalian bone. Schaffler et al. [179] conducted cyclic tests on bone samples and reported a systematic decrease in Young's modulus similar to that reported in this study, though of lower magnitude (up to 7 % decrease) [179], with a drop in stiffness of 10% frequently used as an indicator of failure in bone [171]. Figure 5.10a shows their results. This study also detected microdamage in the form of cracks of average length 80μm [179, 180]. Cracks were rarely seen at the surface, being contained within the bone. The detection of these cracks required specialised techniques, such as the use of liquid chelating dyes capable of penetrating through to the cracks.Figure 5.10b shows a typical example of the appearance of these microcracks. Taylor [181] found that the reduction in Youngs modulus could be used to make predictions about the growth characteristics of microcracks in bone and their influence upon failure.

The same process is presumed to be occurring in insect cuticle during the experiments described in the present work, since there is no other explanation for the observed decrease in elastic stiffness. It was not possible to detect this damage by examining the surface of the cuticle using SEM. However this is perhaps not surprising, given the difficulty which earlier workers had in detecting microdamage in bone. Cracks which develop during the

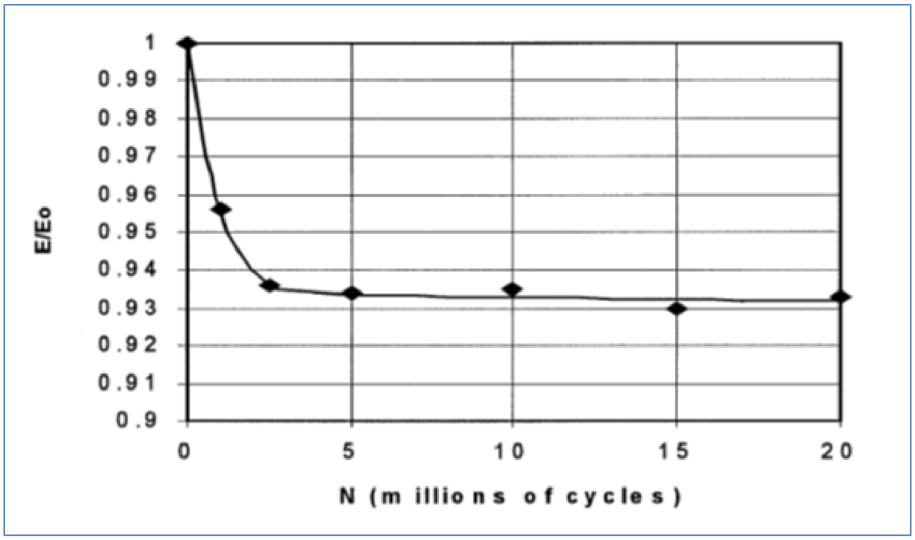

(a)

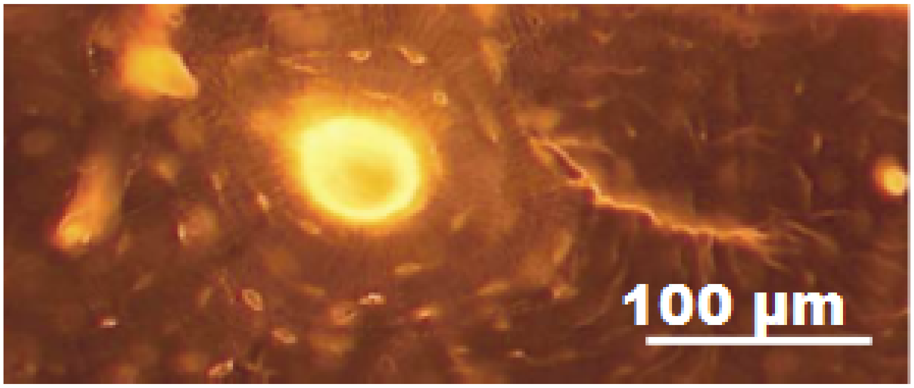

(b)

Figure 5.10: (a) Data from Schaffler et al. [179] showing reduction in Young's modulus during cycling at applied strains of 0-1200 μ ϵ) (b) Results from O'Brien et al. [171] showing the typical appearance of a microcrack in bone after treatment with a fluorescence dye to enhance its visibility.

cyclic loading of bone are similar in size to other microstructural features such as osteons, and they tend to close up when the load is removed, so without the specialised dyes it is almost impossible to see them. Furthermore the great majority of microcracks lie inside the bone rather than on the surface.

Cuticle is chemically different from bone and so probably it will not be possible to use the same dyes, though basic fuschin was used as an initial trial, confirming its unsuitability for this purpose: further work will be needed to develop new dyes or other methods capable of visualising microdamage in this material. Attempts to stain the cuticle were ultimately unsuccessful, and the development of new dyes may be necessary for further work in this field. Though the cracks made in the cuticle did stain more heavily than the overall cuticle, these were large cuts put into the cuticle using a scalpel. It also still remained difficult to distinguish any cracks from the presence of bubbles of dye that had risen up inside the cuticle due to capillary action. Microcracks were not visible using the dye.

Additionally even if the dye had worked at staining cracks, the time required for the staining process makes it incompatible with staining cuticle and then retesting it. Whilst bone can be dyed and retested relatively successfully [172], the same is not true of cuticle which dries out rapidly, and the need to store the cuticle in an ethanol solution permanently warps the properties. Though water is a good temporary storage solution [182], fuschin and many other chelating dyes are not water soluble, though this may serve as a good indicator for what sort of dyes could be utilised in future. However the need to dye and then retest the cuticle is a necessary step to ensure the damage being observed is due to the testing procedure.

This is the first study looking into the effect of microdamage upon the mechanical behaviour of insect cuticle. Overall this work serves as a starting point into the evaluation of microdamage and repair in insect cuticle, and how it may influence the behaviour of the animals particularly in relation to jumping insects and other species that store energy via cuticle deformation.

5.5 Conclusions

This was the first recorded study to investigate the repair of micro damage in insect cuticle, as well as being the first to evaluate how this microdamage affects the mechanical properties. After cyclical loading a significant decrease in the elastic stiffness (Young's modulus) of the cuticle was observed, indicating that microdamage had been induced. When tested again after up to 24 hours there was still a significant decrease in stiffness, showing that some microdamage remained. However in the samples left for 1 week or 4 weeks before retesting, the stiffness had returned to its original value, indicating that the microdamage had been repaired.

It is a highly significant finding: Very little study has been done into the fatigue of insect cuticle, and what has been done has been focused upon the wings [183, 184]. This work suggests that, within a time period of the order of a few days, the insect can fully restore the mechanical function of an overloaded leg and thus return to normal activities.

5.6 Future Work

A gap in this work is the lack visual confirmation of the damage. Visual confirmation would aid in understanding where microcracks form as well as understanding the mechanisms surrounding their formation and development. Supporting this, new stains and dye techniques particularly tailored to insect cuticle will need to be devised. Alternatively owing to the autofluorescent nature of cuticle, and the fact that the clotting material produced upon damage contains large amounts of melanin, multiphoton microscopy could be used alongside mechanical testing, as it allows living animals to be tested [185].

Additionally tests at more realistic loading rates could be conducted, as the loading rate used here is much slower than what the cuticle typically undergoes during jumping. It can be expected to behave as a much stiffer material under those conditions, and perhaps suffer less deformation.

Chapter 6

Additional Studies on Insect Cuticle

6.1 Introduction

It has been know for some time that the UTS of the insects cuticle increases rapidly in the first few days and weeks after moulting. This is to be expected; immediately after ecdysis the cuticle is soft and compliant to allow for the insect to grow, but it must rapidly harden to allow normal locomotory function. This occurs via the sclerotisaion process [49], as outlined in Chapter 2.

However recent work by Dooley et al. [186] investigated how the mechanical properties of the insect cuticle change over the course of the insects' life. Most previous studies had only observed the first 2-3 weeks post moult [45, 145, 146], ignoring any changes that may be occurring after this time point. What Dooley et al. [186] found is that the Young's modulus increases rapidly over the first three weeks of the insects life, consistent with previous work. However after this point the sharp rise begins to level off, but then a gradual increase in UTS occurs over the insects life. Parle and Taylor [76] found similar results in their study, finding that the UTS of the tibia also increases as the insect ages. The reason for this change has yet to be fully elucidated, though presumably it is an effect of the ageing process.

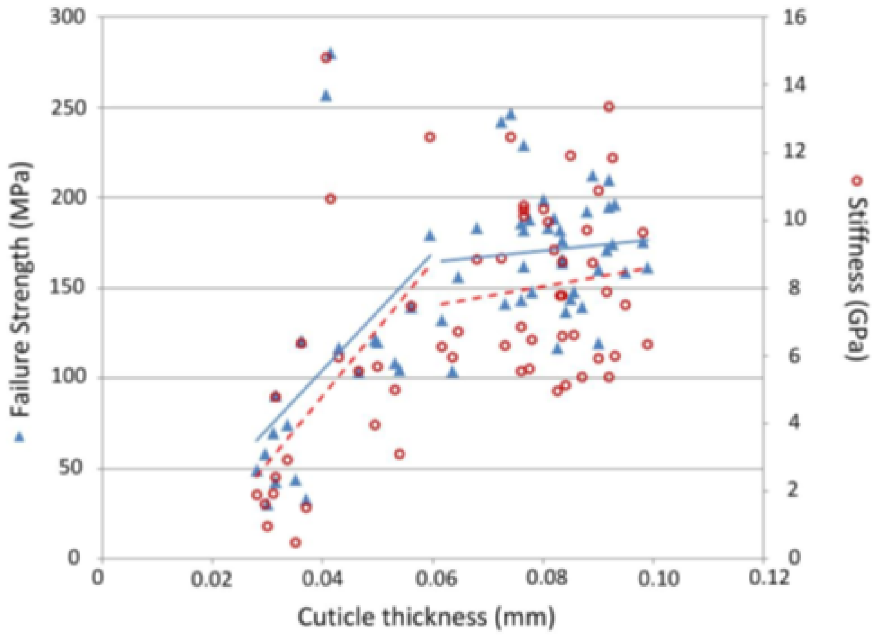

Figure 6.1: Increase in Youngs Modulus (right axis) and UTS (left axis) against cuticle thickness [140].

This hypothesis was examined in greater depth by Parle [140], who examined the way the cuticular layers are deposited during this extended time period. Their plot of Young's modulus against cuticular thickness can be observed in Figure 6.1. It is evident that the cuticular thickness increases as the insect gets older, corresponding with increases in the Young's modulus. This increase in cuticular thickness was anticipated to be the cause for the increase in UTS; the exocuticle is hard and stiff and increased amounts of it would confer additional strength. But this was not found to be the case.

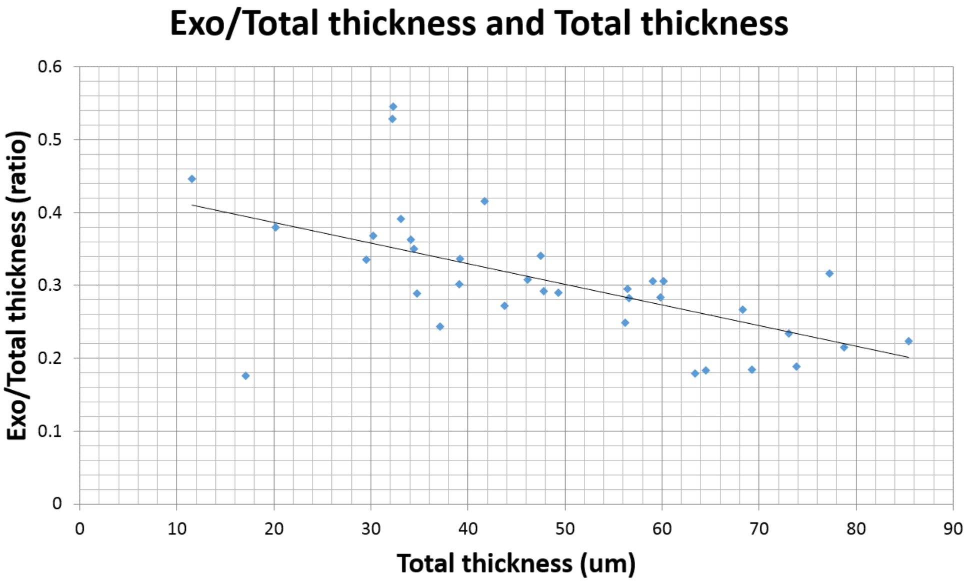

Figure 6.2: Changes in Exocuticle thickness in comparison to total thickness over the first 10 weeks of adult life [140].

Histological staining revealed that exocuticle is exclusively laid down in the first few days immediately after moulting; rapidly increasing to a thickness of 10 μm, with little further changes over the subsequent 10 weeks. This can be observed in Figure 6.2. But the total cuticle thickness continues to increase, albeit at a decreased rate, consistently over the insects life, reaching 90 μm in thickness after 10 weeks. This is due to continued deposition of endocuticle material. This is counter intuitive and further complicates the effect of age upon UTS and stiffness. As the endocuticle is tougher and more compliant, increased amounts of it would be expected to lead to a soft, more compliant tissue rather than the reverse. Consequently the mechanism causing the observed changes in mechanical results remains to uncovered.

The counter-intuitive nature of the changes in UTS and the work outlined in Chapter

4 raised questions about the root cause and mechanisms behind this effect.

6.2 Sex and mating differences

The initial changes in cuticle properties, though they vary between species and body part - due to differing functions - are well understood. But the reason for any further changes remain to be elucidated. They can be assumed to be age related; several studies have found reduced compliance in the adhesive pads of older insects [187], along with reduced locomotion [155]; an addition to this explanation is the hypothesis that these differences are driven by mating patterns and sex. Differences in age related decline amongst humans across the sexes and based on pregnancy are well established: osteoporosis affects far more woman than it does men [188–190].

This leads to the question ‘Perhaps the insects display these changes as they reach mating age¿. Egg-laying has been reported by Schmidt and Albutz to begin occurring from 3 weeks [147]. Insects were observed mating in our study from 2 weeks of age, though no egg-laying material was provided, so thus a comparison cannot be fully drawn. Animals that have not mated by this stage, or at least by 8-9 weeks of age may begin to become redundant to their species. Animals that mate may not display the same changes, and remain ‘young‘ as they age. Schmidt and Albutz [147] observed that females that did mate had comparatively shorter life spans. Alternatively the ageing process may simply be delayed in these insects. Female desert locusts have been found to be able to lay eggs (though in smaller quantities) up to the age of 4 months [147].

6.2.1 Materials & Methods

For these tests male and female insects were ordered as 5th instar nymphs. Animals were kept separate based on sex until moulting occurred. 7 days later, two groups of females were added to the males (the animals were in two separate tanks - the size of the tanks being the limiting factor), with another group of females kept isolated from the males in a separate tank, to act as controls. The animals were left to mate for approximately 3 weeks before testing the females in the same fashion as before, outlined in Chapter 3. Though there is the possibility of the presence of nearby males having an effect on the control females, I unfortunately did not have access to multiple housing facilities. The animals were kept on separate shelves from each other, surrounded by wooden boarding. As the effect is primarily due to sight and pheromones (if physical interaction is constrained), which both require close contact, this is sufficient to mitigate any effect that may occur.

6.2.2 Results

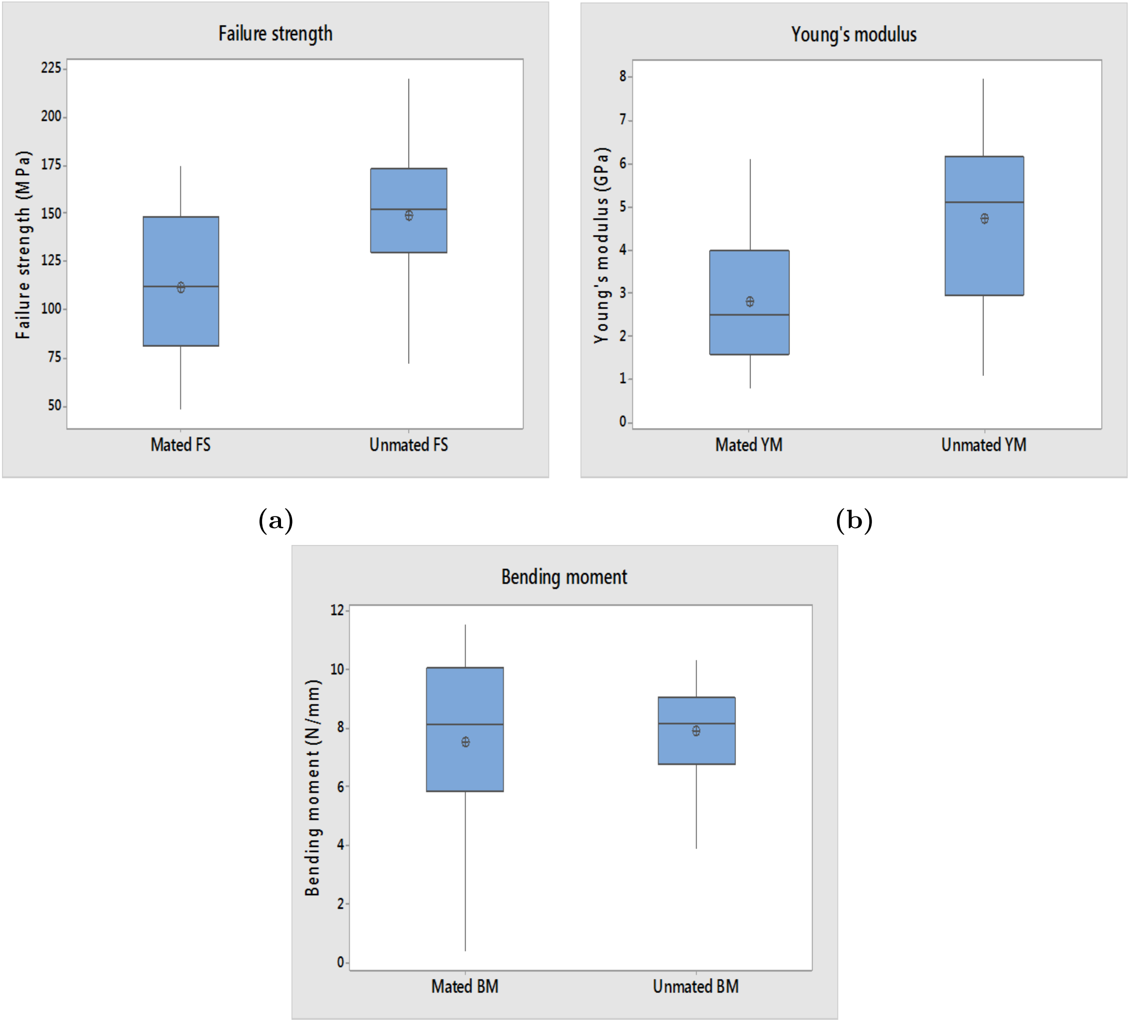

(a) (b)

(c)

Figure 6.3: (A) UTS for insects allowed to mate and the controls. (B) Young's modulus for insects allowed to mate and the controls. (C) Bending moment for insects allowed to mate and the controls.

Females that had been able to mate had lower values of UTS and values for Young's modulus compared to their unmated control counterparts. Both of these decreases were found to be highly statistically significant ($p<0.005$). The bending moment to failure was also lower, but this was not statistically significant ($p=0.6$).

The values for the control insects for all three properties (UTS, Young's modulus and bending moment) were comparable to those observed by previous researchers for insects of that age [4, 76]. Consequently the decrease in the mated insects is directly tied to the presence of the male insects (none of whom were tested). The results can be seen in Figure 6.3. Though both the thickness and the diameter was larger in the mated insects, being 94.4 μm to 78.6 μm and 1122.3 μm to 1050.6 μm respectively, there was no statistical difference in either the thickness ($p=0.32$) or the diameter ($p=0.6$) of the two groups. These increasing values lead to an increased value for the second moment of area (I) this change was also insignificant, an average of 0.044 for the mated insects and 0.029 for the unmated insects ($p=0.43$).

6.2.3 Discussion

It has previously been shown that the UTS and stiffness of an insects cuticle increases as the insect ages [76], at the same time as increasing amounts of tough, flexible endocuticle are being laid down [140]. Consequently the deposition of additional stiff exocuticle is not responsible for the changes observed, and mating habits was proposed as a potential factor in these changes. It was found that mating had a huge impact upon the mechanical properties of the insect cuticle, with only the insects that had not mated showing the previously documented gradual increases in UTS and stiffness. The mated insects continued to act like their younger counterparts, with the cuticle remaining more flexible, but still strong enough to withstand normal locomotory loads.

Why mating would have such a strong influence remains unclear, and no male insects were used in this or previous studies beyond keeping them in tanks with the females, so it is unknown if they experience such changes and if mating would prevent the change. Typically studies involving larger insects such as the desert locust only utilise females as they are significantly larger than their male counterparts. However this study has consequences for future work, as mixed colonies may produce different results compared to single sex colonies for older insects.

6.3 Water content

Loss of water from the material itself was proposed as a possible cause of the changes in mechanical structure. A precedent does exist for this line of thinking; water has previously been identified as being a factor affecting the mechanical properties of numerous materials, both natural and man-made [191–193].

Water content also has a large impact on the properties of the cuticle, alongside the protein to chitin ratio. In soft cuticle, where the chitin to protein ratio is normally 50:50, the water content varies from 40-75%. In contrast, in hard cuticle, chitin only makes up 15-30% of the dry weight and the water content rarely exceeds 12% [45]. The process of sclerotisation itself is the driving of water from the cuticle matrix [156].

This effect of water content has also been observed directly in a lab environment; Work carried out by Klocke and Schmitz [141] compared the Young's modulus and hardness of dehydrated cuticle, and then later the same cuticle re-hydrated by submersion in water. They found that depending on the type of cuticle and direction, the presence of water decreased the Young's modulus from 5 GPa to less than 0.5 GPa, an order of magnitude in difference [141].

This relationship between stiffness and water content correlates with work carried out by Dirks and Taylor [194] who looked at the relationship between percentage water saturation and Young's modulus. What they found is that as the water saturation drops from 100% to 10%, the Young's modulus of the cuticle increases from 3 GPa up to as high as 9 GPa [194] as the cuticle dries out. This data can be observed in Figure 6.4. Evidently there is a precedent for water acting as a modulator of the mechanical properties in insect cuticle. As to why this may occur naturally remains to be elucidated. However if water content can be easily identified as playing a role in the UTS of the cuticle, causing the changes observed in older insects, at least the mechanism can be identified, even if the driving factor cannot.

This problem was addressed in several ways; trying to track the water content in samples using infrared spectroscopy, examining the loss of water from excised samples (presented as changes in weight), and investigating if storage in water or PBS would impact the mechanical properties.

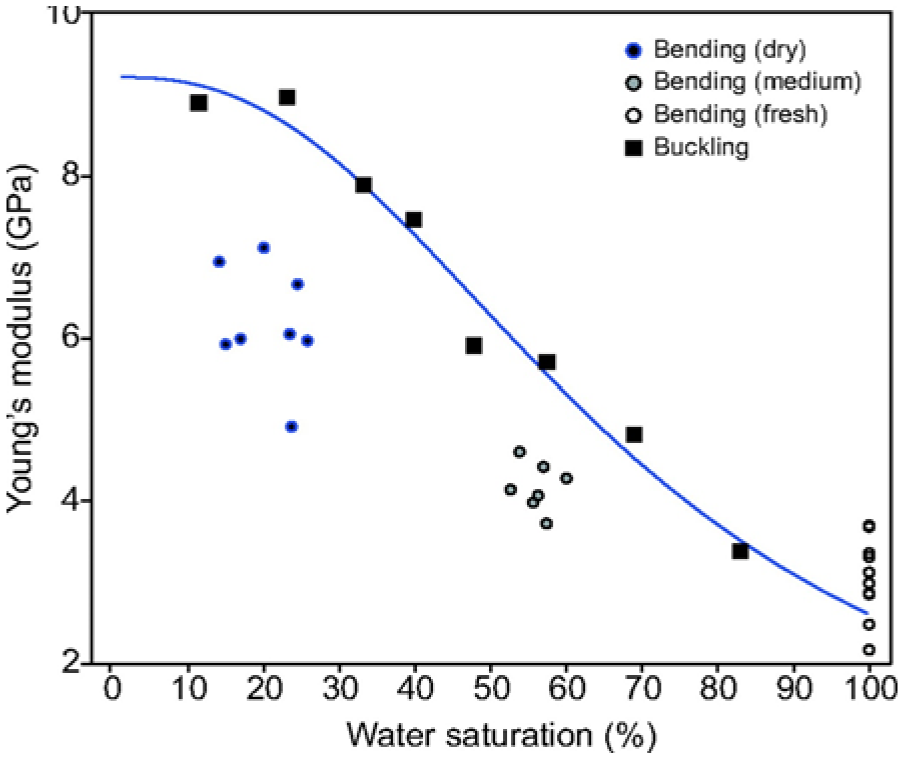

Figure 6.4: Relationship between Young's modulus and percentage water content for a variety of failure modes [194].

Infrared Spectroscopy

Fourier transform and attenuated total infrared spectroscopy (FTIR spectroscopy and ATR spectroscopy respectively) were utilised to try and investigate the water content in insect cuticle of different ages. FTIR has been used quite a lot in the biomedical community for tissue imaging [195], primarily because it is quick and relatively easy to perform, with only small samples required to receive a wealth of chemical knowledge; Functional groups, bonding types, conformations amongst others. In fact because the spectral bands in vibrational spectra give such narrow bounds, in some cases it is possible to identify chemical bonds within a given molecule [196].

Attenuated total reflectance (ATR) is a sub-type of FTIR spectroscopy, was chosen for this study as samples do not require preparation, as well as the results being independent of the sample thickness. ATR can also be used as a way of tracking water content in tissues, as water has a unique and strong absorption spectrum, and the water content can theoretically be quantitatively measured from spectrum [197]. Though this may not always be possible due to overlap between different molecules in a spectra.

6.3.1 Materials & Methods

ATR

For the evaluation of water content in insects of different ages an (ATR) was used. The young insects were five days after their final moult, and the oldest ones more than 180 days old. Insects of an indeterminate mid age (acquired as adults) were also examined, they were estimated to be about 14-21 days post moult. All measurements were carried out using a Thermo Scientific Nicolet is5 with a diamond background, with 16 scans taken for the background between each sample. Legs were removed from anaesthetised insects just below the tibiofemoral joint. Samples were then immediately placed under the sample holder. Damage to the tissue was avoided, and where damage was significant the sample was discarded. All the spectra were corrected and the peaks smoothed. All samples were taken at a resolution of 4 cm^{-1} and a data spacing of 0.482 cm^{-1}.

Rehydration

The hind leg was removed just below the tibiofemoral joint from sedated insects. The legs were then immediately placed in fresh deionised water, or fresh PBS solution for 24, 48 and 72 hours respectively. These samples were stored at an ambient temperature in small eppendorf tubes. After the given length of time the samples were removed from their given solutions and mounted and tested to failure via cantilever bending as outlined in Chapter 3. Once again failure was characterised by a drop in the load, and samples which were discovered to be compromised were neglected.

In the case of the samples stored in water for 24 hours, all of the insects had only one leg removed and stored in water, the other was left attached to the insect for the same length of time. When it came to test the sample the remaining leg was then excised in order to allow a paired comparison between the two legs.

Weight Loss

It had previously been noted that the tibial sections began to dehydrate very rapidly once they were excised [65]. However this study only examined loss of water in insects that were approximately 14 days post moult. This raises the question of whether or not water loss increases as insects get older? It is possible that the waxy outer layer of their cuticle gets abraded as they age, or they simply become inefficient at maintaining homoeostasis, and dehydrate, which could lead to mortality. This could also explain the increase in stiffness and UTS observed. Consequently experiments were set up to examine the loss of water over the course of three hours for insects of various ages.

Excised tibial samples were placed on a Labquip CENT 203 fine balance, and the initial mass of the leg recorded. The mass was recorded every minute for the first five minutes, then every five minutes until the thirty minute mark; thereafter recordings were taken every thirty minutes until three hours had passed. Masses were recorded to the nearest tenth of a milligram. This was done for insects up to the age of 50 days after their final moult. All tests were carried out at room temperature and were left inside the chamber throughout the course of the experiment to avoid mass changes due dust or breezes, causing an incorrect reading.

6.3.2 Results

FTIR AND ATR

Fresh cuticle was observed to lose up to 30% of its weight over the first three hours after removal. This loss was tracked over the course of 12 hours (see Figure 6.5a). A large peak is present in the fingerprint region, at 3300 cm^{-1}, a peak associated with the O-H stretching mode [198], indicating the presence of water. This peak decreases over time, with little change in peak size, only height, suggesting a decreasing number of O-H bonds. Similar investigations on insects of various ages using an ATR attachment revealed a trend. Whilst the spectra appeared to be identical, with no peak shift, or additional peaks observed, the peak height intensity for the same characteristic O-H stretching mode was greatly decreased (see Figure 6.5b).

When the average of the peak height intensities for numerous samples were taken (see Figure 6.6) the average for the young samples was 0.109 ±0.029 A.U. and the adult samples 0.065 ±0.042 A.U.. There was a statistically significant difference between the two, however the ATR equipment is vulnerable to changes in the humidity and air temperature, and the results proved difficult to replicate (the results presented having all been taken in succession.

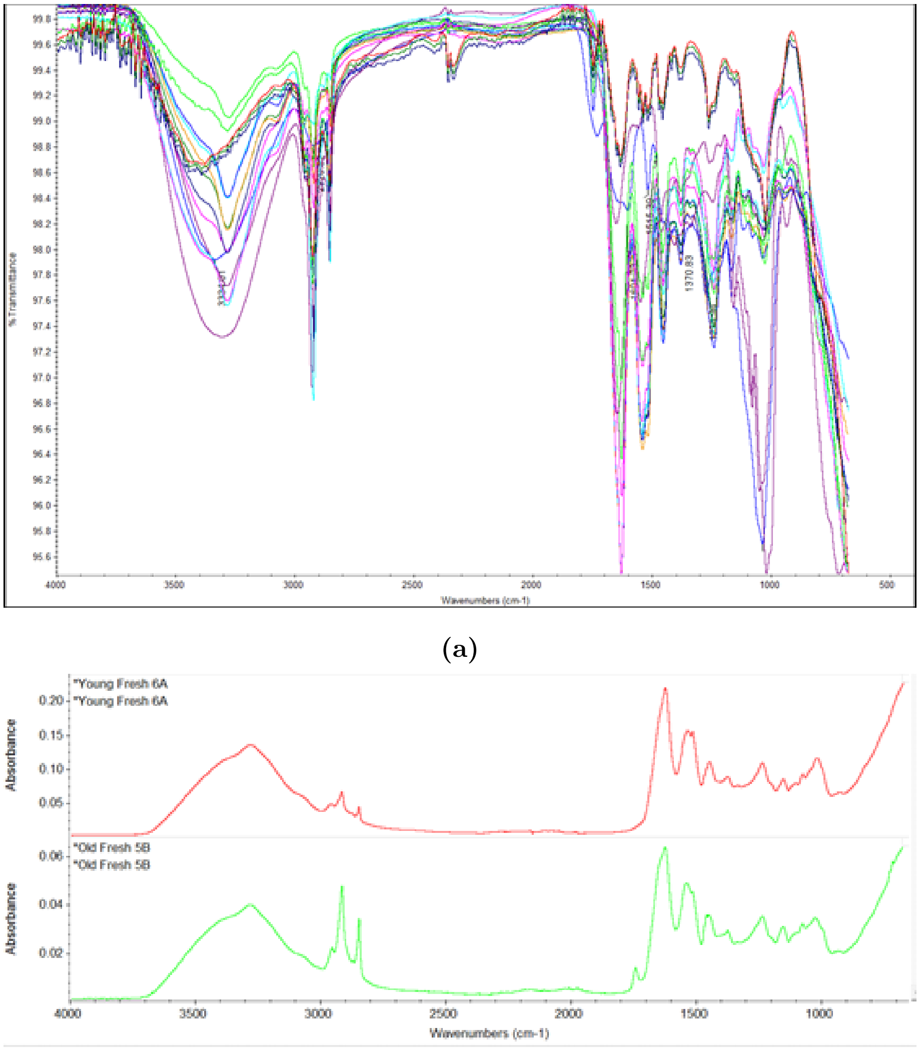

(a)

(b)

Figure 6.5: (a) Spectra of % transmittance against wavenumber recorded over the course of 12 hours, the peak associated with O-H bonding can be seen to decrease in this time period. (b) Peak intensity versus wavenumber, for old and young fresh cuticle. The height of the O-H peak can be seen to be drastically different between the two images.

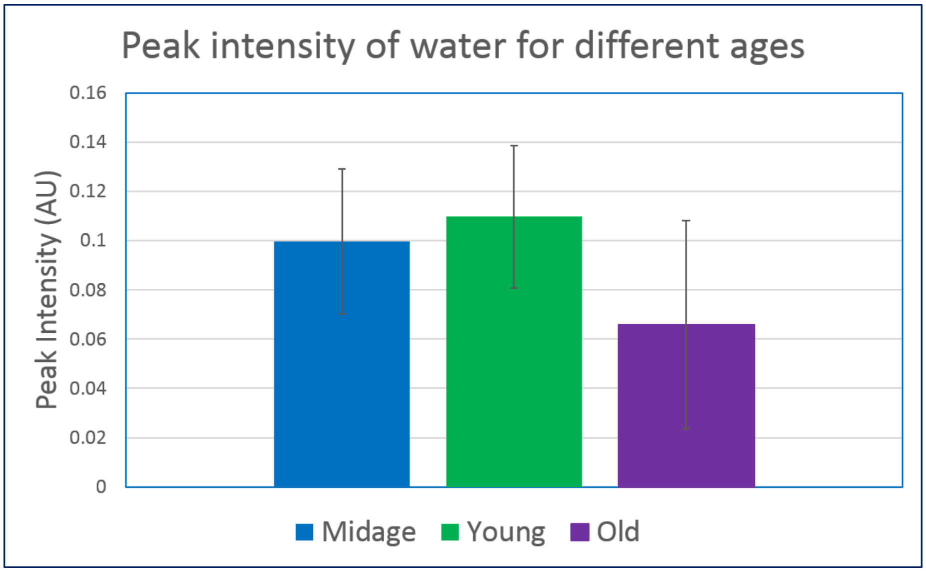

Figure 6.6: Average of peak intensity heights for (L-R) mid-age, young and old insects

Rehydration

For the samples submerged in water a decrease could be observed in both the Young's modulus and the UTS when compared to samples tested fresh, but neither were statistically significant ($p>0.05$ for both measurements). The Young's modulus for the fresh samples was 3.6 GPa and it was 3.7 GPa for the rehydrated samples. For the UTS the mean for the fresh and rehydrated samples respectively were calculated to be 186.8 MPa and 168.9 MPa.

Storing samples in PBS was similarly ineffective, with the stiffness and UTS of the stored samples increased in comparison to the controls. The stiffness and UTS of the fresh samples was 2.5 GPa and 125.5 MPa, increasing to 3.7 GPa and 157.4 MPa after storage in PBS. There was no difference between the PBS storage times.

Weight loss

The loss of water from the tibia also proved to be inconclusive. Overall the older cuticle showed a tendency to lose weight more rapidly than the younger ones, but due to large amounts of scatter in the data no trend between the different age groups could be discerned.

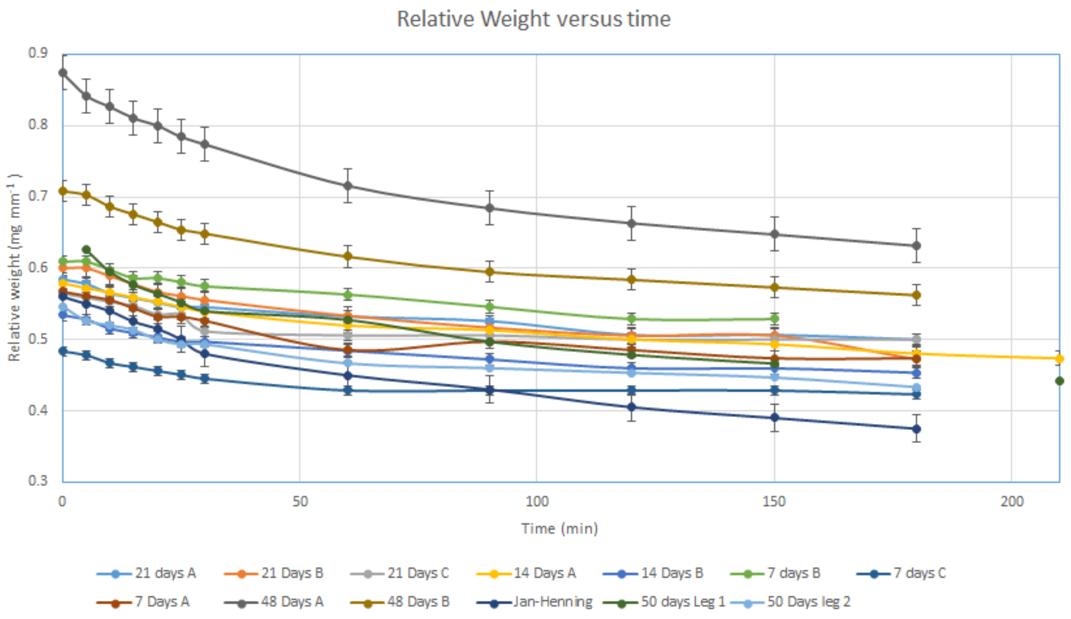

Figure 6.7: Loss of mass (as a function of mass per unit length) for insects of various ages

6.3.3 Discussion

Water was proposed as the mechanism causing this change in mechanical properties; insect cuticle is known to be strongly affected by water content [142, 199, 200]. The reason for the changes occurring with age were also sought to be elucidated.

Younger cuticle was found to have a greater water content than its older counterpart, when examining the ATR spectra. However ultimately this method was found to be difficult to reproduce, owing to the sensitivity of the machine to outside factors (it did not have a controlled environment). But even if this could be mitigated, the results were found to vary throughout the day, presumably due to how recently or how much the insect in question had eaten, a factor that would be difficult to control. Additionally due to the shape of the cuticle (a hollow cylinder) the water content being recorded is probably only in the outer layer of the cuticle, as opposed to the inner layer. The cuticle could be prepared for ATR spectroscopy in future by perhaps crushing the sample, or sectioning it to reveal the inside, but this then exposes the sample to dehydration effects, which already impact intact cuticle in less than 15 minutes [65]. Consequently these studies were not continued any further.

Samples stored in deionised water displayed a slight decrease in comparison to fresh samples. This is comparable to work carried out by Aberle et al. [182] who found that storage in water for 48 hours resulted in a slight decrease in Young's modulus, but leaving the samples for longer resulted in increasing stiffness. Storage in PBS had the opposite effect, increasing the stiffness and UTS of the tibia even after just 24 hours, indicating that this may not be an appropriate storage method for future testing.

As to the reasons why the cuticle would begin to dry out, this remains unclear. Dehydration and then rehydration of cuticle are seen to be reversible effects, indicating that the uptake of water is a fast fundamental physical effect [141]. However attempts to hydrate older cuticle back to its younger, softer, state proved to be unsuccessful, with no significant change observed for the cuticle stored in either PBS or deionised water. This indicates that the changes causing the ‘alive‘ cuticle to become stiffer are stable changes, that are not easily reversed.

More work is necessary to connect water loss with the increasing stiffness observed. It is quite possible that as the insects age, minor abrasions appear on the cuticle which can let water out, it has been well documented that abrasions make the cuticle much more susceptible to dye infiltration [201] indicating that the epicuticle can be removed. The epicuticle is known to control transpiration and water loss [202, 203], so a lack of it could easily be a problem for the animals. One way to investigate this is by raising insects in different environments, such as using sand as bedding, installing sections of sandpaper in the enclosure.

6.4 Conclusions

It was found that mating plays a large role in the changes in mechanical properties observed as the insects age, with mated insects displaying significantly lower stiffness and UTS compared to their unmated counterparts. This is important for future research, as the use of just a single sex may produce different results compared to an experiment where the opposite sex is used. Additionally the lifespan of mated females is typically shorter [147], and this may be tied to these changes in stiffness, though further work is required to see if mated females undergo the same changes but at a later point in life.

Water loss was identified as a potential mechanism driving these changes, with lowered water content found in the older insects. However the results, which were initially promising, were found to be difficult to reproduce. Further work with IR spectroscopy would be necessary to confirm these changes. If water is the driving factor, these changes are permanent stable changes, unlike those that occur in the desiccation of the samples during testing.

6.5 Future Work

Future work on this topic could involve investigating the male insects as previous studies [76, 125, 161] only used female insects. The mated females could also be studied at a variety of time points over the course of their lives to see if they suffer the same changes, just with a delay. Additionally if the stiffening happens to all cuticle, examination of softer tissue may display a more substantial increase in stiffness where changes may be more obvious. This is one possible route for further study.

Water still remains a potential culprit and further study could involve the use of an ATR machine with a controlled environment removing some of the variables in such tests. Finally various staining techniques could be conducted, in order to identify living epidermal in the cuticle, as additional exocuticle has already been exonerated as a culprit. Perhaps as the insects age they simply have less epidermal cells, or the quality of the cells reduce, which could be linked to the observed changes.

Chapter 7

Fracture Toughness of Limpet Shells

7.1 Introduction

Many biological materials fail by brittle fracture; the formation of a crack leading to sudden failure. Common examples are eggshells [204], bone [205], and insect cuticle [65]. Soft tissues such as skin and cartilage also fail by crack formation [206]. Consequently understanding how cracks propagate throughout the material is important in order to understand the function and limits of the material, as well as being essential for any biomimetic applications. Fracture toughness in biological materials is typically evaluated using two engineering parameters; the crack propagation energy (or energy per unit crack formed) G_C and the fracture toughness K_C, as discussed in more depth in Chapter 2.

Though easily defined, fracture toughness is frequently difficult to measure in biological materials due to complications such as anisotropy, difficulties with sample preparation and complex geometry (which can make obtaining traditionally shaped samples impossible). A classic example of such a problem is bamboo; different fracture toughness values ranging across three orders of magnitude have been reported [134]. This is in part due to the difficulties associated with the mechanics of the shape; through thickness bending can occur due to the curved shape of the bamboo. Hydration and temperature is also a factor when testing some biological materials, though for the limpet shells this effect is negligible, as they contain very little water. An additional factor that can complicate matters is the presence of toughening mechanisms within the material. The presence of these will mean that though crack initiation is relatively easy, as the crack gets longer, the fracture toughness gets increasingly large for continued propagation [134]. This phenomenon has been observed repeatedly in both nacre [82] and in bone where osteons act as crack stopping mechanisms [33, 207]. Consequently the calculation of fracture toughness in biological materials must be undertaken quite cautiously.

Despite the associated difficulties in measuring these values there has been increasing interest in the fracture toughness of stiff biological materials, as they often display superior mechanical properties. This observation led to a study on limpet shells, the fracture toughness of which had not been measured until recently [208, 209]. These shells primarily suffer failure due to the presence of debris in the water [133], as well as due to failed predation attempts [86]. For the species in this study, *P. vulgata*, the main failure mode is spalling, causing the formation of holes in the apex. For many biological materials, such as bone, the hierarchical structure is built in such a way that it is optimally designed to resist certain types of loading [32]. The same has been observed in insect cuticle [65]. Consequently, in addition to determining the fracture toughness of the limpet shell the study also sought to discover if the hierarchical structure or any microstructures within the shells [90, 208] act to help resist spalling.

This study primarily concerned itself with delamination cracks as these are the primary failure mode observed in *P. vulgata* [93, 209] but thickness cracks of the layers, in both a radial and circumferential direction, have all been reported frequently for other mollusc species [99, 133, 210].

7.2 Methods

For this purpose shells were impacted with either 10% or 20% of their critical energy. The required energy to cause failure of a shell of a given size could be evaluated by reversing equation 7.1, taking E_{cr} to be 8.8 $MJm^{-4.6}$, taken from Taylor [93]. The shells could then be impacted at sub-critical amounts of this energy.

$$E_n = \frac{E_c r}{L^{4.6}} \tag{7.1}$$

A detailed description of the origins of this equation and the impact test method are outlined in Chapter 3.

Before impacting the shells, they were initially polished to a smooth surface, using a polishing machine, with silicon carbide paper (P360), to remove any irregularities at the shell rim. The jagged edges can prevent the shells from lying flat against the testing plate - causing large amounts of the applied compressive forces to be concentrated in very small areas, leading to high stresses. Given the stiff nature of the shell, this can easily cause a crack to grow, leading to failure.

The length was only measured after polishing to ensure that any changes were accounted for. The shells were then loaded in a quasistatic fashion using an Instron compression machine (Instron 3366, see Figure 7.1) to a maximum load of 200 N and at a rate of 1 mm/min. This load was chosen based off of experimental results that showed that some of the smaller shells begin to crack and spall at 250N. It was sought to keep the quasi-static testing at low loads to prevent any damage to the shell. In this way the slope of the force-displacement curve could be determined and thus the stiffness of the material could be observed.

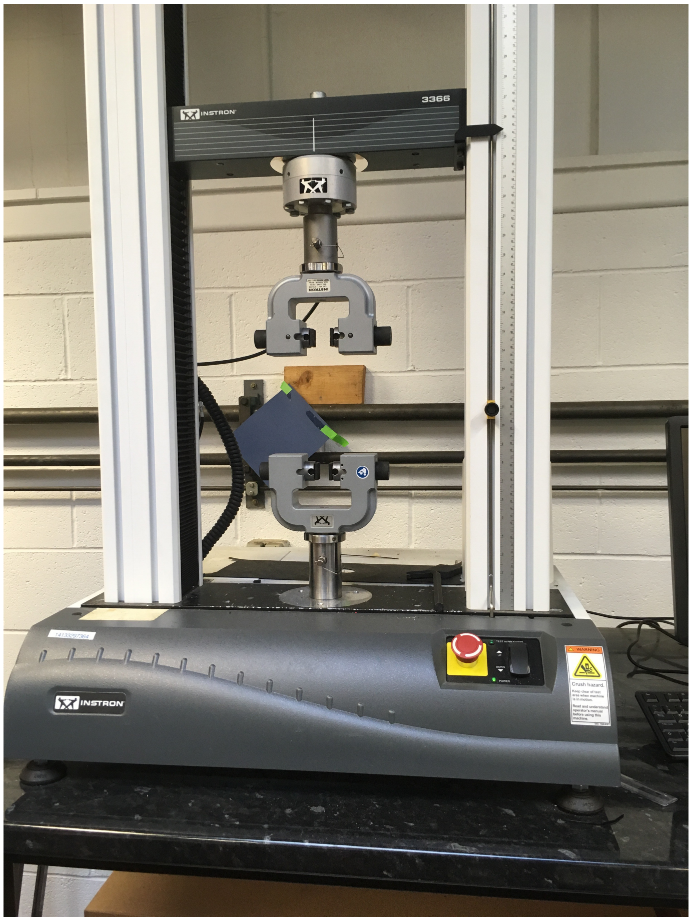

Figure 7.1: Instron machine used during testing.

The shells were then impacted at the desired force before being compressed *again*, in an identical manner. By observing the load-displacement curves of the two compressions, as in Figure 7.2, the ratio of the slopes of the two curves could be determined and used as an estimate of the energy actually used in crack formation, as opposed to other energy dissipation's such as through recoil of the weight. For each shell the energy loss is expressed as an applied energy, and there was no correlation between shell size and the amount of energy dissipated through the shell. The impact energies can then be corrected as appropriate. On average the slope decreased by 27%, as in Figure 7.2, indicating that only 27% of the impact energy went into forming cracks within the shell so this correction was applied to the energies used in calculations. As the slopes were linear until failure it is assumed that the amount of energy lost to viscoelasticity and plastic deformation is negligible.

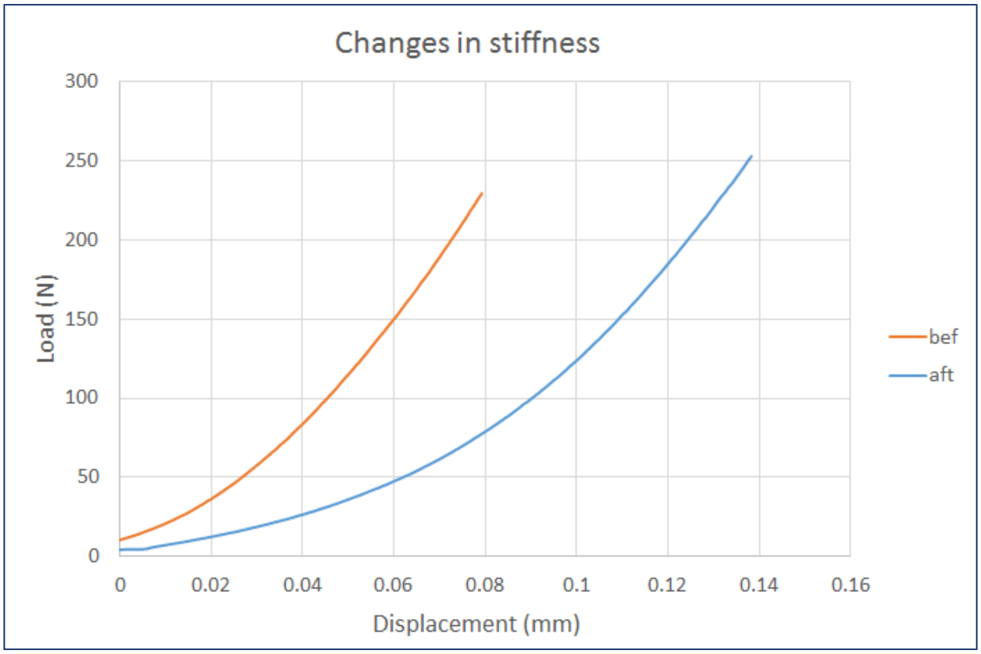

Figure 7.2: Slope of the load-displacement curve for a shell before and after impact.

Thereafter shells were initially cut through with a handsaw to remove some of the shell material before polishing. The shells were then polished using several machines (See figure 7.3), initially with increasingly fine silicon carbide paper (P360 and P800), before using a solution of diamond particles, initially at a size of 6 and then 1 μm to ensure a highly reflective surface that was free of any scratches made by the rougher polishing methods.

A light microscope (Leica DMLM) was then used to observe the cracks and record them photographically (using a Dino Lite digital microscope). The cracks were categorised into 3 different types. Type a: parallel delamination cracks, type b: cracks that run parallel and suddenly jump between laminae, and type c: running perpendicular to them, and finally cracks that ran from one surface of the shell to the other. They were also categorised by the location of the crack in the shell. Region 1: in the apex, region 2: the middle of the shell, region 3: or at the rim. This categorisation of crack types gives an insight into the distribution of energy throughout the shell and the way in which the damage propagates. A schematic of the shell with the regions and examples of the crack types included can be seen in Figure 7.4.

KNUTH-ROTOR
PHOENIX 4000
Jean Wirtz

(a)

Figure 7.3: Images of the polishing machines used.

The crack lengths were measured using ImageJs Fiji software [174]. Knowing both the crack length and the number of cracks, the work of fracture for the shell could be calculated. This was done by treating the crack as a semi-annulus and making the assumption that any vertical section taken was typical of the overall shell, and as such that any crack observed can be assumed to visible on every section around the circumference [208]. In this way the area of the crack can be calculated as

$$A = \frac{\pi}{2}(R_{1i}^2 - R_{2i}^2) \tag{7.2}$$

Where R_{1i} and R_{2i} are the longest and shortest radius of the annulus. This area can then be multiplied by the number of cracks in the shell to give the total area of the cracks.

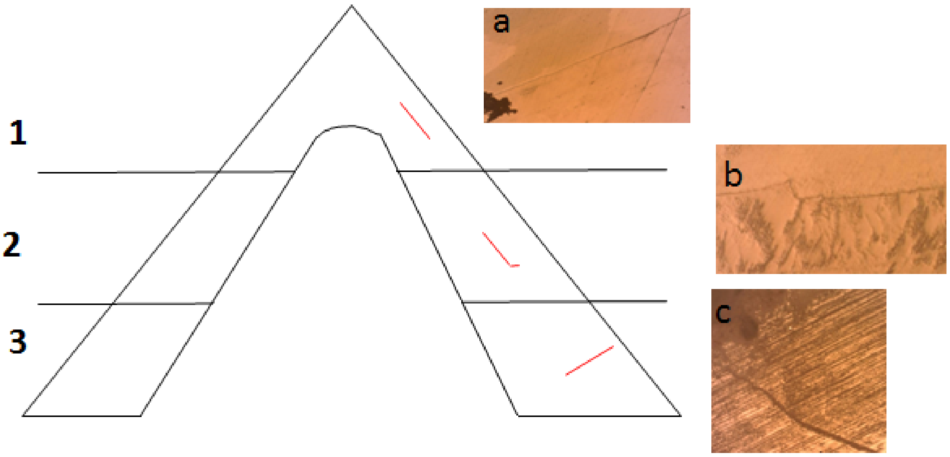

Figure 7.4: Different regions and crack types indicated on the shell. Example images of the three different crack types can be observed.

The change in the total area of the cracks between the shells impacted at 10% and 20% can then be caclulated as the difference in the areas. This can be combined with the impact energy can be utilised to calculate the crack propagation energy value G_C

$$G_c = \frac{\Delta U}{\Delta A} \tag{7.3}$$

Where ΔU is the change in energy, i.e. the change in energy between the shells impacted at 10% and 20%. The fracture toughness can then be calculated from G_c

$$K = \sqrt{GE} \tag{7.4}$$

10 shells were tested impacted at 10% of their impact energy and 10 more were tested for 20% of their impact energy.

7.3 Results

The number of cracks in each sample, the length of their cracks and the cracks location can be viewed in the table below.

640 cracks were counted across all 20 samples. The vast majority of the cracks were delamination cracks, making up 87 % and 83 % of the cracks in the 10 % and 20 % groups respectively, indicating that this is the main failure mechanism. This aligns with

% of E_{cr}	10%	20%
Samples	10	10
cracks (± s.d.)	24.1 ± 9.2	39.8 ±13.6
crack length (± s.d.)	2.7 ± 1.8 mm	2.7 ± 2.1
Crack location		
apex	77 %	73 %
rim	10 %	5 %
main body	13 %	22 %

Table 7.1: The number of samples in each group, the number of cracks, their length (mm) and a percentage breakdown of where in the shell cracks were found.

the behaviour observed in shells impacted at higher energies, as these typically fail due to spalling at the apex. Although the initial impact energy is only 10 % of the expected critical energy, doubling the impact energy to 20 % caused the number of cracks to nearly double. However despite the increase in impact energy, the average crack size across both groups was found to be 2.7 mm with increases in impact energy only increasing the number of cracks. The average length of the cracks is also uniform across the various regions of the shell.

The majority of the cracks (73-77 %) form in the apex of the shell, where the shell is at its thickest, rather than the lower, thinner, regions, suggesting that the apex of the shell may be designed to absorb the damage from the blows.

The crack propagation energy can be calculated using Equation 7.3 and was found to be 150 Jm^{-2} ± 21 Jm^{-2}. Then taking E= 46 GPa [136], and using Equation 7.4, the work was found to be 2.6 MPa$m^{\frac{1}{2}}$. This value is much higher than can be expected for pure calcium carbonate. This can be explained when examining the shells under SEM. Though initially the fracture surface seems quite smooth, roughness on a variety of scales can be observed. In Figure 7.5a, macroscale roughness can be observed on the exposed surface of the shell. This may serve to deflect cracks, forcing them to twist around, and delaying their growth. In Figure 7.5b individual crystals and layers can be observed. The fact that the cracking and separation of these layers occurred in a staggered fashion suggests that the cracks have to twist around between the layers in order to propagate. And finally, the layers of the shell have a structure similar to a corrugated iron roof, with many small

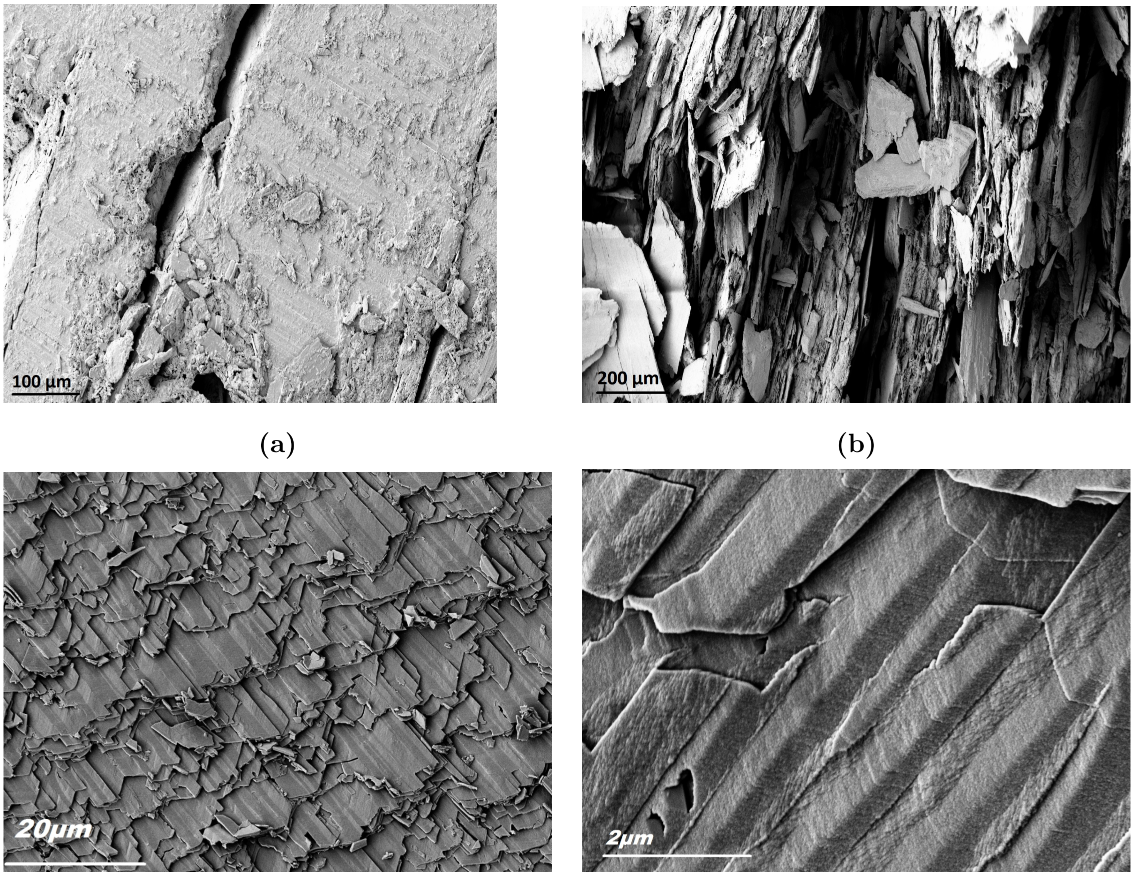

(a) **(b)**

(c) **(d)**

Figure 7.5: SEM photos depicting the layered structure of the shell, along with the nano-structured pleats. (a) and (b) are images of shells polished to reveal the surface. (c) and (d) are of spalled material after a fracture and by Dr. Dooley.

‘pleats‘ approximately 100 nm in height protruding from the layers surface. This can be observed in Figure 7.5c and 7.5d. When impacted the shells layers will experience a mixture of compression and shear stresses. It is expected that these pleats would then ‘lock‘ together between different layers, resisting shear movement, and helping reduce the stress intensity at the cracks. It is assumed that these pleats exist due to the crystal structure of the layers.

7.4 Discussion

The experiments proved to be a valid and successful method of measuring delamination toughness in limpet shells. The value for fracture toughness, K_{IC} of 2.6 $MPam^{\frac{1}{2}}$ is lower than the value reported for nacre. Barthelat and et al [82] reported K_{IC} values of 5.2 $MPam^{\frac{1}{2}}$ from crack initiation, up to 11.6 $MPam^{\frac{1}{2}}$ during propagation for nacre , with the increasing values due to nacre's toughening mechanisms. Though the value found for the limpet shells is substantially lower than that of nacre, it is an order of magnitude tougher than its constituent parts, with pure calcium carbonate (in its calcite form) having a fracture toughness K_{IC} of $\approx$ 0.2 $MPam^{\frac{1}{2}}$. Evidently, similar to nacre [7, 81], the limpet shells must contain some toughening mechanisms. Other natural materials, such as eggshell that are also made of calcite, but without any complex microstructures, have toughness values comparable to pure calcite, with eggshells having a reported K_{IC} value of 0.3 $MPam^{\frac{1}{2}}$ [204].

This toughening effect can be related to the complex microstructure making up the shells, alternating layers of aragonite and calcite as discussed by Oritz and et al. [94]. Whilst these layers have been investigated, little work has been done examining how these microstructures affect the toughness of the shells. This study found several scales of roughness in both the shell structure and the individual layers [208], which may help resist the propagation of delamination cracks. On a macroscopic scale there is evidence of some roughness in the shell structure which may deflect cracks, conferring some toughness, as observed in Figure 7.5a. On a microscopic scale, in Figure 7.5b, individual crystals can be observed. The layers appear to be staggered, which once again may be acting as an additional toughening mechanisms, as any cracks are forced to travel along the length of the crystal face. Finally on a nanoscale, many small asperities, similar in appearance to a corrugated iron roof can be observed, in Figure 7.5c and 7.5d. These layers potentially lock together when the shell experiences compressive forces, which then resists separation of the layers under shear stress; a combination of compressive and shear stress being what is expected when a shell is impacted. This indicates that similar to bone, which displays trabeculae oriented in such a way to resist their main loading conditions [32], the shells have adapted to resist impacts, one of their primary failure modes. This works in addition to the overall structure of the shell, where the spines, ribs and curvature can help to strengthen the shell further [92].

This study only investigated crack propagation in a single direction. Though this is the primary mode of failure some shells were observed to fail due to the propagation of cracks from the rim of the shell. Consequently at the same time as the study outlined in this chapter, several other fracture modes were investigated, outlined in O'Neill et al. [208]: through thickness cracks propagating in both a radial and circumferential direction. The fracture toughness (K_{IC}) value for cracks propagating in the circumferential direction was evaluated by machining small samples of the SENB type from the shell, and introducing a notch, before testing with a 3-point bend test. It was found to be 0.98 $MPam^{\frac{1}{2}}$. Though considerably lower than the values reported for nacre and other shells, it is still substantially larger than that of pure calcium carbonate. Some toughening mechanism is at work, presumably linked to the macro and microscale roughness which may deflect cracks as they progress through the shell. The difference in the two values for delamination toughness and cracks in a circumferential directions also highlights how the shells have evolved additional resistance to impacts.

Attempts were also made to determine the fracture toughness (K_{IC}) for cracks growing in the radial direction. However due to the shape and curvature of the shell, it was not possible to machine samples for testing in the radial direction. Instead a notch was made into the shell before beginning compression testing, and recording the force to failure. FE models were then created to investigate K_{IC}, however the results proved somewhat less successful, generating very high values for the toughness, being very sensitive to the boundary conditions used. More complex models that include all the features of the shell may help to bring greater clarity. Additionally this study also found that even when the cracks were several mm in length, only slightly less energy was required to cause failure, indicating the shells are well designed to resist crack growth developing from the rim. Un-notched samples primarily fail at the apex, and one of the notched samples did too, indicating some competition between the two failure modes. It also indicates that the shells have evolved resistance to failure from crack propagation at the rim.

Though only two of the methods used were reliable, they demonstrate the shells resistance to crack propagation, both between layers and for cracks propagating through the shell. Delamination failure is a weakness in building materials in layers, and it is a common failure in many layered composites, with smooth cracks running along the edges where layers meet [135]. This can lead to failure via spalling, which is very common in building materials, such as concrete [139].

7.5 Conclusions

This outlines the first published study to measure the fracture toughness of limpet shells, along with their cracking and failure behaviour. It was found that impact tests reliably cause delamination cracks to form in *P. vulgata*, ultimately leading to failure due to the collapse of the apex, though occasionally failure due to crack propagation from the shell rim was observed. This delamination indicates a fundamental weakness associated with layered structures. The crack propagation energy was found to be 0.15 kJm^{-2} and the fracture toughness for delamination to be 2.6 $MPam^{\frac{1}{2}}$. Reliable estimates for cracks propagating in the circumferential direction were also determined, with the fracture toughness being 0.98 $MPam^{\frac{1}{2}}$.

Delaminated shell material had a smooth surface but scanning electron microscopy unveiled an array of roughness on a variety of length scales that may serve as toughening mechanisms. One of these mechanisms was nano-asperities: regular, ordered pleats of $\approx$ 100 nm in size, observed within the shell structure. These pleats may aid the shell in resisting crack propagation and delamination failure when experiencing shear and compress

This optimisation of a material to resist specific loading conditions is quite common, and observed in materials such as bone [32], and is achieved on a variety of length scales. Consequently nature can be identified as an ongoing source of inspiration for materials design, particularly in the use of traditionally brittle composites.

7.6 Future Work

One potential avenue for future work can be identified from this study is the development of more sophisticated finite element (FE) models that incorporate the ridges on the shell which may help to stiffen the shell. Measurements in the radial direction proved to be unreliable, and more sophisticated FE models could address this challenge too, as well as including the tendency for radial cracks to deviate to the circumferential direction. This may give greater insight into how the cracks grow through the shell and how the microstructures resist and deflect them. Further investigations into the microstructures could also be carried out, and perhaps more identified at different length scales by looking at samples from various portions of the shell. Those presented here were all taken from the apex region, and different mechanisms may be in place at the rim of the shell.

Chapter 8

Repair & Remodelling in Limpet Shells

8.1 Introduction

Limpets and other molluscs rely on shells to protect them: if the shell becomes damaged this may significantly impair its function. There are several ways in which a shell can become damaged. Not primarily from wave action, as limpet shells can resist much larger forces than those produced by waves [91], but due to failed predation attempts [86]. Another important factor is the presence of small debris in the water, such as stones and pebbles. Shanks & Wright [133] found that in areas with large numbers of loose pebbles the population of limpets was much smaller than in similar areas with fewer pebbles. A similar effect was observed by Cade [210] with regards to ice scouring and rocks in the Antarctic. This damage typically presents itself as cracks or holes in the apex region of the shell, or at the rim where the shell meets the rocks [99, 210]. This is problematic not just due to increased predation risk but also due to the threat of desiccation at low tide, due to the loss of water through the damaged shell. These threats mean that it is important for long lived gastropods to be able to repair their shells and it has been known for some time that molluscs are capable of repairing injuries to prevent their death. The presence of these repairs has even been used to determine common predators [91, 211]. These repairs often leave scars on the shell in the form of large protrusions with jagged edges. Blundon and Vermeij [131] found that these scars do not act as fault lines, having little effect on crushing resistance. However this study only examined fully healed shells, with no consideration for a period of weakness that may have occurred whilst the repair was being carried out. This is significant as the amount of time it can take for shells to fully repair damage can range from 1-4 months [80, 100], depending on the species and water temperature. Repair usually initiates as an occlusion of the holes or damage site [101, 212, 213]. However initially this material is easily removed, leaving the shells very vulnerable. Finally it is quite plausible that a shell could sustain some damage that does not pierce the shell fully. Whether or not limpets are able to detect such damage and repair it, or if the damage persists as a fault in the shell remains an open question that this work seeks to answer.

The ability of the limpet shells to respond to even more subtle repetitive damage was also evaluated. Taylor [93] found that the shells perform very poorly in fatigue conditions; with the single impact failure energy being 8.06 $MJm^{-4.6}$ and that for fatigue being only slightly higher at 10.58±6.2 $MJm^{-4.6}$. A plot of the normalised impact energy against the number of impacts to failure (N_f) can be seen in Figure 8.1. The data follows a linear slope, except at large values of N_f. This shows that damage accumulates almost linearly in the shells. Consequently it can be expected that limpets struck repeatedly at low energies will fail rather quickly unless they are able to respond to repeated stressors, as opposed to the large impact incidents.

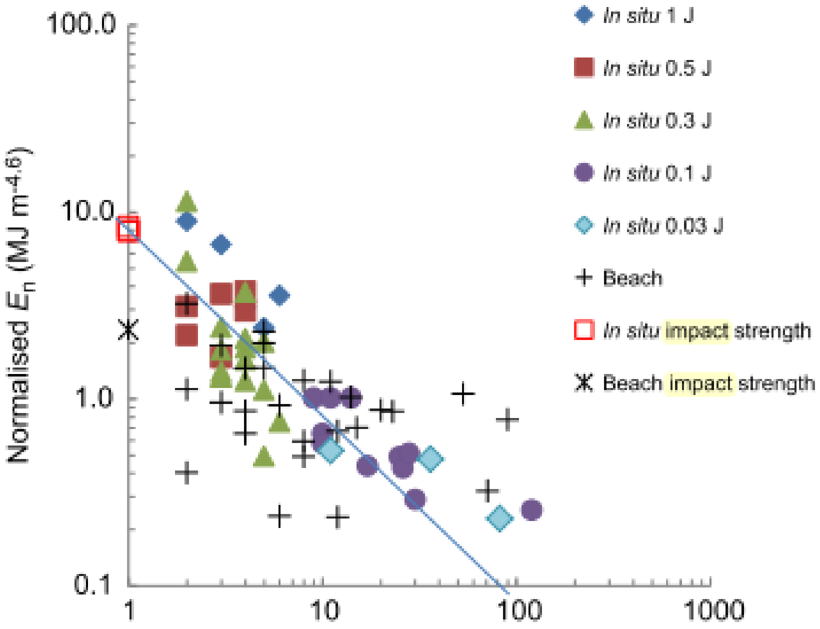

Figure 8.1: Plot of E_n against N_f. The straight line represents a constant value of the total accumulated E_n, here 8.06 $MJm^{-4.6}$. Graph taken from Taylor [93].

Linear accumulation of damage is unusual even for stiff composites; if you stress the material at 50% of its failure strength it will not fail after two loads-it is common for composites to endure a number of cycles several orders of magnitude higher than this [214–216]. Though for a biological material remodelling might be possible - in fact this is the very thing this study set out to investigate - this behaviour is very poor. Cortical bone cycled at roughly one third of it's ultimate tensile strength (UTS) can withstand close to 100,000 cycles before failure [171, 217]. This means limpets are especially vulnerable to repeated damage events, such as a proliferation of heavy storms, something that will get more likely as global warming continues. As a result it seems reasonable to assume that limpets and indeed other molluscs, have some ability to remodel and respond to small amounts of repeated damage. This study sought to to evaluate this hypothesis.

It has been speculated before that the apex of the shell acts as a sacrificial point in the shell, absorbing most of the energy of the impact and protecting the rest of the shell and the animal inside [93]. Sacrificial points are not uncommon in nature, although they are generally in the form of sacrificial bonds, such as hydrogen structures in bone, that break following impact and absorb energy whilst increasing fracture toughness [5]. Consequently the potential role of the apex as a site to absorb damage is not unprecedented.

8.2 Materials & Methods

The energy to failure for shells was evaluated through impact testing, as outlined in Chapter 3. Sub-critical impact damage to shells was also carried out in the same fashion, but with smaller weights or lower heights utilised to ensure the impact energy was lower.

8.2.1 Compression testing

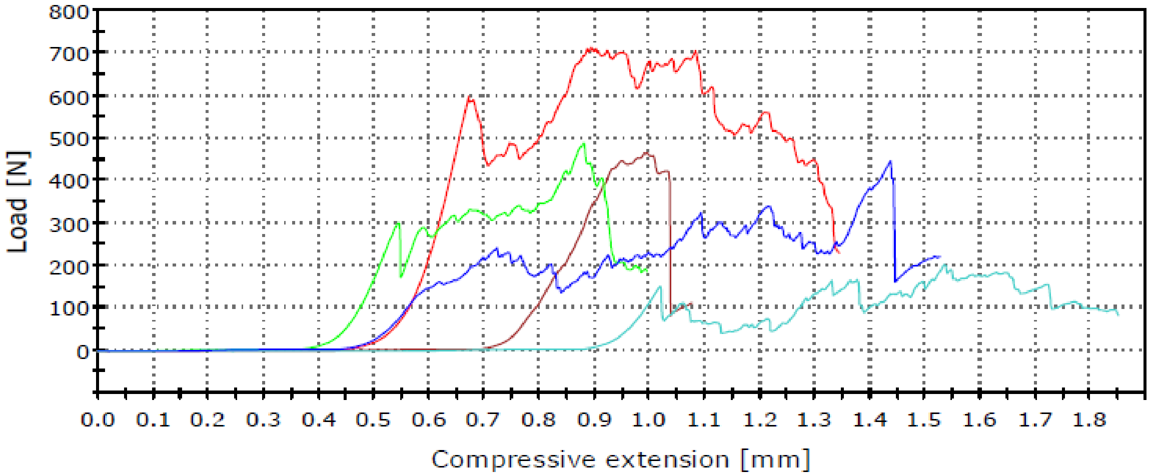

Figure 8.2: Typical load-displacement curve produced by the Instron. The different colour lines represent different tests.

The strength of the shells was investigated via quasistatic compression testing using an Instron compression machine (Instron 3366), as discussed previously in Chapter 7. The shells were polished to a smooth surface as in the previous study. Shells were then tested at a rate of 1 mm/min, focusing the force on the apex. The machine then produces a load-displacement force, an example of which can be seen in Figure 8.2.

Intact shells and shells that were collected from the beach (shells that were found empty with significant abrasion due to the sand) were tested, along with shells that had been manually abraded and some that had been impacted with 0.3 J of energy before being left to repair for 30 days. This was to see if the abrasion had any significant effect on strength and to see if quasi-static testing was an effective way of investigating shell strength.

8.2.2 Damage Repair

Three different types of damage were investigated. The first consisted of an impact of 0.3 J to the apex of the shell. This was applied to shells which were sufficiently large so that the impact was non-critical (i.e. it did not cause immediate failure). The second type of damage recreated natural abrasion (caused by sand) by using a metal file to remove material from the apex. The final repair case involved the creation of a small hole in or near the shell apex, using a nail (diameter 2.5 mm). In each case some shells were damaged and immediately collected. Other shells were left at the rocky site and groups collected at the following time points; 10, 30 and 60 days. For the shells with holes, shells were also collected at 63 days. The number of samples in each group can be seen in Table 8.1. Shell location varied slightly depending on the type of damage. For shells in the impacted and abraded categories, limpets in open locations attached to flat rocks were chosen, the rocks being near-horizontal for the impacted group. Previous work [93] had found that limpets with holed shells in open locations tended to die quickly, possibly due to dehydration or predation, so in the present study holes were applied to limpets in more sheltered locations, in crevices. Fresh undamaged shells were also collected at the same time to serve as controls. Shells in all damage categories were subjected to impact testing as described in Chapter 3.

At the same time, additional shells in the abraded, impacted and control groups (n= 10-12) were sectioned vertically through the apex and polished down using silicon carbide paper (P360) to measure thickness of material at the apex. These shells were not tested to failure like the others, as doing so would destroy the apex and make investigations

	Impacted	Abarded	Apex hole
0 days	14	11	21
10 days	-	8	-
30 days	20	16	-
60 (63) days	33	12	16

Table 8.1: Number of shells tested for each type of damage and time period. For the apex hole shells the time period was actually 63 days as above. In cases where no data is given either an insufficient number of shells displayed repair at that stage to collect them, or the number of shells chosen were all of the same size.

impossible. Consequently they are not included in the numbers indicated in Table 8.1. Thickness was measured using both an electronic vernier callipers and a toolmakers microscope. Apex thickness is reported as a percentage of shell size (L), in order to allow comparisons between shells of different sizes. (Regression analysis of length as a predictor of thickness $R^2_{adj} = 66\%$). A relationship between thickness and length has been previously identified in other species, the results are comparable to that reported in this study [91, 99]. Shells were then examined under SEM, following the protocol outlined in Chapter 3.

8.2.3 Fatigue & Remodelling

Shells were tested cyclically by impacting them at 10% or 20% of their critical energy, leaving them for a given time period before impacting them again over a four month period. 221 samples were considered as four groups, controls, those impacted with 10% of the critical energy every week, and those impacted at 20% of their critical energy week or every two weeks. The number of samples in each group can be seen in Table 8.2.

Limpets were chosen in a range of sizes from 26 to 46mm, and only those living on a horizontal surface were considered. All shells chosen lived within a small range of rocks, so that at most individual limpets were not more than a few metres apart, to reduce any habitat variability. Shells were measured *in situ* using a callipers. The impact equipment described previously (see Chapter 3) was modified slightly: additional notches were added to the tube, and a variety of weights (28.9, 57.9, 115.6 and 231.3 g) were used. This of

Shells	Impact Energy	Repair Period
57	10%	weekly
54	20%	weekly
63	20%	fortnightly
46	-	-

Table 8.2: Number of shells tested for each energy level and the repair periods. The final group are control shells; they were monitored to ensure no outside factor we were not aware of was influencing our results.

varying weights and heights allowed the delivery of an impact as close as possible to 10% or 20% of the shells critical energy. The shells were also measured at every time interval to avoid a build up of systematic errors.

After each session shells were classified as follows: survived if the shell was intact afterwards, missing if the shell could not be found, broken if the shell had developed a hole before being impacted (presumably due to predators or wave action), or failed if the impact caused the apex to break.

Shells were then prepared for microscopy by polishing the shell down across the thickness to the apex, as outlined in Chapter 3.

The effect of injury location, and the ability of the apex to absorb damage was also investigated, by making holes either on or off the apex of the shell, that is on the side of the shell, close to the top, (rather than the rim of the shell). The impact energy of the shells were then evaluated, in the same manner as before to investigate if there was any noticeable effect.

8.3 Results

8.3.1 Quastistatic testing

After testing of the shells by applying a compressive load, the results of the fresh and the beach shells (i.e. those that had been naturally abraded) were grouped into boxes by size (18-25, 26-30, >30, and >40 mm) to allow for increasing strength as shell size increases. There is a relatively large size effect on strength; unsurprisingly as shells get bigger the strength of the shell increases. Fitting regression models shows that in both cases the relationship between size and force is statistically significant ($p<0.05$). It can also be seen that the presence of sand abrasion drastically reduces the strength of the shells compared to their intact rock counterparts, and this decrease holds true across all size groups (see Figure 8.3a). However the relationship between force and size is constant across both intact and beach shells, with the slope of the models being the same ($p>0.05$). These models and data are plotted in Figure 8.3.

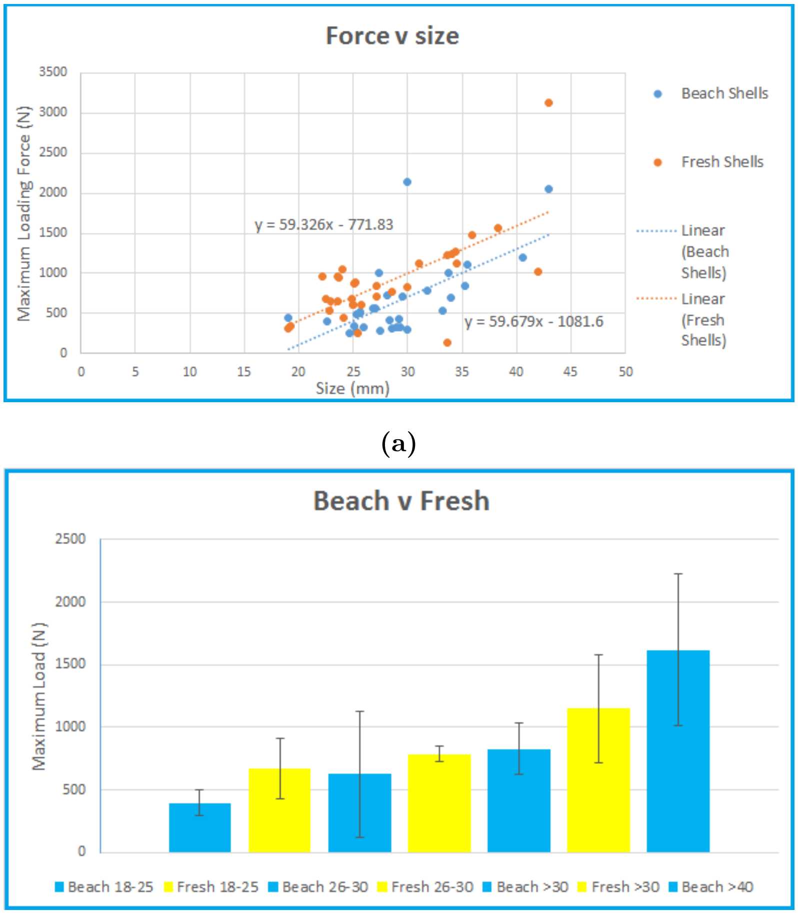

(a)

(b)

Figure 8.3: (A) Regression models fitted to data from both fresh and beach shells. The gradients indicate a strong relationship between size and force to failure. (B) Force for failure for size bins of beach (yellow) and fresh (blue) shells. Data for the fresh shells bigger than 40 mm is not included as only two values occurred here, one of which is a significant outlier, disrupting the graph.

The shells that were manually abraded, all the shells that were collected were under

26 mm. A statistically significant decrease was found in the force at failure between the two groups ($p<0.05$), representing a fall of a third in the strength of the shell.

The impacted and then repaired shells, these samples all ranged in size from 26-37 mm and were compared to shells of a similar size. No significant decrease in strength was observed ($p>0.05$).

8.3.2 Mechanical repair

Shells were damaged in one of three ways: abrading the apex, impacting with 0.3J of energy and making small holes. After leaving the shells for various time periods to repair they were collected and tested. Over the course of this repair periods for the abraded category none of the animals were lost. For the impacted shells 6% were lost over the course of the tests, a loss rate we did not consider to be abnormally high. For the shells containing holes the rate of loss was much larger: 50% after 63 days.

A control value the normalised failure energy for shells with no pre-existing damage was calculated to be 8.3 $MJm^{-4.6}$. Immediately after impact the strength of the damaged shells decreased to approximately half of the control value, to 4.2 $MJm^{-4.6}$. After 30 days of repair this increased to 5.14 $MJm^{-4.6}$, and after 60 days repair was complete, at least from a mechanical perspective. At this time point the shells were statistically indistinguishable from their control counterparts with strengths of 7.10 $MJm^{-4.6}$. This represents a repair of 86% of the original failure strength. These results are presented in Figure 8.4a.

The same trend of increasing strength with repair was also observed for the abraded shells. Abrasion had a significant impact upon the shells failure energy, reducing it to just 2.52 $MJm^{-4.6}$. This is comparable to results found by Taylor [93] who found that shells on beaches suffered natural abrasion from the sand, presenting much more blunted apexes. This resulted in a decrease in the energy to failure for the shells. However when the shells were left to repair for 30 days the strength was repaired back to 5.0 MJ$m^{-4.6}$. As for the impacted shells, after 60 days repair was mechanically complete, with the failure energy of the shells back to 7.55 MJ$m^{-4.6}$, representing a 91% repair of the original energy. At this point they were statistically indistinguishable from controls shells. These results are presented graphically in Figure 8.4b.

Results for shells with small apex holes were not as clear. As for the two previous cases, shells were examined at 10 and 30 days but there was little evidence of repair at this stage, bar some white deposition around the site, but this was easily dislodged. Shells were examined again after 63 days and at this point sufficient repair had occurred that they were collected. At this stage the shells had repaired their failure energy back to 6.6 $MJm^{-4.6}$, representing a 79% recovery of the control value.

8.3.3 Thickness and Deposition

During the mechanical testing of the damaged samples, additional samples at each time point from the abraded and impacted categories were collected and the thickness of the apex examined. 10 days after the initial impact shells were statistically thinner than intact control shells ($p<0.05$). However by 30 days the shells had increased their thickness by a significant amount ($p<0.05$), corresponding to the increase in failure energy observed. No significant difference in thickness was observed between shells after 30 and 60 days ($p>0.05$), though after 60 days shells were still statistically thinner than their control counterparts ($p<0.05$). As after 60 days the mechanical strength is almost completely restored this suggests that the shells may have other strengthening mechanisms available to them. The effect of thickness upon impact energy can be seen in Figure 8.4a.

Similarly, and not surprisingly, when given no time to repair the abraded shells were significantly thinner than their intact counterparts, having lost about two thirds of their total thickness ($p<0.05$). As with the impacted shells, this thickness increased over time, reflecting the improvement in strength observed. After 30 days the shells were significantly thicker than immediately after abrasion ($p<0.05$), but little increase in thickness was observed over the next 30 days ($p>0.05$). After 60 days, as with the impacted shells, although the strength has increased until it was almost comparable with the control samples, the thickness of the shells was still statistically less than the controls ($p<0.05$).

After thickness measurements had taken place, many of the same shells were examined by SEM to search for evidence of repair. Figure 8.5b depicts a shell impacted and investigated after 60 days passed. There is little to no obvious evidence of repair, with lots of cracking and delamination evident. A large void between the layers is evident, presumably caused by spalling of the material. There is nothing to indicate any repair

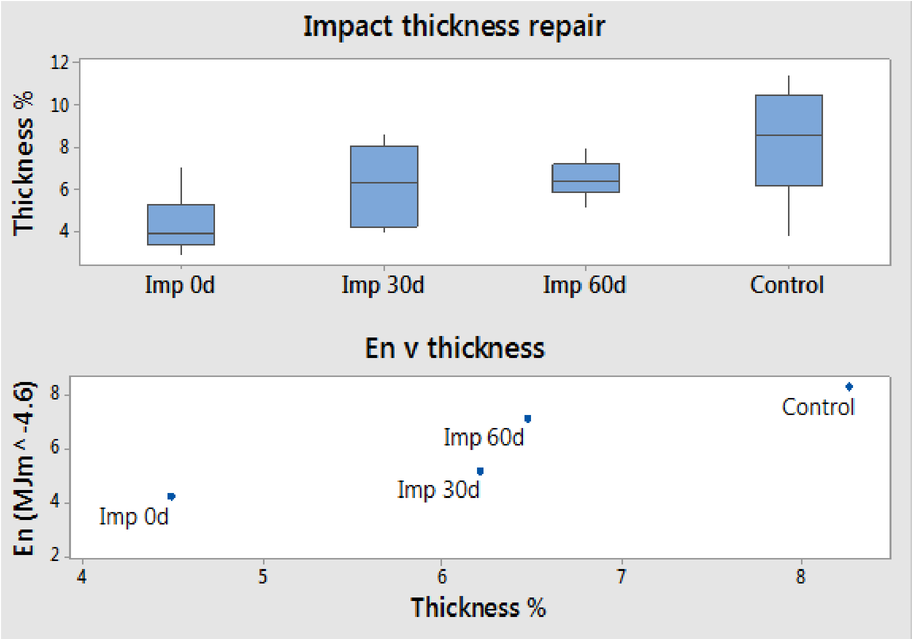

(a)

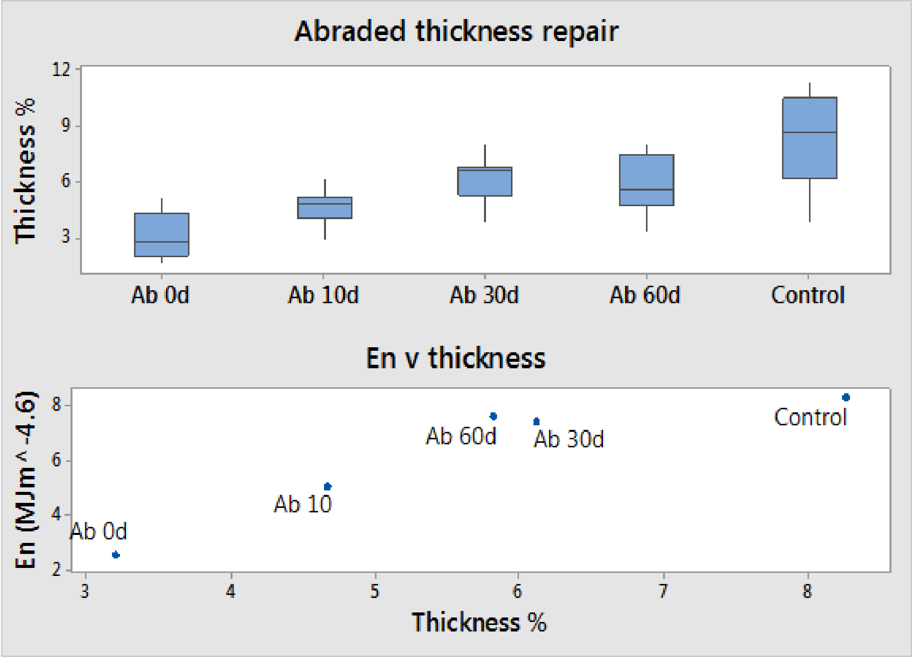

(b)

Figure 8.4: (A) Increasing apex thickness for impacted shell, over time. This correlates with the increase in impact strength depicted in the lower plot. It can be seen that the mechanical strength approaches the control values even as the thickness remains reduced. (B) Increasing thickness for shells that were abraded and then left to repair. The same trend is observed as for the impacted shells.

to the damaged layers, especially at the apex of the shell, suggesting any and all repair must occur on the inside of the shell. In Figure 8.5c an abraded shell can be observed. There is no evidence of any damage through the thickness of the shell. This once again indicates that all repair must occur on the inside of the shell. However, in neither case is fresh deposition abundantly clear, suggesting that it may be indistinguishable from normal growth material.

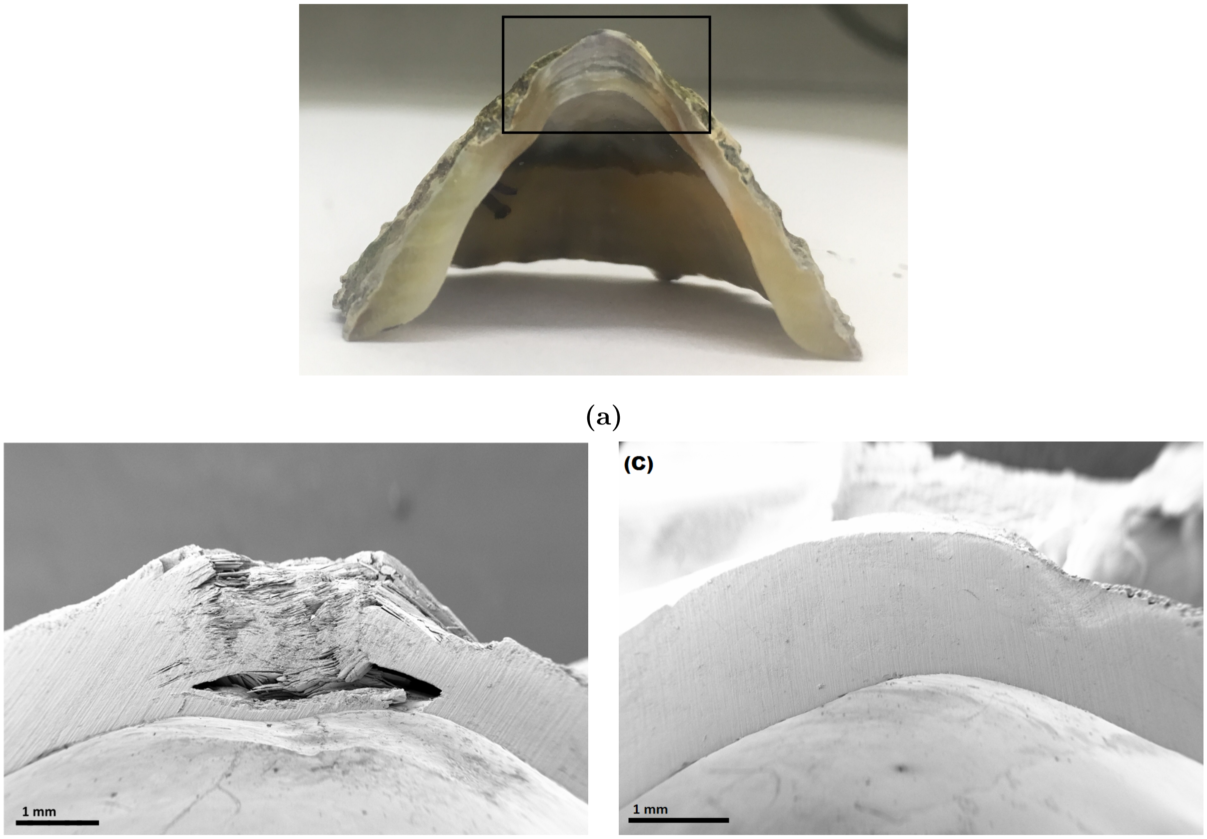

(a)

(b) (c)

Figure 8.5: (a) Depicts a shell polished down to expose the thickness through the apex. In this way thickness can be measured and the internal structure and damage can be seen under SEM. The apex of the shell has been indicated with a black rectangle. (b) Depicts a shell impacted with 0.3J and left to repair for 60 days. Evidence of damage is still clearly present. (c) Depicts a shell abraded and left to repair for 30 days. In contrast to (b) there is little evidence of damage.

8.3.4 Crumple Zones

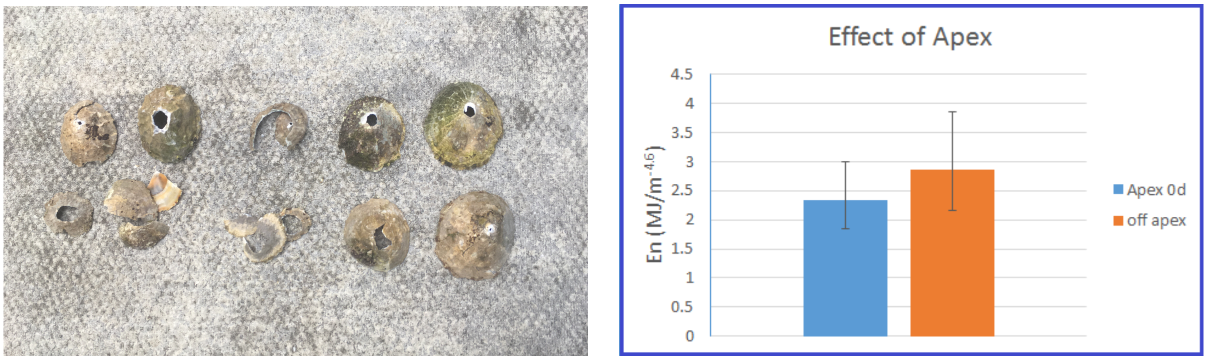

(a) (b)

Figure 8.6: (a) Depicts a variety of shells with holes either on or slightly off the apex that have failed. (b) Depicts the effect of hole location upon the impact strength for shells with holes on their apex, and those with the holes moved slightly off centre.

The location of the injury was found to make a statistically significant difference ($p<0.05$) to the energy required to cause failure. A hole through the thickness of the shell caused a drop in strength to 2.2 $MJm^{-4.6}$. Placing the hole just slightly off the apex had a large effect, with the strength now being reduced to 2.8 $MJm^{-4.6}$. This suggests that the apex is designed to absorb energy in an impact to prevent overall failure of the shell. This is highlighted in SEM images of damaged shells through the apex, such as Figure 8.6b which shows that most of the damage is confined to a narrow band around the apex, with little damage spreading outward.

8.3.5 Fatigue Behaviour

Shells were found to be very susceptible to fatigue failure. The damage a shell receives accumulates inside the shell in a very linear fashion.

An early problem encountered in this study was the occurrence of hurricane Ophelia, a very rare weather event in Ireland's normally mild climate. Ophelia struck on October 16th resulting in unusually large waves and very high winds, particularly concentrated in coastal areas. Unfortunately as a result a number of samples were lost, particularly in the groups that were impacted at 20%. The number of shells lost can be seen in the table below.

	10% (weekly)	20% (weekly)	20% (fortnightly)
Loss	7%	31.5%	38.1%

Table 8.3: Number of shells lost across groups during Ophelia meteorological event. Results presented as percentages

All of the control shells survived the impact, indicating that though the shells had only received a couple of weeks worth of impact at this stage, damage was beginning to accumulate inside the shells. None of the shells lost in Ophelia were considered for further analysis, though the potential weakening of surviving shells could not be mitigated.

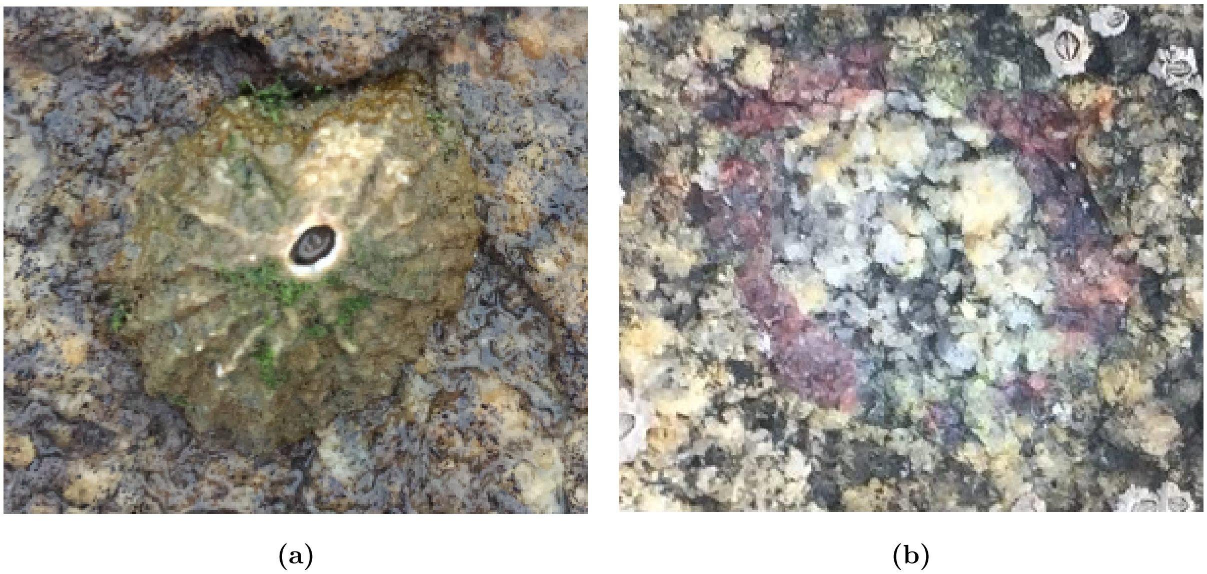
(a)

(b)

Figure 8.7: (a) A shell found broken with the animal still inside (b) Imprint on a rock where a shell once was; the animal has gone missing and its grazing scar is left behind. Photos taken by R. Mala.

Ultimately the goal here was to see if the limpets are capable of remodelling their shells when experiencing frequent damage - damage accumulates in a linear fashion in the shell, so if the shell can survive a number of impacts that in total exceed its critical energy it can be thought of as responding to and repairing this damage. Shells that are found broken or go missing in between impact events are consequently somewhat problematic, as we do not know the exact reason for the loss. It can be assumed that this is due to the repeated impacts - the shell accumulates damage until it is barely held together before being washed off, or eaten as the damage makes it more susceptible to predators. These data points are recorded separately to shells which actually failed under impact. Examples of this sort of damage can be seen in Figure 8.7. The results can be seen in Table 8.4.

% impact energy	Energy	Survived	Missing	Broken	Failed
10% (weekly)	140%	42.3%	50%	7.7%	-
20% (fortnightly)	140%	40.5%	54%	5.5%	-
20% (weekly)	260%	2.5%	82%	7.7%	7.7&-
Control	-	97.8%	2%	-	-

Table 8.4: Cyclical loading outcomes. The accumulated energy is written as the percentage of the shells critical energy, taken to be 8.3 $MJm^{-4.6}$. All results are percentages

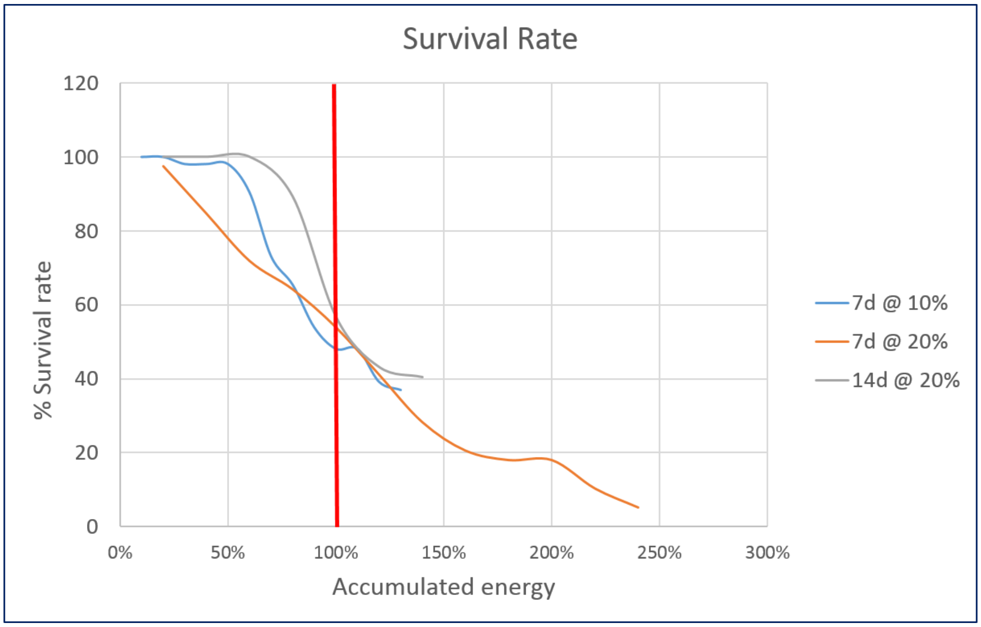

Figure 8.8: Survival rates of the three groups with varying impact energies evaluated, corrected for the effects of hurricane Ophelia. The red line marks the point where the accumulated energy meets the critical energy.

The groups impacted at 10% every 7 days and 20% every 14 days displayed similar survival rates, with a little under half of the shells surviving in both cases. The third group, impacted at 20% every 7 days did very poorly, with nearly all of the shells having failed by the end of the experiment. However it must be noted that these shells absorbed twice as much energy as the other groups, so this increased failure rate is to be expected. If the percentage of surviving shells is plotted against the accumulated energy, after correcting for the effects of Hurricane Ophelia (removing shells lost in this storm from the results and the total number of shells in each group) another interesting trend emerges: The shells impacted at 20% every 7 days start to experience a high rate of loss almost immediately, beginning at 20% of the critical energy, with a reasonably steady rate maintained thereafter.

A little over half of the shells were still intact when the accumulated energy reaches the critical energy. In sharp contrast, the shells impacted at 20% every 14 days only suffer their first loss when the accumulated energy hits 80% of the critical energy, with the number of surviving shells falling rapidly thereafter, with roughly half of the shells lost once the accumulated energy reaches the critical energy. A similar trend is observed in the shells impacted at 10% every 7 days, though they begin to experience a fall off in numbers earlier, with shells beginning to be lost once the accumulated energy reaches at 30% of the critical energy. Just under 50% of the shells were still intact once the accumulated energy reached the critical energy. This data can be seen in Figure 8.8.

The overall survival rate at 100% of the critical energy is 50%, comparable to what would be expected if simply impacting the shells in a consecutive manner, as some would fail before or after the accumulated energy, with some scatter, as seen in Figure 8.1. That some shells survived up to 140% of their critical energy (in this case 40-42%) does indicate that some remodelling process may be occurring, but it is still within the realms of what could be scatter.

If remodelling processes are occurring, the mechanism of repair once again is quite unclear. When looking at the SEM photos (see Figure 8.9) as for the repair groups discussed above, there is no clear signs of repair. Figure 8.9a depicts a shell impacted every 14 days at 20% of its critical energy, close to half of the apex appears to have spalled away, with extensive delaminations in the remaining material evident. Internal delamination of the shell can also be seen. Figure 8.9b is an even more extreme case of a shell impacted every 7 days at 20% of its critical energy. The apex is very badly damaged, seemingly consisting of layers barely held together. In this case the damage seems to spread much further, with much larger pieces having already been lost to spalling. It is quite evident that higher impact energies result in greater internal damage to the shell, explaining the greater fail rate, not that this was a surprising result.

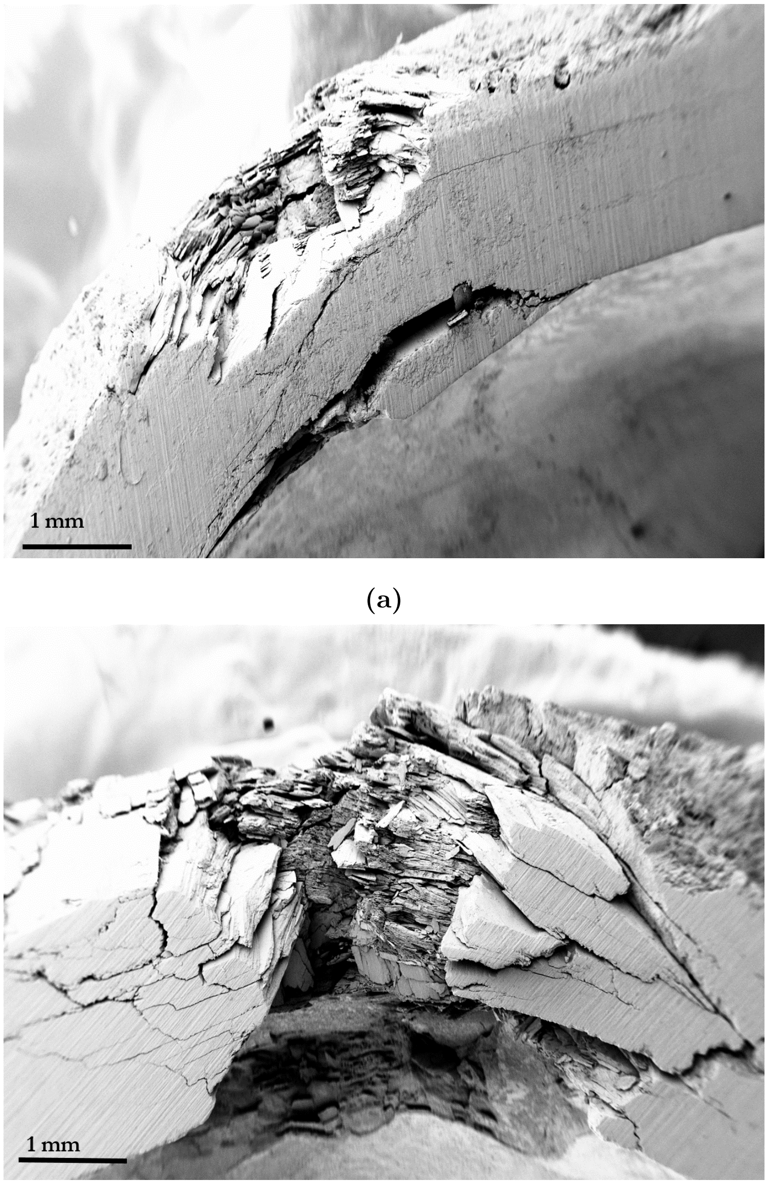

(a)

(b)

Figure 8.9: (a) Shell impacted at 20% of its critical energy every 14 days (shown here after reaching 160 % of the critical energy) (b) Shell impacted at 20% of its critical energy every 7 days (shown here after reaching 240% of the critical energy)

8.4 Discussion

8.4.1 Quasi-static testing

Ultimately it was necessary to abandon the use of the quasi-static testing when testing the shells, for several reasons. Though up until now it has been the most used test when investigating the strength of shells [91, 131], it has always led to a large amount of scatter in data. Even when the shells are polished smoothly, it is difficult to prevent stress concentrations, unless testing on the exact site of the shells initial location. This is not always practical or even feasible when using traditional machines such as the Instron described in this study. Additionally it was frequently difficult to identify the exact moment when the shell failed. Occasionally a crack developed and the load-displacement curve fell rapidly when the shell failed. However typically the shells fail due to the destruction of the apex; in this case the gradient of the compressive force versus displacement declines very gradually with many minor peaks, gradually crushing the apex and corresponding layers. This made it difficult to determine when the apex initially failed, as opposed to the force applied just leading to a larger hole forming. This led to inconsistent results and as a result impact testing was determined to be the best course of action for further investigations.

8.4.2 Repair

In this study shells that were given time to repair experienced modes of failure consistent with those observed by previous researchers [133, 210], with most shells failing due to formation of a large hole at the apex. Many empty shells with holes in the apex were observed in the area of the test site, suggesting that hole formation is a large cause of mortality in the species, as well as indicating that the damage presented here is similar to damage that occurs naturally. Shells with evidence of repair in them were noticed during these experiments (and were described previously in the literature by Taylor [93], Harper and et al. [99], Cadee [210], Checa [218]), indicating that repair is something that happens naturally, rather than as an artefact of the experiments, though the causes are difficult to determine.

The results show that limpets are very effective in repairing damage to their shells.

After 60 days, for the impacted and abraded shells strength had been restored to 92% and 83% of the control values, respectively. The process was slower for the shells with holes in them, with shells being restored to 79% of the control strength after 63 days. This longer timescale is presumably due to the greater magnitude of the damage. Whilst the damaged part of the shell may be smaller than in the other cases, it penetrates the whole shell, and the repair process takes longer. Additionally it is possible that the newly-formed occlusion material is washed away by high tides, as it is easily dislodged, causing the limpets to have to begin repair once more. This may explain why some limpets were unable to repair holes even after long periods. Similarly the apex seems to act as a sacrificial point in the shell [93], absorbing most of the damage (see section 8.4.3).

The results showed an approximately linear relationship between the energy needed for impact failure and the thickness of the shell at the apex (see Figure 8.4). This differs from the much stronger effect of limpet size on failure energy, which was previously established to scale to the power of 4.6 [93]. The scaling of impact strength is strongly dependent on material and specimen type. For the abraded shells the reduced strength was expected to be caused by the reduction in thickness, so this was no surprise. What was not expected was that this also turned out to be the case for the impacted shells. In fact the relationship between energy and thickness was found to be almost the same for the two groups (see Figures 8.4a and 8.4b). This suggests that the main reason for loss of strength after impact is not the internal damage (visible in Figure 8.5) but the reduction in thickness, which occurs due to surface compression and loss of material by spalling, both internally and externally. This finding also merits further investigation, to elucidate more systematically the relationship between impact strength, damage and thickness.

The fact that the limpets are able to repair the non-critical impacts and also the damage done by abrasion raises other questions, namely how the animal is able to sense the damage. In neither of these cases is the shell pierced. The limpets could perhaps sense the impact damage due to the internal crack formation, but in the abraded case it remains unclear. The animal may be able to detect increased stress and strain in the shell, both during the damage event and later, as water passes over the shell. This would be a very interesting subject for future work. Additionally these results could be used to create characteristic finite element models, similar to those published by O'Neill et al. [208] to model crack propagation through the shells. This would allow greater insight into how stresses are dispersed throughout the shell at the time of impact.

How the limpets are actually repairing their shells is another question that requires further investigation. The shells are getting increasingly thicker over time. This suggests that deposition of fresh material could be the repair mechanism. This would make sense, as this is also the manner in which the shells grow, by depositing material on the inside of the shell. It is also a repair mechanism widely observed in arthropods, such as in insects [4, 70, 152]. However when viewed under SEM, in neither the impacted nor abraded case is fresh material evident. But this could be due to the fact that as the shell was not completely breached, the limpet did not have to plug the damage, and rather had time to repair by normal, gradual deposition, which would be indistinguishable from normal growth. Given the size of limpets which we examined, they can be assumed to be at least 5 years old. During the repair process they were able to more than double the thickness of their shells near the apex over two months, which suggests that they were depositing material in this area at a much faster rate than normal. This implies a system of deposition targeted to the appropriate area, involving cells capable of detecting and orchestrating a specialised repair process.

But the continued increase in impact strength compared to controls even as the thickness lags behind does suggest another factor may be at work. The new layers the animal is depositing could be reinforced in some way, or could have a different crystallographic structure or arrangement of organic layers, such as identified by Suzuki et al. [219].

The time required for repair varied depending on the type of damage. Abrasion was speedily repaired, being mostly complete after 30 days; after impact damage the strength continued to increase approximately linearly up to 60 days (the end of the test period), and the repair of holes was likewise incomplete even after more than 60 days. This could indicate an inability to withstand multiple blows or predatory attacks occurring over a relatively short timescale of the order of weeks. This might explain the smaller number of limpets observed by Shanks and Wright [133] in areas with lots of very small pebbles rather than areas with many large boulders. In this study no such comparison could be made, as the sandy area nearby had little to no rocks suitable for limpets to live on, and a large amount of human foot traffic which would dissuade the growth of limpets.

8.4.3 Crumple Zones & Fatigue Behaviour

It has been suggested before [93] that the apex of the shell acts similarly to crumple zones in cars, i.e. it is a sacrificial point designed to fail and absorb damage, protecting the overall structure [220]. This was found to be the case with the limpets; damage was primarily reserved to the apex of the shell, with little extending further into the rest of the shell, preserving the more important structures within. This is especially evident, as damage to the apex dramatically decreases the strength of the shell. Moving the damage slightly off the apex leads to a comparatively stronger shell; Whilst it is still damaging to the shell, the apex is still somewhat intact. However forces and stresses from off apex damage may distribute stresses and forces in a different way, causing greater structural damage that could propagate throughout the shell - it may also lead to an increased chance to damage to the animal itself. FEA modelling could be utilised here to try and understand how damage spreads through the shell, but as the mechanisms involved are impact based it would be technically difficult. However, despite the reduced effect of placing the damage off the apex, in both cases damage through the shell (i.e. through to the animal) requires extensive repair, even if the area affected may be smaller than for impact damage, as discussed in greater detail above.

This also has an effect upon the fatigue behaviour of the shells; Just as it is not a good idea to get back in and drive a car with a crushed bonnet, the shells react poorly to repeated loading, presumably due to the destruction of this crumple zone, as even minor impacts of 10% or 20% of the critical energy can cause extensive delamination.

How shells respond to this damage, and whether they are able to repair it is what this study aimed to elucidate. No shells actually failed during the tests when impacted, even when the critical energy had been comfortably exceeded, with 40% of two groups surviving when the accumulated energy had reached 140%. However many specimens began to be lost as the accumulated energy reached the critical energy. Figure 8.8 with only approximately 50% surviving past the critical energy in all three groups. It is evident the shells are not designed to endure multiple blows. Whether it points to some remodelling process similar to bone, that enhances fatigue performance, remains to be elucidated. It is quite common for biological materials to exist below their lifetime safety factor [160], using remodelling processes to maintain integrity, but the large number of shells lost means the survival rate could be purely due to scatter. However the loss rate includes shells that went missing or were found broken between the time intervals, and the fate of these shells cannot be definitively known. Few control shells went missing during this time period, so the higher rate loss can be ascribed to the shells being weaker due to the damage, but the exact cause cannot be known, as predation both from sea birds and other gastropods that bore into the shells are other factors that can impact survival. Further studies are required to confirm whether or not the shells are capable of repairing damage, either by reducing the amount of damage, perhaps 5% every 2 weeks, or 10% every 3-4 weeks, as the current data is to unclear to come to definitive conclusions about remodelling processes.

Why all 3 groups have roughly the same survival rate at the 100% accumulated energy but have different paths to this point remains to be explained. This result has been corrected for the effects of Ophelia, so particularly inclement weather can be somewhat ruled out as a factor. It is intuitive that the group impacted at 20% every 7 days suffers the first loss-that the group impacted every 14 days only experiences losses when the energy reaches 80% indicates that if a remodelling process is occurring, it is able to mitigate the initial damage due to the increased time between impacts, though these capabilities begin to be exceeded after two months of repeated impacts. This is also supported by the behaviour of the 10% group impacted every 7 days. Large losses in the number of shells begin at 60% of the critical energy, falling at a steeper rate than the group impacted with 20% every 14 days. Though the energy being imparted with each impact is higher than for the 10% group the longer time interval seems to be the determining factor, at least in the earlier stages of the study. The 10% every 7 days group however falls at an even steeper rate than the 20% every 7 days group; the reason for this is unclear.

Unsurprisingly shorter repair times and higher energies led to much higher loss rates. This is also evident in the much larger amounts of damage evident in the samples impacted at 20% - even getting images of the samples was very difficult, due to the fragile nature of the apex. Consequently this indicates that whilst there may be a remodelling process at work in the shells, 2 weeks is an insufficient time to repair damage at least when impacted regularly. For example, for a shell of 35 mm in length, an impact energy of 10 % would correspond to 0.17 J. Consequently a shell impacted every 3 weeks may fare better, with impacts of 0.3 J taking between 4-8 weeks to fully repair [209]. Even the abraded shells which suffered no internal delaminations required 4 weeks to fully restore mechanical strength, which may be the limit of increased deposition of fresh shell material, it is not yet clear if such a limit is due to limits in the mechanism of shell repair or if it is due to environmental constraints, such as insufficient quantities of calcium ions in the water.

8.5 Conclusions

This study represents the first work examining how limpets repair their shells and how the mechanical properties change during repair. Impact studies were found to be the most effective means of investigating the mechanical behaviour of the shells. The quasistatic testing previously used has several major drawbacks and is a poor representation of the loads experienced in nature. Impact testing produced much more reliable results, suggesting a revision to the status quo.

It was revealed that limpets have the ability to repair damage to their shells. Though previous workers have noted the capacity of these animals to repair through-thickness holes [99, 210], it has been discovered that they actively respond to other, more subtle kinds of damage. The limpet is able to sense the reduction in the strength of its shell as a result of external abrasion or low-energy impacts, and to take action to restore that strength in a relatively short period of time.

Measurements of the thickness of the shell at the apex suggests that the main effect of low-energy impact and abrasion is a reduction in thickness, which correlates linearly to the impact energy needed for failure. During the repair process the thickness of the shell increased, as did the impact strength of the shell, so the deposition of fresh shell material is believed to be the main method of repair, though the fresh material could not be identified specifically. However after 60 days the shells were still statistically thinner than the controls. Consequently there may be some other strengthening mechanism at work.

The ability of the limpets to remodel their shells when experiencing multiple more minor loading conditions, and their long term fatigue behaviour was also evaluated. The shells were found to perform very poorly in fatigue, with damage accumulating in a linear fashion. Ordinarily, shells impacted repeatedly fail as soon as the accumulated energy meets the critical energy. This is presumably due to the crumple zone behaviour of the apex, which is unable to withstand multiple blows. When given some time to repair between impacts, over half of the shells were still intact, more than would be expected to be seen if the shells were consecutively impacted. Though it is not definitive, and further experiments are required to confirm that these increased survival rates are not purely scatter in the data, it does seem that the shells are capable of some amount of remodelling of more minor damage.

8.6 Future Work

This work itself raises several further questions. The most obvious of which appears to be how the shells are actually strengthening after repair, in addition to the fresh deposition of new material. This is possibly due to changes in the crystallographic structure of the new material, a question that could be answered using crystallographic techniques such as electron beam scatter diffraction, utilised successfully by Suzuki et al. [219] to identify differing layers of calcite and aragonite. That a reduction in thickness is the main reason for loss in strength also merits further investigation. How the shells sense damage is another mystery yet to be elucidated. Related species have mechanoreceptors in their bodies [221], and it may be possible that those in the limpet shells are sensitive enough to detect the changes in the stiffness of the shell. The explanation for the scaling of the impact energy with an exponent of 4.6 is also unclear and merits further investigation, for example using computer simulations.

Chapter 9

Conclusions

This work has focused on the mechanical properties of insect cuticle (*Schistocerca gregaria*), and limpet shells (*Patella vulgata*), with an emphasis on how they respond to damage, and their ability to repair changes in their mechanical properties after damage has occurred. The results of this thesis are compiled in Table 9.1, where they are compared to bone, a widely studied biological material, and steel, a widely used human-made material. These comparisons are made to give greater insight into how properties vary across the natural world, as well as the advantages and disadvantages associated with using human-made materials or biological ones.

	Bone	**Cuticle**	**Shell**	**Steel**
Young's Modulus (GPa)	20	5	46	200
Energy Density (MJ/m^3)	3.3	12	1.38	50
U.T.S (MPa)	150	158	48	500
Repair time (weeks)	6-12	1-3	4-8	N/A
Repair Mechanism	Tissue regrowth	Deposition	Deposition	N/A
Scaling Relationship	Length L^3	Thickness t^4	Length $L^{4.6}$	Length L^3
Lifespan	>70 years	≈ 6 months	>30 years	Usage dependent
Structure	Hierarchical: collagen fibres form lamella-orientation & % of hydroxyapatite affect bone type	Hierarchical: chitin nanofibres in protein matrix. Arrange in lamella. Extent of bonding influences properties	Hierarchical: layers of calcite & aragonite, & small amounts of proteins & organic matter	Microstructure varies with phase or phases.
Humidity Effect	Strongly affected	Strongly affected	Potential effect at very low values	N/A

Table 9.1: N/A means this effect does not occur in this material. Scaling relationship displays the property that the UTS of the sample scales with. For cuticle all values are reported for insects 4 weeks after moulting. The scaling relationship is valid for the first 3 weeks.

The beginning of this work focused upon the desert locust cuticle. Younger insects were found to be more effective at repairing injuries than their older counterparts, confirming a link between age and repair capability in insects. Despite the difference in the effectiveness of the repair, both groups carried out repair in the same manner, via the targeted deposition of new cuticle. It was also discovered that injuries have a greater effect on older insects than their younger counterparts. Small puncture injuries had a large effect on older insects, but negligible effect in young ones. This was linked to the fracture toughness of the cuticle in various age groups, with older insects having a fracture toughness less than half that of their younger counterparts. This leads to minor injuries becoming more serious due to the potential for crack propagation from the initial site. This corresponds to similar effects observed in bone, where older samples are more brittle and prone to fracture.

Having elucidated a greater understanding of how the mechanical properties of cuticle and repair ability change with age, the next area of research was to investigate if the insects could respond not just to macroscale damage, but microscale damage too. This was done by applying a stress to living tibia, and then leaving it to repair for various time periods. Cuticle was found to be a viscoelastic material, behaving as a stiffer material when loaded more rapidly, as well as undergoing significant hysteresis when cyclically loaded. The tibia itself also suffers a large degree of apparent plastic strain, $\approx 20\%$ after one cycle. This indicates that the cuticle is absorbing a large amount of energy, potentially leading to microscale damage, presumably via the formation of microcracks, though they could not be explicitly identified. The presence of damage is confirmed via the large reduction in stiffness between cycles, with the stiffness in the second cycle half that of the first, too large a value to be explained by viscoelastic behaviour alone. The insects were capable of repairing this damage within 1 week. How the insects are sensing this microdamage remains to be determined though it is quite possibly linked to the campaniform sensilla, which may experience local stresses or strains if a microcrack occurs near them. It also raises further queries about the reduced fracture toughness of older cuticle; if it is more prone to defects and breaking its energy storage abilities would also be affected. This ability to detect and repair microcracks is similar to effects observed in bone-mammalian bone is constantly remodelling to repair microscale cracks, before catastrophic failure occurs.

Having identified the effects of ageing on the mechanical behaviour of insect cuticle, how it repairs damage, and the link between these two factors; triggers, and mechanisms for these changes were investigated. Whether or not the insects had mated proved to have a very strong effect on the mechanical properties, with the mated females displaying none of the increasing stiffness observed in their unmated counterparts. This change was tenuously connected to loss of water from the insects cuticle. This ties in with the mechanical results in the prior studies; the critical crack length for older cuticle was substantially smaller than that for the younger insects. However the results were ultimately inconclusive and further work is necessary to confirm if a dehydration process is really occurring.

The concept of mechanical behaviour and repair was expanded upon and then applied to a second organism, the common limpet. Initially the work focused on determining the fracture toughness of the shells. The crack propagation energy and fracture toughness were found to be 0.15 kJm^{-2} and 2.6 $MPam^{\frac{1}{2}}$ respectively, approximately half that of nacre. This is still an order of magnitude higher than pure calcium carbonate, reported to be $\approx$0.2 $MPam^{\frac{1}{2}}$. One of the explanations for this difference is the intricate microstructure observed in the shell. This could be observed on a variety of length scales, from macro to nano, with various structures all acting to deflect cracks, hampering their growth. The most notable of these was the presence of nano-asperities with the appearance of multiple 'pleats'. It is hypothesised that when the shell experiences compressive and shear loads, as it does when impacted, these layers lock together and resist shear movement, helping to prevent delamination. Such strengthening microstructures are well documented throughout the natural kingdom: bone possesses numerous microstructures that prevent crack propagation, increasing the toughness.

Whilst carrying out the fracture toughness study, it was noticed that the shells have remarkably poor fatigue performance, typically failing once the accumulated impact energies surpassed the critical energy. This would seemingly leave them very vulnerable to repeat impacts unless they are capable of repairing sub-critical damage.

Shells were found to be able to repair damage to their shells, even damage that did not fully pierce the shell, though how they detect such damage remains to be seen. Impacts, abrasion and small holes were all found to dramatically reduce the strength of the shell, with the impact strength being just 30-50% of the intact shells. After 60 days all three groups of shells were able to repair strength such that they were statistically indistinguishable from their control counterparts. For the abraded and impacted shells, an increase in shell thickness was identified as one mechanism of repair, similar to the cuticle repair observed in the insects. The shells were still statistically thinner than controls, even after mechanical strength was restored, indicating that some other unidentified strengthening mechanism is at work. The shells ability to remodel when experiencing consistent, repeated stress was also investigated to examine if when given time between impacts, the shells can produce a better fatigue performance. This was found to be the case, with numerous shells surviving past the critical energy. However further studies are required to confirm if this effect is real, with longer time scales. The apex of the shell was found to be acting as a crumple zone for the rest of the shell, absorbing the majority of the damage in an impact. This can be linked to the poor fatigue performance observed, as the sacrificial behaviour of the apex means extensive damage occurs even at lower energies.

Finally, though all of these findings are very novel with respect to the organisms in question they reflect similar research and findings in mammalian bone, to which comparisons have been made throughout this thesis. The repair process of the cuticle and shell are similar, involving deposition of fresh material. This is in contrast to bone where the damaged material is removed and replaced, indicating that nature has evolved a variety of mechanisms to repair damage, a feature sorely lacking in human-made materials such as steel. These differing mechanisms may affect the time the repair takes with cuticle able to repair damage in as little as one week, with bone potentially taking several months. Limpet shells fall between the two. This also corresponds to the lifetime of the animal, with locusts being much shorter lived, which may be a factor in repair mechanisms. Bone scales in a manner similar to steel, with larger samples being stronger [222]. For the shells the relationship is more complex scaling to the length of the shell raised to the power of 4.6. This is comparable to the insects where the strength scales with the thickness of the cuticle to the power of 4. The UTS of bone and cuticle are reasonably similar, albeit less than half that of most steels. The shells perform more poorly, being an order of magnitude lower, but this is presumably due to them being designed to resist the compressive forces associated with impacts, rather than tensile forces, as reported in this table. The

Young's modulus and energy density of all 3 biological materials is an order of magnitude lower than that of steel. The values for bone and the shells are very similar; this is not surprising as they are both primarily ceramic composites, though the value for the shells may be higher as the energy density here is once again for tests in tension, and they may perform better under compression. The energy density of cuticle is 3 times that of the other two biological materials, which may be linked to its role as an energy store when jumping. From these comparisons it is evident that though biological materials display poorer properties than that of materials such as steel their ability to repair enables them to exist below their lifetime fatigue limit. This is in stark contrast to human-made materials which need to be over designed with large safety factors at work to prevent premature failure.

The work presented here, whilst primarily blue skies research does have several avenues for biomimetic applications. The microstructures observed in the shells could be applied in future composite design. As ceramic matrix composites become increasingly popular, their lack of toughness remains a concern, and toughening microstructures are a potential solution. The presence of the crumple zone observed in the apex could also be used in the design of ceramic parts exposed to impacts, such as turbine blades and bird strikes, to limit damage to a single zone, preventing catastrophic failure. How the shells repair an acellular material is also of potential interest. Most repair mechanisms documented in mammals rely on the proliferation of cells, something that is not currently feasible in human-made materials. The mechanisms by which the shells detect damage (though still unknown) and repair strength may be a more realistic method for self-healing materials. The means by which the insects sense damage, through deformations of the campaniform sensilla would be an ideal mechanism for sensing strain in small robots: composed of a deformable 'dome' spread over the dendrites of a nerve, this mechanoreceptor could easily be mimicked and adapted, to be applied in a human-made setting. The mechanisms by which insects store energy for jumping are already being utilised in jumping robots [107]. Understanding the viscoelastic effects at work, as well as the potential for damage and fatigue (important for materials that cannot repair) is crucial to take these studies farther. Finally the how the tibia of the locust is designed and changes with age in order to resist buckling, whilst still being robust against fracture is of potential interest for future design of columns.

Chapter 10

Future Work

This research has uncovered new information about both the mechanical behaviour and the repair response of various biological materials, raising multiple avenues for future exploration.

For gaining greater insight into what is causing the changes in older insect cuticle confocal laser scanning or multiphoton microscopy seem like ideal choices, as if water is being lost from the cuticle, it is possible that further cross-linking, a dehydration process, is occurring. As cuticle is autofluorescent, and more heavily sclerotized cuticle emits at longer wavelengths, changes in the extent of cross-linking could be observed in insects of different age groups. The potential loss of water from cuticle could also be explored further by raising the insects in a more abrasive environment, such as the sand they would normally experience in the wild. This may affect the epidermal layer and result in different changes to those observed in insects raised on oats.

The driver for the changes observed in older cuticle also requires further study; mating behaviours have tentatively been identified as a factor, but further study is required. This could be carried out in the form of artificial pheromones, or actually allowing the females to lay eggs, which did not occur in this study. As the females need to carry greater loads before depositing their eggs, the changes observed in the mated females (or rather lack of changes) could be related to this additional demand. Male insects could also be observed as they may not experience this change in stiffness and strength with age, or they may experience it regardless of mating habits. Additionally the insects could be observed or fed remotely to confirm if the reduced locomotion seen in the older insects is purely due to increased acclimation to humans or is in fact related to age.

Identification of micro-damage is also important in elucidating further information about how cuticle responds to loads, and how this affects the energy storage capabilities. Further studies into these effects could investigate the behaviour of cuticle in response to repeated loads, perhaps by cycling once a day, or for a larger number of cycles to a lower strain. Doing so would give greater insight into any active remodelling process and help determine if the repair process is still targeted even when the injury has not pierced the epidermis. This raises additional questions such as how the animals manage to sense the damage at all. Sensing of damage may be linked to the campaniform sensilla, oval-shaped mechanoreceptors in the cuticle that can detect strain in the cuticle as they are sensitive to compression along their short axis. There is great scope for further investigations into the evolution of such cells in the cuticle, and the energy storage capabilities of cuticle. Such information would be essential for any cuticle-inspired biomimetic material that could be used in the future. Given the materials light weight, high strength, and good fracture toughness it is not hard to imagine a biomimetic version being used in the future. It is also biocompatible and bioresorbable, and chitin derivatives are already being utilised in the medical sphere. Future utilisation of cuticle inspired materials will require greater information about the fatigue properties of the material, a field of study that this research only begins to touch upon. Dyeing, as utilised in bone studies is one potential route for identifying microcracks and how they influence mechanical properties.

The limpet shells also possess potential for future biomimetic applications. Most ceramics are much lighter, and have higher melting points than metals. Despite this obvious appeal to industries such as aerospace, one key factor has hindered their use. Ceramics are typically very brittle, with a low fracture toughness. Nature may hold the key to identifying how we can improve the strength of ceramics. Additionally many man-made composites are layered structures, which are prone to delamination failures, similar to those seen in the shells. But evidently nature has evolved a multitude of ways to strengthen even ceramic composites through the use of micro or nano structures. Consequently further study of how these structures form and the identification of other toughening mechanisms could be useful in future biomimetic composite design. Finite element models could also be utilised; the use of more sophisticated models of crack propagation through materials such as the limpet shells could be useful in elucidating more information about how cracks grow around these microstructures and how structures such as the spines on the shell help to increase stiffness. Further identification of microstructures, and how they are formed via crystal orientation and growth is another route to explore.

How materials respond to and repair damage is also an important area, and one where our knowledge is lacking. Though one mechanism of repair in limpet shells has been identified, at least one more factor is at work. The primary mechanism is an increases in thickness but the maximum rate of this deposition and the factors that control it still remain as open questions. These are important questions, as they will effect the ability of limpets and other similar species to survive the threats posed by climate change, in particular rising frequency of extreme storms, which already had an effect on the population. The other strengthening mechanism or even mechanisms could potentially be identified via micro- or nano-CT scans which may identify other structures within damaged shells. Shells could also be fixed immediately after collection, which may allow the presence of organic matter to be observed. This could present differently in damaged shells and may confer information about how crystal growth could be different in repair materials, as the presence of different crystal layers or different orientations may aid in increasing the strength of the shell. The fatigue behaviour of the shells also requires further studies to understand it better, and confirm the ability of the shells to remodel. The use of lower energies and longer time frames would be an easy way to establish this.

The studies contained within this thesis have filled gaps in the literature about both the mechanical properties and the repair capabilities of the locust and the limpet, whilst opening up several avenues for further study. As biomimetics becomes an ever expanding field it is important to glean information about the mechanical behaviour of the biological material in question. Additionally, as most biological materials rely upon repair mechanisms for continued use, these must be identified and used to inform any applications of such material.

References

[1] N. Lepora, P. Versuche, and T. Prescott. The state of the art in biomimetics. *Bioninspiration Biomim.*, 8(1), 2013.

[2] B. Rich and B. Pokroy. A study on the wetting properties of broccoli leaf surfaces and their time dependent self-healing after mechanical damage. *Soft Matt.*, 14:782–7792, 2018. doi: 10.1039/C8SM01115J.

[3] Y. B. G. C. Gurtner, S. Werner and M. T. Longaker. Wound repair and regeneration. *Nature*, 453, 2008.

[4] E. Parle, J. Dirks, and D. Taylor. Bridging the gap: wound healing in insects restores mechanical strength by targeted cuticle deposition. *J. R. Soc. Inter.*, 13(117), 2016. doi: 10.1098/rsif.2015.0984.

[5] M. Meyers, J. McKittrick, and P. Chen. Structural biological materials: Critical mechanics-materials connections. *Science*, 339(6121), 2013. doi: 10.1126/science.1220854.

[6] L. Wen, J. Weaver, and G. Lauder. Biomimetic shark skin: design, fabrication and hydrodynamic function. *J. Exp. Biol.*, 217:1656–1666, 2014. doi: 10.1242/jeb.097097.

[7] F. Barthelat and R.Rabiei. Toughness amplification in natural composites. *J. Mech. Phys. Solids*, 59:829–840, 2011. doi: 10.1016/j.jmps.2011.01.001.

[8] U. Wegst and M. Ashby. The mechanical efficiency of natural materials. *Philos. Mag.*, 84(21):2167–2186, 2004. doi: 10.1080/14786430410001680935.

[9] G. Musumeci and et al. New perspectives for articular cartilage repair treatment through tissue engineering: A contemporary review. *World J Orthop*, 5(2):80–88, 2014. doi: 10.5312/wjo.v5.i2.80.

[10] M. Tiku and H. Sabaawy. Cartilage regeneration for treatment of osteoarthritis: a paradigm for nonsurgical intervention. *Ther. Adv. Musculoskelet. Dis.*, 7(3):76–87, 2015. doi: 10.1177/1759720X15576866.

[11] Y. Yang, X. Ding, and M. Urban. Chemical and physical aspects of self-healing materials. *Prog. Polym. Sci*, 49-50:34–59, 2015. doi: 10.1016/j.progpolymsci.2015.06.001.

[12] D. Wu, S. Meure, and D. Solomon. Self-healing polymeric materials: A review of recent development. *Prog. Polym. Sci*, 33(5):479–522, 2008. doi: 10.1016/j.progpolymsci.2008.02.001.

[13] J. Li and et al. Pathophysiology of acute wound healing. *Clin. Dermatol.*, 25:9–18, 2007.

[14] H. Frost. Wolff's law and bone's structural adaptations to mechanical usage: an overview for clinicians. *The Angle Orthodontist*, 64:175–188, 1994. doi: 10.1043/0003-3219(1994)064⟨0175:WLABSA⟩2.0.CO;2.

[15] S. Cowin. Wolffs law of trabecular architecture at remodeling equilibrium. *J. Biomech. Engin.*, 108, 1986.

[16] S. W. et al. The effect of prolonged physical training on the properties of long bone: a study of wolff's law. *J Bone Joint Surg Am*, 63, 1981.

[17] A. Parfitt and et al. Structural and cellular changes during bone growth in healthy children. *J. R. Soc. Inter.*, 27(4), 2000. doi: 10.1016/S8756-3282(00)00353-7.

[18] D. Taylor, J. Hazenberg, and T. Lee. Living with cracks: Damage and repair in human bone. *Nat. Mat.*, 6(4):263 – 268, 2007. doi: 10.1046/j.1469-7580.2003.00194.x.

[19] T. Einhorn and L. Gerstenfeld. Fracture healing: mechanisms and interventions. *Nat Rev Rheumatol.*, 11(1):45–54, 2015. doi: 10.1038/nrrheum.2014.164.

[20] D. Burr. Targeted and nontargeted remodeling. *Bone*, 30(1):2–4, 2002. doi: 10.1016/S8756-3282(01)00619-6.

[21] L. Raggatt and N. Partridge. Cellular and molecular mechanisms of bone remodelling. *J. Biol. Chem.*, 285(33):25103–8., 2010. doi: doi:10.1074/jbc.R109.041087.

[22] G. Jones. Upper extremity stress fractures. clin. *Clin. Sports Med.*, 25:159–174, 2006. doi: 10.1016/j.csm.2005.08.008.

[23] K. Bennell and P. Brukner. Preventing and managing stress fractures in athletes. *Compos. Struct.*, 6(4):171–180, 2005. doi: 10.1016/j.ptsp.2005.07.002.

[24] T. Bayley, G. Sutton, and M. Burrows. A buckling region in locust hindlegs contains resilin and absorbs energy when jumping or kicking goes wrong. *J. Exp. Biol.*, 215 (7):1151–1161, 2012. doi: 10.1242/jeb.068080.

[25] M. Sabick, M. Torry, Y.-K. Kim, and R. Hawkins. Humeral torque in professional baseball pitchers. *Am. J. Sports Med.*, 32:892–898, 2004. doi: 10.1177/0363546503259354.

[26] T. Branch and et al. Spontaneous fractures of the humerus during pitching: a series of 12 cases. *Am. J. Sports Med*, 20:468–470, 1991. doi: 10.1177/036354659202000419.

[27] K. Kaufman, S. Brodine, and R. Shaffer. Military training-related injuries: Surveillance, research, and prevention. *Am. J. Prev. Med.*, 18(3:1):54–63, 2000. doi: 10.1016/S0749-3797(00)00114-8.

[28] R. Baron and M. Kneissel. Wnt signaling in bone homeostasis and disease: from human mutations to treatments. *Nat. Med*, 19:179–192, 2013.

[29] E. Orwoll and et al. Skeletal health in longduration astronauts: Nature, assessment, and management recommendations from the nasa bone summit. *J. Bone Miner. Res.*, 28(6):1243–1255, 2013. doi: 10.1002/jbmr.1948.

[30] F. Sabet, A. Najafi, E. Hamed, and I. Jasiuk. Modelling of bone fracture and strength at different length scales: a review. *Interface Focus*, 6(1), 2015. doi: 10.1098/rsfs.2015.0055.

[31] J. Wolff. *Das Gesetz der transformation der knochem.* Hirschwald, 1892.

[32] N. Willems, G. Langenbach, V. Everts, and A. Zentner. The microstructural and biomechanical development of the condylar bone: a review. *Eur J Orthod.*, 36(4): 479–485, 2014. doi: 10.1093/ejo/cjt093.

[33] z. Seref-Ferlengz, O. Kennedy, and M. Schaffler. Bone microdamage, remodeling and bone fragility: how much damage is too much damage? *Bonekey Rep.*, 4(644), 2003. doi: 10.1038/bonekey.2015.11.

[34] C. Turner, A. Robling, R. Duncan, and D. Burr. Do bone cells behave like a neuronal network? *Calcif. Tissue Int.*, 70:435–442, 2002. doi: 110.1007/s00223-001-1024-z.

[35] J. Klein-Nulen, R. Bacabac, and A. Baker. Mechanical loading and how it affects bone cells: The role of the osteocyte cytoskeleton in maintaining our skeleton. *Eur. Cell Mater.*, 24:278–291, 2012. doi: 10.22203/eCM.v024a20.

[36] S. Tatsumi and et al. Targeted ablation of osteocytes induces osteoporosis with defective mechanotransduction. *Cell Metab.*, 5:464–475, 2007.

[37] M. Schaffler and O. Kennedy. Osteocyte signaling in bone. *Curr. Osteoporos. Rep.*, 10(2):118–125, 2012. doi: 10.1007/s11914-012-0105-4.

[38] L. Cardoso, B. Herman, and O. Verborgt. Osteocyte apoptosis controls activation of intracortical resorption in response to bone fatigue. *J. Bone Miner. Res.*, 24(4): 597–605, 2009. doi: 10.1359/jbmr.081210.

[39] A. Aiyer. untitled, 2018. URL `www.orthobullets.com\/basic-science/9009/fracture-healing`.

[40] L. Gerstenfeld, D. Cullinane, and G. Barnes. Fracture healing as a post-natal developmental process: molecular, spatial, and temporal aspects of its regulation. *J. Cell Biochem.*, 88(5):873–884, 2003. doi: 10.1002/jcb.10435.

[41] R. Marsell and T. Einhorn. The biology of fracture healing. *Injury*, 42(6):551–555, 2011. doi: 10.1016/j.injury.2011.03.031.

[42] Unknown. Iucn redlist, 2018. URL `https://www.iucnredlist.org/`.

[43] T. Daimon and et al. A *Bombyx mori* gene, *BmChi-h*, encodes a protein homologous to bacterial and baculovirus chitinases. *Insect Biochem Mol Biol*, 33(8):749–759, 2003. doi: 10.1016/S0965-1748(03)00084-5.

[44] L. Duo-chuan. Review of fungal chitinases. *Mycopathologia*, 161, 2006.

[45] J. Vincent and U. Wegst. Design and mechanical properties of insect cuticle. *Arthropod Struct. Dev.*, 33(3):89–1002, 2004. doi: 10.1016/j.asd.2004.05.006.

[46] T. Minamoto and et al. Saccharification of β-chitin from squid pen by a fermentation method using recombinant chitinase-secreting *Escherichia coli*. *Appl Biochem Biotechnol.*, 175(8):3788–3799, 2015.

[47] H. Li and et al. Molecular characterization and expression analysis of chitinase from the pearl oyster *Pinctada fucata*. *Comp. Biochem. Physiol. B Biochem. Mol. Biol.*, 203:141–148, 2017. doi: 10.1016/j.cbpb.2016.10.007.

[48] I. Weiss, S. Kaufman, B. Heiland, and M. Tanaka. Covalent modification of chitin with silk-derivatives acts as an amphiphilic self-organizing template in nacre biomineralisation. *J. Struc. Biol.*, 167(1):68–75, 2009. doi: 10.1016/j.jsb.2009.04.005.

[49] R. Chapman. *The Insects: structure and function.* Cambridge Universities Press ltd., 2013.

[50] P. Butler and et al. Variability of marine climate on the north icelandic shelf in a 1357-year proxy archive based on growth increments in the bivalve *Arctica islandica*. *Palaeogeogr. Palaeoclimatol. Palaeoecol.*, 373:141–151, 2013. doi: 10.1016/j.palaeo.2012.01.016.

[51] S. Moffett. *Nervous System Regeneration in the Invertebrates.* Springer, 1996. doi: 10.1007/978-3-642-79839-9_2.

[52] F. Muijres and et al. Flies compensate for unilateral wing damage through modular adjustments of wing and body kinematics. *Interface Focus*, 7(1), 2017. doi: 10.1098/rsfs.2016.0103.

[53] A. Chapman. Numbers of living species in australia and the world. *Canberra: Australian Biological Resources Study*, 2006.

[54] S. S. G.A. Sword, M. Lecoq. Phase polyphenism and preventative locust management. *J. Insect Physiol.*, 56(8):949–957, 2010.

[55] B. Uvarov. Grasshoppers and locusts. *Centre for Overseas Pest Research, London*, 2, 1977.

[56] R. Jayakumar and et al. Biomedical applications of chitin and chitosan based nanomaterialsa short review. *Carbohydr. Polym.*, 82(5):227232, 2010.

[57] M. Dash and et al. Chitosana versatile semi-synthetic polymer in biomedical applications. *Prog. Polym. Sci.*, 36(8):9811014, 2011.

[58] A. Anitha and et al. Chitin and chitosan in selected biomedical applications. *Prog. Polym. Sci*, 39(9):16441667, 2014.

[59] V. Wigglesworth. *The Principles of Insect Physiology.* Butler & Tanner ltd, 1951.

[60] S. Nikolov and et al. Robustness and optimal use of design principles of arthropod exoskeletons studied by ab initio-based multiscale simulations. *J Mech Behav Biomed Mater*, 40(3):166–178, 2011. doi: 10.1016/j.ibmb.2009.10.007.

[61] Y. Bouligand. Twisted fibrous arrangements in biological materials and cholesteric mesophases. *Tissue Cell*, 14(2):189–217, 1972. doi: 10.1016/S0040-8166(72)80042-9.

[62] D. Raabe, C. Sachs, and P. Romano. The crustacean exoskeleton as an example of a structurally and mechanically graded biological nanocomposite material. *Acta Materialia*, 53(15):4281–4292, 2005. doi: 10.1016/j.actamat.2005.05.027.

[63] S. Andersen. Insect cuticular sclerotization: A review. *Insect Biochem Molec Biol*, 40:166–178, 2010. doi: 10.1016/j.ibmb.2009.10.007.

[64] S. Reynolds. The mechanical properties of the abdominal cuticle of rhodnius larvae. *J. Exp. Biol.*, 62(1):69–80, 1975.

[65] J. Dirks and D.Taylor. Fracture toughness of locust cuticle. *J. Exp. Biol.*, 9(77), 2012. doi: 10.1242/jeb.068221.

[66] M. Locke. Cell interactions in the repair of wounds in an insect (*RHODNIUS PROLIXUS*). *J. Insect Physiol.*, 12:389–395, 1966.

[67] V. Wigglesworth. Wound healing in an insect (*Rhodinius prolixus hemiptera*). *London School of Hygiene & Medicine*, 1937.

[68] M. Lavine and M. Strand. Insect hemocytes and their role in immunity. *Insect Biochem. Mol. Biol.*, 32(10):1295–1309, 2002. doi: 10.1016/S0965-1748(02)00092-9.

[69] U. Theopold, O. Schmidt, K. Söderhäll, and M. Dushay. Coagulation in arthropods: defence, wound closure and healing. *Trends Immunol.*, 25(6):2643–2650, 2004. doi: 10.1016/j.it.2004.03.004.

[70] M. Dushay. Insect hemolymph clotting. *Cell. Mol. Life Sci.*, 66(16):26432650, 2009. doi: 10.1007/s00018-009-0036-0.

[71] A. Rowley and N. Ratcliffe. A histological study of wound healing and hemocyte function in the waxmoth *Galleria mellonella. J. Morph.*, 157(2):181–199, 1978. doi: 10.1002/jmor.1051570206.

[72] T. Muta and S. Iwanaga. The role of hemolymph coagulation in innate immunity. *Curr. Opin. Immunol.*, 8(1):41–47, 1996. doi: 10.1016/S0952-7915(96)80103-8.

[73] G. Bidla, M. Lindgren, U. Theopold, and M. Dushay. Hemolymph coagulation and phenoloxidase in drosophila larvae. *Dev. Comp. Immunol.*, 29(8):669–679, 2005. doi: 10.1016/j.dci.2004.11.007.

[74] L. Cerenius and K. Söderhäll. The prophenoloxidase-activating system in invertebrates. *Immunol. Rev.*, 198:116–126, 2004.

[75] A. Nappi and E. Ottaviani. Cytotoxicity and cytotoxicmolecules in invertebrates. *Bioessays*, 22(5):469–480, 2000.

[76] E. Parle and D. Taylor. The effect of aging on the mechanical behaviour of cuticle in the locust *Schistocerca Gregaria*. *J. Mech. Behav. Biomed. Mater .*, 68:247–251, 2017. doi: 10.1016/j.jmbbm.2017.02.008.

[77] C. Oritz and M. Boyce. Materials sciencebioinspired structural materials. *Science*, 319(5866), 2008. doi: 10.1126/science.1154295.

[78] G. M. M. Sarikaya. Rigid biological composite materials: Structural examples for biomimetic design. *Exp. Mech.*, 42(4):395403, 2002.

[79] E. Munch and et al. Tough, bio-inspired hybrid materials. *Science*, 322(5907): 1516–1520, 2008. doi: 10.1126/science.1164865.

[80] V. Sleight and et al. Transcriptomic response to shell damage in the antarctic clam, *Laternula elliptica*: Time scales and spatial localisation. *Tissue Cell*, 40:207–218, 2015. doi: 10.1016/j.margen.2015.01.009.

[81] A. Jackson, J. Vincent, and R. Turner. The mechanical design of nacre. *Proceed. R. Soc. Lon.*, 234(1277):415–440, 1988. doi: 10.1098/rspb.1988.0056.

[82] Barthelat and et al. On the mechanics of mother-of-pearl: a key feature in the material hierarchical structure. *J. Mech. Phys. Solids*, 55(2):225–444, 2007.

[83] Chris73. Nautilus half-shell showing the camerae in a logarithmic spiral, 2009. URL `https://en.wikipedia.org/wiki/Nautilus#/media/File:NautilusCutawayLogarithmicSpiral.jpg`.

[84] F. Meldrum. Calcium carbonate in biomineralisation and biomimetic chemistry. *Int. Mat. Rev.*, 48(3), 2003. doi: 10.1179/095066003225005836.

[85] L. D.R. Reproduction, ecology, and evolution of the indo-pacific limpet scutellastra flexuosa. *Bull. Mar. Sci.*, 81(2):219–234, 2007. doi: 10.1016/S0965-1748(02)00030-9.

[86] V. G.J. *Evolution and Escalation.* Princeton University Press, 1987.

[87] G. Ellem, J. Zurst, and K. Zimmerman. Shell clamping behaviour in the limpet *Cellana tramoserica*. *J. Exp. Biol.*, 205:539–547, 2002.

[88] A. Smith. The role of suction in the adhesion of limpets. *J. Exp. Biol.*, 161:151–169, 1991.

[89] A. Smith. Alternation between attachment mechanisms by limpets in the field. *J. Exp. Mar. Biol. Ecol.*, 160(2):205–220, 1992. doi: 10.1016/0022-0981(92)90238-6.

[90] W. K.M. and S. A.S.M. *The Mollusca: Physiology part 2.* Aacdemic Press, 1983.

[91] J. Cabral and R. Jorge. Compressibility and shell failure in the european atlantic patella limpets. *Mar. Biol.*, 150(4):585–597, 2007. doi: 10.1007/s00227-006-0379-0.

[92] K. Szabó and B. Koppel. Limpet shells as unmodified tools in pleistocene southeast asia: an experimental approach to assessing fracture and modification. *J. Archaeol. Sci.*, 54, 2015. doi: 10.1016/j.jas.2014.11.022.

[93] D. Taylor. Impact damage and repair in shells of the limpet *Patella vulgata*. *J. Exp. Biol.*, 219(24):3927–3935, 2016. doi: 10.1242/jeb.149880.

[94] J. Oritz and et al. Protein diagenesis in patella shells: Implications for amino acid racemisation dating. *Quat. Geochronol.*, 27, 2015. doi: 10.1016/j.quageo.2015.02.008.

[95] N. Watabe. *Biology of the Integument.* Springer, 1984. doi: 10.1007/978-3-642-51593-4_25.

[96] F. Marin and G. Luquet. Molluscan shell proteins. *CR PALEVOL*, 3(6-7):469–492, 2004. doi: 10.1016/j.crpv.2004.07.009.

[97] K. Elliot and D. FitzSimons. *Hard Tissue Growth, Repair and Remineralization.* John Wiley & Sons, 2009.

[98] A. Barber, D. Lu, and N. Pugno. Extreme strength observed in limpet teeth. *J. R. Soc. Inter.*, 12(105), 2015. doi: 10.1098/rsif.2014.1326.

[99] E. Harper and et al. Iceberg scour and shell damage in the antarctic bivalve *Laternula elliptica*. *PLOS One*, 7(9):1–12, 2012. doi: 10.1371/journal.pone.0046341.

[100] B. Bulkley. Shell damage and repair in five members of the genus *Acmaea*. *Veliger 11 (suppl)*, pages 64–66, 1968.

[101] C. Fleury and et al. Shell repair process in the green ormer *Haliotis tuberculata*: A histological and microstructural study. *Tissue Cell*, 140(3):207–218, 2008. doi: 10.1016/j.tice.2007.12.002.

[102] S. Kapur and A. Gupta. The role of amoebocytes in the regeneration of shell in the land *Pulmonate*, *Euplecta indica*. *Biol. Bull.*, 139(3):502–509, 1970. doi: 10.2307/1540369.

[103] S. Uozumi and S. Suzuki. 'organic membrane-shell' and initial calcification in shell regeneration. *Jour. Fac. ScL, Hokkaido Univ., Ser. IV*, 19(1-2):37–74, 1979.

[104] A. Mount, A. Wheeler, R. Paradkar, and D. Snider. Hemocyte-mediated shell mineralization in the eastern oyster. *Science*, 304(5668), 2004. doi: 10.1126/science.1090506.

[105] D. Sud and et al. A cytological study of the mantle edge of *Haliotis tuberculata* l. (mollusca, gastropoda) in relation to shell structure. *J. Shellfish Res.*, 21(1):9201–210, 2002.

[106] A.-M. Lin, P.-Y. Chen, and M. Meyers. The growth of nacre in the abalone shell. *Acta. Biomat.*, 84(1):131–138, 2008. doi: 10.1016/j.actbio.2007.05.005.

[107] M. Ilton and et al. The principles of cascading power limits in small, fast biological and engineered systems. *Science*, 360(6387), 2018. doi: 10.1126/science.aao1082.

[108] L. Rome and S. Lindstedt. The quest for speed: Muscles built for high-frequency contractions. *Am. Physiol. Soc.*, 13(6):261–268, 1998. doi: 10.1152/physiologyonline.1998.13.6.261.

[109] R. Alexander and H. Bennet-Clark. Storage of elastic strain energy in muscle and other tissues. *Nature*, 265:114–117, 1977.

[110] M. Burrows and O. Morris. Jumping and kicking in bush crickets. *J. Exp. Biol.*, 206:1035–1049, 2003. doi: 10.1242/jeb.00214.

[111] M. Burrows, S. Shaw, and G. Sutton. Resilin and chitinous cuticle form a composite structure for energy storage in jumping by froghopper insects. *BMC Biol.*, 6(41), 2008. doi: 10.1186/1741-7007-6-41.

[112] M. Burrows and G. Sutton. Locusts use a composite of resilin and hard cuticle as an energy store for jumping and kicking. *J. Exp. Biol.*, 215(5):3501–3512, 2012. doi: 10.1242/jeb.071993.

[113] S. Vogel. Living in a physical world iii. *J. Biosci.*, 30(3):303–312, 2005. doi: 10.1007/BF02703667.

[114] G. Sutton and M. Burrows. Insect jumping springs. *Curr. Biol.*, 28(4):142–143, 2018. doi: 10.1016/j.cub.2017.11.051.

[115] M. Blanco and S. Patek. Muscle trade-offs in a power amplified prey capture technique. *Evolution*, 65(5):1399–1414, 2014. doi: 10.1111/evo.12365.

[116] M. Burrows. Morphology and action of the hind leg joints controlling jumping in froghopper insects. *J. Exp. Biol.*, 209:4622–2637, 2006. doi: 10.1242/jeb.02554.

[117] M. Burrows. Jumping performance of froghopper insects. *J. Exp. Biol.*, 209:4607–4621, 2006. doi: 10.1242/jeb.02539.

[118] H. Bennet-Clark. The energetics of the jump of the locust *Schistocerca gregaria*. *J. Exp. Biol.*, 65:53–83, 1975.

[119] R. Brown. The mechanism of locust jumping. *Nature*, 214(939), 1967. doi: 10.1038/214939a0.

[120] S. Katz and J. Gosline. Ontogenic scaling and mechanical behaviour of the tibiae of the african desert locust (*Schistocerca Gregaria*). *J. Exp. Biol.*, 168:125–150, 1992.

[121] W. Heitler. The locust jump. specialisations of the metathoracic femoraltibial joint. *J. Comp. Physiol.*, 89(1):93–104, 1974.

[122] S. R. et al. Motor activity and trajectory control during escape jumping in the locust *Locusta migratoria*. *J. Comp. Physiol A*, 191(10):965–975, 2005. doi: 10.1007/s00359-005-0023-3.

[123] H. W. B. M. The locust jump. i. the motor programme. *J. Exp. Biol.*, 66:203–219, 1977.

[124] G. Sutton and M. Burrows. The mechanics of elevation control in locust jumping. *J. Comp. Physiol A*, 194:557–563, 2008. doi: 10.1007/s00359-008-0329-z.

[125] E. P. at et al. Buckling failures in insect exoskeletons. *Bioninspiration Biomim.*, 11 (1):378–391, 2015. doi: 10.1088/1748-3190/11/1/016003.

[126] D. Taylor and J. Dirks. Shape optimization in exoskeletons and endoskeletons: a biomechanics analysis. *J. R. Soc. Inter.*, 9(77):3480–3489, 2012.

[127] J. M. Timoshenko, S. & Gere. *Theory of Elastic Stability.* McGraw Hill, 1961.

[128] B. L.G. On the flexure of thin cylindrical shells and other thin sections. *Proc. R. Soc. A.*, 116, 1927.

[129] V. R. Knaster J, Tortoa G. The brazier effect and its influence in the design of beampipes for particle colliders. *Vacuum*, 64, 2003.

[130] Y. Takahashi. Evaluation of leak-before-break assessment methodology for pipes with a circumferential through-wall crack. part i: stress intensity factor and limit load solutions. *Int. J. Pres. Ves. Pip.*, 79(6):385–392, 2002. doi: 10.1016/S0308-0161(02)00036-4.

[131] J. Blundon and G. Vermeij. Effect of shell repair on shell strength in the gastropod *Littorina irrorata*. *Mar. Biol.*, 76(1):41–45, 1983. doi: 10.1007/BF00393053.

[132] J. Currey and J. Taylor. The mechanical behaviour of some molluscan hard tissues. *J. Zool. Lond.*, 173:395–406, 1974. doi: 10.1111/j.1469-7998.1974.tb04122.x.

[133] A. Shanks and W. Wright. Adding teeth to wave action: the destructive effects of wave-borne rocks on intertidal organisms. *Oceologia*, 69(3):420–428, 1986. doi: 10.1007/BF00377065.

[134] D. Taylor. Measuring fracture toughness in biological materials. *J. Mech. Behav. Biomed.*, 77:776–782, 2018. doi: 10.1016/j.jmbbm.2017.07.007.

[135] B. Schrauwen and A. Peijs. Influence of matrix ductility and fibre architecture on the repeated impact response of glass-fibre-reinforced laminated composites. *App. Comp. Mat.*, 9:331–352, 2002. doi: 1423189/604819.

[136] J. Currey. Further studies on the mechanical properties of mollusc shell material. *J. Zool.*, 180(4):445–453, 1976. doi: 10.1111/j.1469-7998.1976.tb04690.x.

[137] Chris. 4 ways to prevent concrete spalling, unknown. URL `https://concretetoolreviews.com/4-steps-to-prevent-concrete-spalling/`.

[138] F. Norton. A general theory of spalling. *J. Am. Ceram. Soc.*, 8(1):29–39, 1924. doi: 10.1111/j.1151-2916.1925.tb16332.x.

[139] J. Ko. and D. Ryu. The spalling mechanism of high strength concrete under fire. *Mag. Concrete Res.*, 63(5):357–370, 2011. doi: 10.1680/macr.10.00002.

[140] E. Parle. *Investigations into the Mechanical Properties of Insect Cuticle*. PhD thesis, Trinity College Dublin, 2015.

[141] D. Klocke and H. Schmitz. Water as a major modulator of the mechanical properties of insect cuticle. *Acta Biomater.*, 7:2935–2942, 2011.

[142] T. Schöberl and I. Jäger. Wet or dry hardness, stiffness and wear resistance of biological materials on the micron scale. *Adv. Eng. Mater.*, 8(11):1164–1169, 2006. doi: 10.1002/adem.200600143.

[143] W. Heitler. The locust jump: Iii. structural specializations of the metathoracic tibiae. *J. Exp. Biol.*, 67:29–36, 1977.

[144] C. Linnaeus. Systema natur per regna tria natur, secundum classses, ordines, genera, species, cum characteribus, differentiis, synonymis, locis. *Sys. Nat. Ed.*, 10:1–824, 1758.

[145] H. Hepburn and I. Joffe. Locust solid cuticle-a time sequence of mechanical properties. *J. Insect Physiol.*, 20:497–506, 1974. doi: 10.1016/0022-1910(74)90158-9.

[146] M. Jensen and T. Weis-Fogh. Biology and physics of locust flight v. strength and elasticity of locust cuticle. *Philos. Trans. R. Soc. Lond. B. Biol. Sci.*, 215(7):1151–1161, 1962. doi: 10.1098/rstb.1962.0008.

[147] G. Schmidt and R. Albutz. Laboratory studies on pheromones and reproduction in the desert locust schistocerca gregaria (forsk.). *J. Appl. Entomol.*, 118:378–391, 1994. doi: 10.1111/j.1439-0418.1994.tb00815.x.

[148] J. Currey, K. Brear, and P. Zioupos. The effects of ageing and changes in mineral content in degrading the toughness of human femora. *J. Biomech.*, 29(2):257–260, 1996. doi: 110.1016/0021-9290(95)00048-8.

[149] J. Hoffman and et al. Phylogenetic perspectives in innate immunity. *Science*, 284 (5418), 1999.

[150] D. Li and et al. Insect hemolymph clotting: evidence for interaction between the coagulation system and the prophenoloxidase activating cascade. *Insect Biochem. Mol. Biol.*, 32(8):919928, 2002. doi: 10.1016/S0965-1748(02)00030-9.

[151] S. V. R. et al. A comparative study of piscine defense: The scales of *Atractosteus spatula*, *Arapaima gigas*, and *Latimeria chalumnae*. Presentation at the 6th International Conference on Mechanics of Biomaterials and Tissues, 12 2015. Waikoloa, Hawaii.

[152] J. Lai-Fook. The fine structure of wound repair in an insect (*Rhodnius prolixus*). *J. Morph.*, 124(1):37–77, 1968. doi: 10.1002/jmor.1051240104.

[153] J. Snedker and A. Gautieri. The role of collagen crosslinks in ageing and diabetes - the good, the bad, and the ugly. *Muscles Ligaments Tendons J*, 4(3):303308, 2014.

[154] V. J.F.V. *Structural Biomaterials*. Princeton University Press, 1990.

[155] Y. Zhou and et al. Effect of shear forces and ageing on the compliance of adhesive pads in adult cockroaches. *J. Exp. Biol.*, 218(17):2775–2781, 2015. doi: 10.1242/jeb.124362.

[156] J. Vincent. If it's tanned it must be dry: A critique. *J Adhes*, 85(11):755–769, 2009. doi: 10.1080/00218460903291296.

[157] H. Fuchs and R. Stephens. *Metal Fatigue in Engineering*. Wiley, New York USA, 1980.

[158] J. Morley. *High Performance Fibre Composites.* Academic Press, London, 1987.

[159] H. Frost. Presence of microscopic cracks in vivo in bone. *Henry Ford Hosp Med Bull*, 8:25–35, 1960.

[160] D. Taylor. What we cant learn from nature. *Mat. Sci. Engin. C.*, 31(6):1160–1163, 2011. doi: 10.1016/j.msec.2010.12.006.

[161] M. O'Neill, D. DeLandro, and D. Taylor. Age related responses to injury and repair in insect cuticle. *J. Exp. Biol.*, In press, 2018.

[162] R. Johnson, A. Kaiser, M. Quinlan, and W. Sharp. Effect of cuticular abrasion and recovery on water loss rates in queens of the desert harvester ant *Messor pergandei. J. Exp. Biol.*, 1214:3495–3506, 2011. doi: 10.1242/jeb.054304.

[163] C. Mattheck. *Design in nature: learning from trees.* Berlin: Springer, 1998.

[164] S. Patek, B. Nowroozi, J. Baio, R. Caldwell, and A. Summers. Linkage mechanics and power amplification of the mantis shrimp's strike. *J Exp. Biol.*, 210:3677–3688, 2007. doi: 10.1242/jeb.006486.

[165] W. Gronenberg. The fast mandible strike in the trap-jaw ant odontomachus. i. temporal properties and morphological characteristics. *J. Comp. Physiol. A*, 176: 391–398, 1995. doi: 10.1242/jeb.006486.

[166] D. Cofer, G. Cymbalyuk, W. Heitler, and D. Edwards. Neuromechanical simulation of the locust jump. *J. Exp. Biol.*, 2136:1060–1068, 2010. doi: 10.1242/jeb.034678.

[167] M. Burrows and G. Morris. The kinematics and neural control of high speed kicking movements in the locust. *J. Exp. Biol.*, 204:3471–3481, 201.

[168] D. Dudek and R. Full. Passive mechanical properties of legs from running insects. *J. Exp. Biol.*, 209:1502–1515, 2006. doi: 10.1242/jeb.02146.

[169] R. Blickhan. Stiffness of an arthropod leg joint. *J. Physiol.*, 19(5):375–384, 1986. doi: 10.1016/0021-9290(86)90014-X.

[170] A. Sensenig and J. Schultz. Mechanics of cuticular elastic energy storage in leg joints lacking extensor muscles in arachnids. *J. Exp. Biol.*, 206:771–784, 2003. doi: 10.1242/jeb.00182.

[171] F. O'Brien, D. Taylor, and T. Lee. Microcrack accumulation at different intervals during fatigue testing of compact bone. *J. Biomech.*, 36(7):4973–980, 2003. doi: 10.1016/S0021-9290(03)00066-6.

[172] T. Lee and et al. Detecting microdamage in bone. *J. Anat.*, 203(2):161–172, 2003. doi: 10.1046/j.1469-7580.2003.00211.x.

[173] R. Alexander. Leg design and jumping technique for humans, other vertebrates and insects. *Phil. Trans. R. Soc. Lond. B.*, 347:235–248, 1995.

[174] J. Schindelin and et al. Fiji: an open-source platform for biological-image analysis. *Nat. Methods*, 9(7):676–682, 2012. doi: 10.1038/nmeth.2019.

[175] W. Callister. *Fundamentals of materials science and engineering: An integrated approach.* John Wiley and Sons Inc., 2005.

[176] H. Axelson and K. Hagbarth. Human motor control consequences of thixotropic changes in muscular short-range stiffness. *J. Physiol.*, 535:279–288, 2001. doi: 10.1111/j.1469-7793.2001.00279.x.

[177] H. Barnes. Thixotrophy-a review. *J. Non-Newtonian Fluid Mech.*, 70:1–33, 1997. doi: 10.1016/S0377-0257(97)00004-9.

[178] T. Zack, T. Claverie, and S. Patek. Elastic energy storage in the mantis shrimp's fast predatory strike. *J. Exp. Biol.*, 212:4002–4009, 2009. doi: 10.1242/jeb.034801.

[179] M. Schaffler, E. Radin, and D. Burr. Long-term fatigue behavior of compact bone at low strain magnitude and rate. *Bone*, 11:321–326, 1990.

[180] M. Schaffler, E. Radin, and D. Burr. Mechanical and morphological effects of strain rate on fatigue of compact bone. *Bone*, 10:207–214, 1989.

[181] D. Taylor. Microcrack growth parameters for compact bone deduced from stiffness variations. *J. Biomech.*, 31:587–592, 1998. doi: 10.1016/S0021-9290(98)00050-5.

[182] B. Aberle, R. Jemmali, and J. Dirks. Effect of sample treatment on biomechanical properties of insect cuticle. *J. Arthr. Struc. Dev.*, 46(1):138–146, 2017. doi: 10.1016/j.asd.2016.08.001.

[183] J. Dirks, E.Parle, and D.Taylor. Fatigue of insect cuticle. *J. Exp. Biol.*, 216:1924–1927, 2013. doi: 10.1242/jeb.083824.

[184] H. Rabaji and et al. Wing cross veins: an efficient biomechanical strategy to mitigate fatigue failure of insect cuticle. *Biomech Model Mechanobiol.*, 16(6):19471955, 2017. doi: 10.1007/s10237-017-0930-6.

[185] M. Rabasovic and et al. Nonlinear microscopy of chitin and chitinous structures: a case study of two cave-dwelling insects. *J. Biomed. Opt.*, 20(1):19471955, 2015. doi: 10.1117/1.JBO.20.1.016010.

[186] C. Dooley, E. Parle, and D. Taylor. Measuring locust tibia cuticle layers to study mechanical properties and repair. Presentation at the 6th International Conference on Mechanics of Biomaterials and Tissues, 12 2015. Waikoloa, Hawaii.

[187] A. Ridgel and R. Ritzmann. Insights into age-related locomotor declines from studies of insects. *J. Prosthet. Dent.*, 4(1):23–39, 2005. doi: 10.1016/j.arr.2004.08.002.

[188] R. Miller. Osteoporosis in postmenopausal women therapy options across a wide range of risk for fracture. *Geriatrics*, 61(1):24–30, 2006.

[189] R. Renner, L. Boucher, and H. Kaufman. Osteoporosis in postmenopausal women. *Int. J. Pres. Ves. Pip.*, 52(4):581–588, 1984. doi: 10.1016/0022-3913(84)90352-4.

[190] J. Kanis and et al. European guidance for the diagnosis and management of osteoporosis in postmenopausal women. *Osteoporos Int.*, 19(4):399428, 2008. doi: 10.1002/jmor.1051240104.

[191] H.N.Dhakal, Z. Zhang, and M. Richardson. Effect of water absorption on the mechanical properties of hemp fibre reinforced unsaturated polyester composites. *Compos. Sci. Technol.*, 67:1674–1683, 2007.

[192] C. Armstrong and V. Mow. Variations in the intrinsic mechanical properties of human articular cartilage with age, degeneration, and water content. *J. Bone Joint Surg. Am.*, 64:88–94, 1982.

[193] I. Yakimets and et al. Mechanical properties with respect to water content of gelatin films in glassy state. *Polymer*, 46:12577–12585, 2005.

[194] J. Dirks and D. Taylor. Veins improve fracture toughness of insect wings. *PLOS One*, 7(8), 2012. doi: 10.1371/journal.pone.0043411.

[195] C. Krafft and V. Sergo. Biomedical applications of raman and infrared spectroscopy to diagnose tissues. *Spectroscopy*, 20:195–218, 2006.

[196] Z. Movasaghi, S. Rehman, and I. Rehman. Raman spectroscopy of biological tissues. *App. Spec. Rev.*, 42(5):493–541, 2007.

[197] R. Ports and et al. A noninvasive , in vivo technique to quantitatively measure water concentration of the stratum corneum using attenuated total-reflectance infrared spectroscopy. *Arch. Dermatol. Res.*, 277:489–495, 1985.

[198] J. Lambert. *Introduction to Organic Spectroscopy*. Macmillan, 1987. ISBN 9780023673009.

[199] S. Enders and et al. Exploring biological surfaces by nanoindentation. *J Mater Res*, 19:8808–8887, 2004. doi: 10.1557/jmr.2004.19.3.880.

[200] J. Hillerton, S. Reynolds, and J. Vincent. On the indentation hardness of insect cuticle. *J Exp Biol*, 96:45–52, 1982.

[201] E. Slifer. Vulnerable areas on the surface of the tarsus and pretarsus of the grasshopper (acrididae, orthoptera); with special reference to the arolium. *Ann Entomol Soc Am. Entomological Society of America*, 43(2):173–188, 1950.

[202] A. Lees. Transpiration and the structure of the epicuticle in ticks. *J. Exp. Biol.*, 23: 379–4109, 1947.

[203] M. Locke. Permeability of insect cuticle to water and lipids. *J Insect Physiol*, 147: 295–298, 1965.

[204] D. Taylor, M. Walsh, A. Cullen, and P. O'Reilly. The fracture toughness of eggshell. *Acta. Biomat.*, 37:21–27, 2016. doi: 10.1016/j.actbio.2016.04.028.

[205] D. Taylor and T. Lee. Microdamage and mechanical behaviour: predicting failure and remodelling in compact bone. *J. Anat.*, 203(2):203–211, 2003. doi: 10.1046/j.1469-7580.2003.00194.x.

[206] D. J. Adams, K. Brosche, and J. Lewis. Effect of specimen thickness on fracture toughness of bovine patellar cartilage. *J. Biomech. Eng.*, 125(6):927–929, 2003. doi: 10.1115/1.1635405.

[207] R. Nalla, J. Kruzic, J. Kinney, and R. Ritchie. Effect of aging on the toughness of human cortical bone: evaluation by r-curves. *Bone*, 35(6):1240–1246, 2004. doi: 10.1016/j.bone.2004.07.0167.

[208] M. O'Neill, D. Cafiso, R. Mala, G. L. Rosa, and D. Taylor. Fracture toughness and damage development in limpet shells. *Theor. App. Frac. Mech.*, 96:168–173, 2018. doi: 10.1016/j.tafmec.2018.04.013.

[209] M. O'Neill, R. Mala, D. Cafiso, C. Bignardi, and D. Taylor. Repair and remodelling in the shells of the limpet *Patella vulgata*. *J. R. Soc. Inter.*, 15, 2018. doi: 10.1098/rsif.2018.0299.

[210] G. Cadee. Shell damage and shell repair in antarctic limpet *Nacella concina* from king george island. *J. Sea. Res.*, 41(1-2):149–161, 1999. doi: 10.1016/S1385-1101(98)00042-2.

[211] G. Cadee, S. Walker, and K. Flessa. Sgastropod shell repair in the intertidal of baha la choya (n. gulf of california). *Palaeogeogr., Palaeoclimatol., Palaeoecol.*, 136:67–78, 1997. doi: 10.1016/S0031-0182(97)00041-2.

[212] S. Cho and W. Jeong. Prismatic shell repairs by hemoctyes in the extrapallial fluid of the pacific oyster, *Crassostrea gigas*. *Korean J. Malacology*, 27(3):223–228, 2011. doi: 10.9710/kjm.2011.27.3.223.

[213] M. Clark and et al. Hypoxia impacts large adults first: consequences in a warming world. *Glob. Chang. Biol.*, 19:2251–2263, 2013. doi: 10.1111/gcb.12197.

[214] P. Curtis. The fatigue behaviour of fibrous composite materials. *J. Strain Anal. Eng.*, 24(4):235–244, 1989.

[215] S. B. et al. Experimental investigation of static and fatigue behaviour of composites honeycomb materials using four point bending tests. *Compos. Struct.*, 87:263–273, 2009. doi: 10.1016/j.compstruct.2008.01.015.

[216] R. Talreja. Fatigue of composite materials: damage mechanisms and fatigue-life diagrams. *Proceed. R. Soc. A*, 378(1775), 1981. doi: 10.1098/rspa.1981.0163.

[217] R. Martin and D. Boardman. The effects of collagen fiber orientation, porosity, density, and mineralization on bovine cortical bone bending properties. *J. Biomech.*, 26(9):1047–1054, 1993. doi: 10.1016/S0021-9290(05)80004-1.

[218] A. Checa. Non-predatory shell damage in recent deep-endobenthic bivalves from spain. *Palaeogeogr. Palaeoclimatol. Palaeoecol*, 100:309–331, 1993. doi: 10.1016/0031-0182(93)90061-M).

[219] M. Suzuki, J. Kameda, T. Sasaki, K. Saruwatari, H. Nagasawa, and T. Kogure. Characterization of the multilayered shell of a limpet, *Lottia kogamogai* (mollusca: Patellogastropoda), using sem ebsd and fib tem techniques. *J. Struct. Biol.*., 171: 223–230, 2010. doi: 10.1016/j.jsb.2010.04.008.

[220] S. Ashely. Composite car structures pass the crash test. *Mech. Engin.*, 118(12): 59–63, 1996.

[221] R. Olivo. Mechanoreceptor function in the razor clam: Sensory aspects of the foot withdrawal reflex. *Comp. Biochem. Physiol.*, 35(4):761–786, 1970. doi: 10.1016/0010-406X(70)90075-7.

[222] D. Taylor. Scaling effects in the fatigue strength of bones from different animals. *J. Theor. Biol.*, 206(2):299–307, 2000. doi: 10.1006/jtbi.2000.2125.